CIGGT Project No. PRO-145

CIGGT Report No. 83-13
Transport Canada Report No. TP5589E

ELECTRIC LOCOMOTIVE EVALUATION

E.R. Corneil
G.W. English
H. Boumeester

prepared for

Transportation Development Centre, Transport Canada

Canadian Institute of Guided Ground Transport
Queen's University at Kingston, Ontario
K7L 3N6

March 1984

This report resulted from research conducted through the Canadian Institute of Guided Ground Transport. The report represents the views of the authors and does not necessarily have the endorsement of the University or the other participating organizations.

REPORT DOCUMENTATION FORM

1. **Transport Canada Report No.**
5589E

2. **TDC Project No.**
4888

3. **Recipient's Catalogue No.**

4. **Title and Subtitle**
ELECTRIC LOCOMOTIVE EVALUATION

5. **Report Date**
March 1984

6. **Performing Organization Report No.**
83-13

7. **Author(s)**
E.R. Corneil, G.W. English, H. Boumeester

8. **Transport Canada File No.**
D1465-317-5

9. **Performing Organization Name and Address**
Canadian Institute of Guided Ground Transport (CIGGT)
c/o Queen's University
Kingston, Ontario K7L 3N6

10. **DSS File No.**
48SZ.T8200-2-2562

11. **DSS or Transport Canada Contract No.**
OSZ 82-00098

12. **Sponsoring Agency Name and Address**
Transportation Development Centre (TDC)
1000 Sherbrooke Street West, Suite 2421
Montreal, Quebec H3A 2R3

13. **Type of Report and Period Covered**
02/83-03/84

14. **Sponsoring Agency Code**

15. **Supplementary Notes**

16. **TDC Project Officer**
C.A. Versailles

17. **Abstract**

Using a train simulation model, the effects of power and tractive effort on train time and energy consumption are evaluated for the range of values typical in available electric locomotives. From this informaton base, extrapolations provide target values for future development. Design requirements such as axle power, overload capacity, traction-motor gear ratio and number of axles are discussed. Models of several different power-conditioning units are developed and used in evaluating measures of performance such as harmonic content, efficiency and power factor. The influence of these factors on the fixed cost of electrification is discussed and in some cases quantified.

18. **Key Words**
Electric locomotives;
Power-conditioning units;
Railway electrification

19. **Distribution Statement**
Available on request from TDC

20. **Security Classification (of this report)**
unclassified

21. **Security Classification (of this page)**
unclassified

22. **No. of Pages**
68 + append.

23. **Price**

TDC 007 79-008

FORMULE DE DOCUMENTATION POUR RAPPORT

1. Nº du rapport Transports Canada
5589E

2. Nº de l'étude — CDT
4888

3. Nº de catalogue du destinataire

4. Titre et sous-titre
ELECTRIC LOCOMOTIVE EVALUATION

5. Date du rapport
Mars 1984

6. Nº du rapport de l'organisme exécutant
83-13

7. Auteur(s)
E.R. Corneil, G.W. English, H. Boumeester

8. Nº de dossier Transports Canada
D1465-317-5

9. Nom et adresse de l'organisme exécutant
Canadian Institute of Guided Ground Transport (CIGGT)
c/o Queen's University
Kingston, Ontario
K7L 3N6

10. Nº de dossier — ASC
48SZ.T8200-2-2562

11. Nº de contrat — ASC ou Transports Canada
0SZ 82-00098

12. Nom et adresse de l'organisme parrain
Centre de développement des transports (CDT)
1000, rue Sherbrooke ouest
Bureau 2421
Montréal (Québec) H3A 2R3

13. Genre de rapport et période visée
02/83 - 05/84

14. Code de l'organisme parrain

15. Remarques additionnelles

16. Agent de projet — CDT
C.A. Versailles

17. Résumé

Ce rapport rend compte des résultats d'une étude par modélisation de la marche des trains, dans laquelle il s'agissait de déterminer l'effet de différents niveaux de puissance par essieu et d'effort de traction sur les temps de parcours et la consommation énergétique, dans la gamme des valeurs types propres aux locomotives électriques courantes. A partir de cette information de base, des extrapolations ont pu être faites pour situer les valeurs-cibles dans l'étude des nouvelles générations de locomotives. Le rapport traite de certains paramètres de base tels que: puissance à l'essieu, capacité de surcharge, rapport d'engrenages des moteurs de traction et nombre d'essieux. Il présente les modèles mathématiques élaborés pour simuler plusieurs groupes de conversion d'énergie qui ont servi à définir les critères à prendre en compte pour mesurer les performances comme: teneur en harmoniques, rendement et facteur de puissance, par exemple. Le rapport traite de l'influence de ces paramètres sur le coût de premier établissement, donnant certains cas chiffrés.

18. Mots-clés
Locomotives électriques. Groupes de conversion d'énergie. Electrification des chemins de fer

19. Diffusion
Ce rapport est distribué sur demande adressée au CDT

20. Classification de sécurité (de ce rapport)
non-classifié

21. Classification de sécurité (de cette page)
non-classifiée

22. Nombre de pages
65 + app.

23. Prix

TABLE OF CONTENTS

1. INTRODUCTION 1
    1.1 Objectives of the Study 2

2. THE APPROACH 2
    2.1 Selection of Track Segments 2
    2.2 Selection of Train Size 3
    2.3 Initial Calculations 5

3. LOCOMOTIVE POWER PER AXLE 9
    3.1 Maximum Overload Rating Defined 9
    3.2 Continuous Powers Defined by a Minimum-Run-Time Criterion 14
        3.2.1 Variability Within a Segment 16
        3.2.2 Variability from Segment to Segment 21
    3.3 Maximum Bounds for Continous Power Ratings 23

4. THE IMPLICATIONS OF THE ANALYSIS 28

5. NUMBER OF AXLES PER UNIT 33
    5.1 Adhesion Requirements 35
    5.2 Power Transmitted Through a Locomotive Pantograph 35
    5.3 Locomotive Weight Considerations 36
    5.4 Reliability Considerations 37

6. CONTROL PHILOSOPHY 37

7. GEAR RATIO CONSTRAINTS 39

8. ADHESION IMPLICATIONS 43
    8.1 General Relationship Between Traction Coefficient and Wheel/Rail Wear 43

9. EFFECTS OF LOCOMOTIVE DESIGN ON ELECTRIFICATION FIXED COSTS 46
    9.1 The Costs of Low Displacement and Power Factors 49
    9.2 Cost of Harmonic Currents 54
    9.3 Comparison of Power-Conditioning Units (PCU) 58
    9.4 Effects of Power-per-Axle 66

10. CONCLUSIONS 67

Appendix A: ELECTRIC LOCOMOTIVE MODELLING, HARMONIC EFFECTS
Appendix B: TRAIN CONFIGURATIONS
Appendix C: TRAIN TIMES
Appendix D: SPEED FACTORS

LIST OF TABLES

1. Segment Classification 4
2. Train Time and Energy 6
3. Maximum Usable Power per Axle for $\psi = 0.25$ 10
4. Maximum Usable Continuous Power per Axle 17
5. Variability Within a Segment -- BICSWN 18
6. Prediction Error Within a Segment - BICSWN 19
7. Variability Between Segments 22
8. Prediction Error, Segment to Segment 24
9. Prediction Error, Segment to Segment 25
10. Substation spacing versus displacement factor 53
11. Average Performance Results for an 800 km Mountain Regional Train Run 65

LIST OF FIGURES

1. Per cent of axle-kilometres vs maximum axle power which might be used on the track segment 13
2. Estimated bound on axle power vs adhesion 21
3. Maximum usable power estimates on a minimum-run-time criterion 26
4. Time spent in "diesel-equivalent" notch position 27
5. Conceptual representation of optimal train speed 29
6. Estimates of maximum potential capacity increase (in per cent) for western line segments 31
7. Elastic and shakedown limits in rolling contact 45
8. Required wheel load 45
9. Structure of the computer simulation package 50
10. Substation spacing versus displacement factor 52
11. Pantograph voltage and current waveforms illustrating resonance effects 55
12. Pantograph voltage and current waveforms with filter connected 55
13. Distributing current for multiple locomotive loads 57
14. Three-bridge phase-control series motor and two-bridge phase control shunt motor 59
15. Two-phase control and symmetric control 61
16. Pulse-width modulated system 63
17. Chopper control 64

1. INTRODUCTION

At present, 38 per cent of all European railways and more than ten per cent of the world's rail lines are electrified. In Canada, both Canadian National and Canadian Pacific have maintained an interest in electrification, but they have adopted the wait-and-see attitude common to most North American railroads. Both CN and CP have made studies of electrification (CP as early as 1895) and have continued to update them. In general, they have found that while there are cost savings, these savings are not sufficiently high to justify commercial interest in conversion. On the other hand, the British Columbia Railway has electrified its new Tumbler Ridge branch line. Also, there has been sufficient interest to warrant the formation, in October 1981, of the Railway Electrification Committee (REC) to assess electrification in the Canadian context. Two working subcommittees were established -- Economic Assessment and Standards. The Economic Assessment Subcommittee undertook a study of the national impacts of electrification which also developed estimates of the costs of conversion.[1]

Supply of electric locomotives was the largest single cost item identified in that study, although this fact is mitigated by the concurrent savings in diesel-electric locomotives. It would be important to achieve a high domestic content for new electric locomotives if electrification were to proceed. North American conditions are different (in terms of both train configuration and terrain) from the majority of electrified rail operations. Also, there is an opportunity to design the electric locomotive as part of the complete electrified system without the constraints of an existing electric infrastructure.

Basically, railway electrification involves the replacement of a portable power source (the diesel engine) with a fixed off-line generating station. Diesel-electric locomotives are limited by the present technology of the diesel engine to approximately 2,700 tractive kilowatts (3,600 horsepower). This power may be delivered to either four or six traction motors without exceeding axle loads commonly accepted by North American railways. Higher-powered diesel engines, suitable for locomotive applications, have been produced, but higher weight and lower reliability have thus far prevented widespread acceptance. Diesel-electric locomotives are in service with up to 560 tractive kilowatts (750 horsepower) per axle, although the majority of units operate at 373 to 448 tractive kilowatts (500 to 600 horsepower) per axle. The possibility of manufacturing acceptable electric locomotives producing substantially more power per axle does exist.

---

[1] Empey, W.F., J.A. Osten (Data Resources of Canada), G.W. English, C. Schwier, F.W.A. Bliemel (CIGGT), National Impact of Railway Electrification, June 1983, TP-4461E, prepared for Transport Canada on behalf of the Railway Electrification Committee.

1.1 Objectives of the Study

The objectives of this study are to identify and discuss the design trade-offs involved in selecting an electric locomotive for Canadian conditions. The effects of power per axle on efficiency and performance, power-conditioning unit design on fixed facilities costs, and the trade-offs associated with wheel size, adhesion and gear size in particular are addressed.

2. THE APPROACH

2.1 Selection of Track Segments

To obtain credible estimates of the effects of increased axle power, it was necessary to simulate realistic train configurations, over existing track profiles, with existing speed and siding constraints. The Train Performance Calculator program (TPC) developed by Canadian National Railways (CN) was used for the simulation.

The analysis was undertaken for a number of different train configurations on a limited number of track segments. A preliminary analysis of mainline trackage for both the CN system and the Canadian Pacific Railway (CP) system was completed to select a range of conditions. This analysis provided:

- an estimate of track speed, based on track speed restrictions and train lengths
- an estimate of total curvature, per unit length, for the track segment
- an estimate of total elevation increase, per unit length, in both the forward and reverse directions, for the track segment

- an estimate of energy required to increase train speed, after a speed restriction, per unit track length, for the segment (in each direction).

Based on this preliminary analysis, each of the mainline segments was categorised by curvature, grading and speed changes. Track segments were then selected to provide a sampling of the possible combinations of the three variables. Two additional segments were added to the selection, to provide three segments bearing the same classifications, to identify the variability within the classification. Table 1 illustrates the "segment classification" for the segments selected for the study. Roughly half of the segments are from each of the two major competing Canadian railways. A total route length of 4,288 kilometres (2,752 miles) was covered by the chosen segments (multiple track was not counted as additional length).

2.2 Selection of Train Size

Train configurations are controlled by a number of factors, most notably traffic mix, siding length, train weight, and controlling gradient. In some cases, locomotive load factor and train time must also be considered. Hence, identification of "typical" trains is not a simple task. To simplify data entry into the TPC computer program, it was decided to initially restrict the car types to a single type for each train. Thus, three major types of trains were considered: box car (mixed freight), bulk car (coal or grain), and TOFC (express with automotive cars, and trailer and container flatcars).

The controlling grade for each segment, and for the trackage between major freight terminals which included the segment, was identified. The design criterion for trailing tonnage per locomotive axle was based on both sufficient adhesion ($\mu = 0.25$ was used) and sufficient power to maintain 20 km/h (12 mph) on the controlling grade. A calculator program produced a list of the numbers of cars and train lengths for locomotive configurations of four, six, eight, etc., axles, increasing the number of axles until car numbers exceeded 140 cars. A comparison of train length to siding length permitted rapid selection of the final train configuration. Each train consisted of N_a locomotive axles (in pairs), N_c cars of the appropriate weight and length, and one van.

TABLE 1

SEGMENT CLASSIFICATION

	Kilometers	Curvature	Grading*	Speed Changes
1. ARTEDM	276.6	Light	Average	Few
2. KINTOR	257.4	Light	Average	Average
3. MOJWAL	356.6	Light	Light	Few
4. SPYSAS	418.0	Light	Light	Average
5. MTLTOR	529.1	Light	Light	Many
6. BICSWN	125.5	Average	Light	Few
7. EDMBIC	241.5	Average	Light	Average
8. IGNKEN	235.0	Average	Light	Average
9. CALSTE	192.3	Average	Light	Average
10. GLDMTL	490.8	Average	Average	Many
11. NBNVAN	204.1	Average	Light	Many
12. STEGOL	71.5	High	High	Few
13. SUXWHT	278.4	High	Light	Average
14. RPSVAN	752.0	High	Light	Many
Total	4,428.8			

* Since grade classification was based on average up-grades in each direction, some steep directional grades such as CALSTE have the same rating as rolling prairie terrain such as MOJWAL.

Note:		
	ARTEDM	is Artland, Saskatchewan to Edmonton, Alberta
	KINTOR	is Kingston, Ontario to Toronto, Ontario
	MOJWAL	is Moose Jaw, Saskatchwan to Walsh, Alberta
	SPYSAS	is Spy Hill, Saskatchwan to Saskatoon, Saskatchewan
	MTLTOR	is Montreal, Quebec to West Toronto, Ontario
	BICSWN	is Bickerdike, Alberta to Swan Landing, Alberta
	EDMBIC	is Edmonton, Alberta to Bickerdike, Alberta
	IGNKEN	is Ignace, Ontario to Kenora, Ontario
	CALSTE	is Calgary, Alberta to Stephen, Alberta
	GLDMTL	is Glendyne, Quebec to Montreal, Quebec
	NBNVAN	is North Bend, B.C. to Vancouver, B.C.
	STEGOL	is Stephen, Alberta to Golden, B.C.
	SUXWHT	is Sioux Lookout, Ontario to Whitemouth, Manitoba
	RPSVAN	is Red Pass, B.C. to Vancouver, B.C.

An evaluation of published rail traffic provided an indication of the predominant train types, in each direction, for each segment. Appendix B illustrates the 125 train configurations used in the study. In some cases, later in the study, siding lengths were adjusted to examine the effects of longer trains.

2.3 Initial Calculations

For each train configuration, TPC calculations were performed for an axle power of 485 kilowatts (650 horsepower) per axle and for 970 kilowatts (1,300 horsepower) per axle. The 970 kilowatts-per-axle figure was identified as the maximum available with existing traction motors, and the lower figure was chosen to provide a factor of two in the power equations. Also, the 485 kilowatts power per axle falls between the two common values for diesel locomotives. The output of these runs is summarized in Table 2. The first segments examined were BICSWN, M0JWAL, and NBNVAN.

The TPC calculations also provided an estimate of energy use for each train configuration. Analysis of these figures confirmed that higher power per axle increased the energy consumption on a mass-distance (ton-mile) basis, although some segments were more sensitive than others. For example, for the MOJWAL segment, the doubling of power reduced running time by 3.3 per cent for a bulk train running west, but the energy consumption increased by 5.5 per cent. For the MOJWAL segment, the controlling grade was outside the segment, and hence the train had surplus tractive capacity for all parts of the segment. On the other hand, the BICSWN segment has a controlling grade which is almost the same as the terminal-to-terminal (zone) grade. The power increase, again by a factor of two, would result in a 28.4 per cent reduction in train time for a bulk train running west. Energy consumption increases by 12.4 per cent. Express trains show a slightly greater increase in energy consumption with increased power per unit mass, but also show a greater reduction in train time with increased power.

TABLE 2

TRAIN TIME AND ENERGY

Segment		Train	Train Run Time		Train Fuel Use				
			650 hp (minutes)	1300 hp (minutes)	650 hp (gallons)	1300 hp (gallons)	Time Reduction (%)	Fuel Increase (%)	Fuel-Time Ratio
ARTEDM									
West:	**Box**	010	272.4	217.6	814.8	1008.6	20.12	23.78	1.1823
	Box	101	248.5	211.0	718.4	865.8	15.09	20.52	1.3596
	Box	102	230.8	207.1	627.8	730.9	10.27	16.42	1.5993
	Bulk	011	265.9	216.6	2091.0	2502.0	18.54	19.66	1.0601
	Bulk	103	264.7	216.3	2078.9	2485.7	18.28	19.57	1.0702
	Bulk	104	243.6	210.8	1826.5	2143.7	13.46	17.37	1.2898
East:	**Bulk**	169	301.9	237.9	1864.9	2325.9	21.20	24.72	1.1661
	Bulk	157	286.1	227.3	1449.1	1799.8	20.55	24.20	1.1775
	Bulk	170	269.2	221.3	1586.5	1934.8	17.79	21.95	1.2338
	TOFC	105	340.8	260.9	743.1	981.5	23.44	31.08	1.3684
	TOFC	012	332.6	253.1	722.9	959.3	23.90	32.70	1.3681
	TOFC	106	271.4	218.9	561.4	738.3	19.34	31.51	1.6289
KINTOR									
West:	**Box**	107	196.1	172.7	1038.2	1209.8	11.93	16.53	1.3852
	Box	013	192.0	171.3	990.0	1140.4	10.78	15.19	1.4091
	Box	108	187.4	169.9	928.6	1056.9	9.34	13.82	1.4795
East:	**Box**	111	198.0	174.1	1038.1	1233.9	12.07	18.86	1.5626
	Box	014	194.1	172.9	999.5	1173.5	10.92	17.41	1.5939
	Box	112	188.5	171.2	932.9	1071.8	9.18	14.89	1.6223
	TOFC	109	220.9	177.5	989.6	1276.8	19.65	29.02	1.4772
	TOFC	015	216.0	176.2	996.0	1228.9	18.43	27.22	1.4770
	TOFC	110	197.3	171.4	856.4	1025.4	13.43	19.73	1.4689
MOJWAL									
West:	**Box**	113	281.0	264.3	1786.3	1932.5	5.94	8.18	1.3772
	Box	016	274.7	263.6	1641.9	1749.3	4.04	6.54	1.6188
	Bulk	114	279.3	266.0	3813.3	4059.5	4.76	6.46	1.3558
	Bulk	017	273.9	265.2	3490.5	3682.8	3.18	5.51	1.7345
East:	**TOFC**	018	291.5	261.6	1196.2	1389.4	10.26	16.15	1.5746
SPYSAS									
West:	**Box**	019	359.0	289.4	1130.0	1433.7	19.39	26.88	1.3863
	Bulk	020	351.7	289.0	2877.1	3497.2	17.83	21.55	1.2090
East:	**Bulk**	171	427.1	309.8	2772.9	3513.5	27.46	26.71	0.9725
	Bulk	159	405.1	300.6	2188.7	2755.4	25.80	25.89	1.0037
	Bulk	172	375.0	290.6	2391.0	2965.5	22.51	24.03	1.0676
	TOFC	021	613.3	395.5	1189.8	1591.4	35.51	33.75	0.9505
	TOFC	115	487.6	348.9	1104.9	1499.3	28.45	35.70	1.2549
	TOFC	116	380.9	290.3	853.3	1161.0	23.79	36.06	1.5160
MTLTOR									
West:	**Box**	022	511.2	441.1	2040.3	2469.1	13.71	21.02	1.5326
	Box	117	476.1	432.1	1804.7	2130.2	9.24	18.04	1.9516
	Box	118	458.8	427.5	1663.7	1922.2	6.82	15.54	2.2775
	Bulk	160	540.7	454.3	4813.5	5720.2	15.98	18.84	1.1788
	Bulk	161	500.5	443.3	4269.7	4987.5	11.43	16.81	1.4710

TABLE 2 (cont'd)

TRAIN TIME AND ENERGY

Segment		Train	Train Run Time		Train Fuel Use				
			650 hp (minutes)	1300 hp (minutes)	650 hp (gallons)	1300 hp (gallons)	Time Reduction (%)	Fuel Increase (%)	Fuel-Time Ratio
East:	Bulk	119	446.7	436.0	4225.8	4779.8	6.58	13.11	1.9930
	Bulk	023	459.6	433.7	3996.7	4509.7	5.64	12.84	2.2777
	Bulk	120	457.2	432.9	3922.1	4424.2	5.31	12.80	2.4086
	TOFC	121	495.3	434.7	2045.8	2484.3	12.24	21.43	1.7519
	TOFC	024	489.7	433.2	2004.3	2422.1	11.54	20.85	1.8067
	TOFC	122	466.2	427.5	1812.1	2134.3	8.30	17.78	2.1419
BICSWN									
West:	Box	025	133.2	97.4	269.3	306.6	26.88	13.85	0.5153
	Box	123	132.4	97.6	266.6	303.4	26.28	13.80	0.5252
	Box	124	121.2	91.2	236.0	269.0	24.75	13.98	0.5649
	Bulk	030	181.5	119.0	785.5	889.8	34.44	13.28	0.3856
	Bulk	155	177.5	116.9	765.5	867.6	34.14	13.34	0.3907
	Bulk	028	134.3	97.5	1065.6	1194.5	27.40	12.10	0.4415
	Bulk	026	133.4	96.9	794.1	892.6	27.36	12.40	0.4533
	Bulk	154	131.8	96.2	1038.6	1164.4	27.01	12.11	0.4484
	Bulk	125	131.9	96.4	780.5	876.1	26.91	12.25	0.4551
	Bulk	126	124.4	92.3	720.7	808.8	25.80	12.22	0.4737
	Bulk	029	119.8	89.8	907.7	1017.3	25.04	12.07	0.4822
East:	Bulk	162	121.0	91.9	667.5	765.1	24.05	14.62	0.6080
	Bulk	163	113.6	89.1	604.9	690.6	21.57	14.17	0.6569
	TOFC	037	146.0	102.3	308.6	360.3	29.93	16.75	0.5597
	TOFC	038	140.2	99.8	308.7	370.5	28.82	20.02	0.6947
	TOFC	027	133.8	101.2	287.4	338.6	24.36	17.81	0.7312
	TOFC	127	125.9	94.6	266.8	316.3	24.86	18.55	0.7463
	TOFC	032	111.5	88.4	419.0	486.0	20.72	15.99	0.7718
	TOFC	128	109.3	87.2	216.4	254.1	20.22	17.42	0.8616
	TOFC	034	102.2	85.2	362.2	413.0	16.63	14.03	0.8432
	TOFC	035	100.0	84.4	372.8	427.1	15.60	14.57	0.9337
	TOFC	031	99.4	84.3	394.3	454.0	15.19	15.14	0.9967
	TOFC	033	90.8	82.0	320.2	356.9	9.69	11.46	1.1826
	TOFC	036	90.3	81.6	318.3	354.4	9.63	11.34	1.1772
EDMBIC									
West:	Box	039	287.6	201.2	661.1	797.4	30.04	20.62	0.6863
	Box	129	284.3	200.1	653.2	788.5	29.62	20.71	0.6994
	Box	130	247.1	188.7	560.2	676.8	23.63	20.81	0.8807
	Bulk	040	284.2	200.3	1945.4	2284.9	29.52	17.45	0.5911
	Bulk	131	279.0	198.8	1907.5	2241.7	28.75	17.52	0.6095
	Bulk	132	250.4	190.5	1689.4	1988.5	23.92	17.70	0.7401
East:	TOFC	041	228.9	191.1	498.1	639.0	16.51	28.29	1.7130
	TOFC	133	220.5	187.9	468.9	591.3	14.78	26.10	1.7656
	TOFC	134	199.7	181.1	385.7	455.4	9.31	18.07	1.9402
IGNKEN									
West:	Box	042	186.3	178.2	749.1	825.1	4.35	10.15	2.3335
	Bulk	164	187.4	179.2	1750.8	1897.7	4.38	8.39	1.9175

TABLE 2 (cont'd)

TRAIN TIME AND ENERGY

Segment		Train	Train Run Time		Train Fuel Use		Time Reduction (%)	Fuel Increase (%)	Fuel-Time Ratio
			650 hp (minutes)	1300 hp (minutes)	650 hp (gallons)	1300 hp (gallons)			
East:	Bulk	043	252.7	189.7	1673.5	2043.2	24.93	22.09	0.8861
	Bulk	135	250.0	189.0	1652.1	2015.8	24.40	22.01	0.9022
	Bulk	136	221.3	182.7	1420.0	1705.1	17.44	20.08	1.1511
	TOFC	044	297.6	208.8	685.3	881.8	29.84	28.67	0.9610
	TOFC	137	283.5	202.5	651.5	841.0	28.57	29.09	1.0180
	TOFC	138	223.8	181.0	497.7	636.6	19.12	27.91	1.4593
CALSTE									
West:	Box	139	232.5	178.3	1271.9	1411.6	23.31	10.98	0.4712
	Box	045	221.6	176.2	1191.6	1317.4	20.49	10.56	0.5153
	Box	140	215.6	175.2	1145.6	1262.7	18.74	10.22	0.5455
	Bulk	142	229.5	178.3	2726.9	2971.2	22.31	8.96	0.4016
	Bulk	046	219.2	176.6	2558.8	2777.4	19.43	8.54	0.4396
East:	Bulk	165	171.2	170.6	422.6	481.2	0.35	13.87	39.5659
	TOFC	141	172.3	171.6	480.5	529.7	0.41	10.24	25.2034
	TOFC	047	171.7	171.1	433.1	480.0	0.35	10.83	30.9887
GLDMTL									
West:	Box	143	403.4	364.3	2459.7	2759.7	9.69	12.20	1.2583
	Box	048	391.8	361.0	2291.9	2531.2	7.86	10.45	1.3287
East:	Bulk	049	419.7	369.9	5107.4	5652.7	11.87	10.68	0.8998
	TOFC	144	461.9	374.3	2134.9	2383.0	18.97	11.62	0.6128
	TOFC	050	448.7	369.8	1842.7	2263.0	17.58	22.81	1.2971
	TOFC	145	435.7	365.9	1769.0	1914.1	16.02	8.20	0.5120
NBNVAN									
West:	Box	051	244.0	239.9	798.7	851.3	1.68	6.59	3.9193
	Bulk	052	246.9	243.2	1632.6	1736.9	1.50	6.39	4.2631
East:	Bulk	166	232.2	230.7	1158.1	1227.3	0.65	5.98	9.2498
	TOFC	146	238.2	236.3	1153.2	1219.1	0.80	5.71	7.1642
	TOFC	053	235.6	234.1	1017.6	1079.2	0.64	6.05	9.5080
STEGOL									
West:	Box	054	137.0	136.9	66.2	83.7	0.07	26.44	362.160
	Bulk	055	137.3	137.3	138.0	176.3	0.00	27.75	999.999
East	Bulk	167	134.7	124.8	1420.6	1459.4	7.35	2.73	0.3716
	TOFC	147	135.4	125.2	1227.9	1262.9	7.53	2.85	0.3784
	TOFC	056	128.8	124.9	1079.8	1112.6	3.03	3.04	1.0032
SUXWHT									
West:	Box	057	264.9	239.7	717.2	806.2	9.51	12.41	1.3045
East:	Bulk	058	279.4	241.3	1929.7	2143.7	13.64	11.09	0.8133
	TOFC	059	307.0	245.9	675.7	804.4	19.90	19.05	0.9570
	TOFC	148	300.6	244.2	657.5	776.8	18.76	18.14	0.9671
	TOFC	149	278.4	238.9	585.2	670.1	14.19	14.51	1.0225
RPSVAN									
West:	Box	060	902.8	887.7	1742.1	1927.8	1.67	10.66	6.3731
	Box	150	897.9	885.3	1643.7	1808.8	1.40	10.04	7.1578
	Box	151	891.6	882.0	1487.1	1626.5	1.08	9.37	8.7061
	Bulk	152	911.0	895.8	3916.5	4318.7	1.67	10.27	6.1549
	Bulk	061	906.9	893.6	3738.4	4104.5	1.47	9.79	6.6776
	Bulk	153	903.5	891.8	3583.9	3919.9	1.29	9.38	7.2398
East:	Bulk	168	975.3	901.5	8889.4	9553.8	7.57	7.25	0.9580
	TOFC	062	993.4	894.1	3006.3	3344.5	10.00	11.25	1.1254

3. LOCOMOTIVE POWER PER AXLE

3.1 Maximum Overload Rating Defined

The maximum power per axle was determined for each segment and train type. This value relates to the tractive force and tractive power required to maintain the track speed on the maximum grade for that speed and track segment. As the maximum grade is, in most cases, relatively short, the value defines an absolute upper bound on useful power in short-term overload conditions.

The maximum track grade for the specific train was located for each different track speed limit, using the detailed TPC printouts. The train resistance for the specific track speed was calculated using the modified Davis train resistance formula incorporated in the TPC. The tractive force was compared to that available from the locomotives, based on a constant adhesion of 0.25.[2] If the computed force exceeded that available from the locomotives, the maximum locomotive tractive force was used to compute the tractive power for the specific track speed. Table 3 presents the results of these calculations, identifying the maximum usable axle power for each segment and train type.

The maximum power that could be used on the ARTEDM segment proved to be limited by adhesion at the track speed limit of 60 mph. The controlling grade is within the segment for westward movements, but outside the segment for eastward movements. The slight variation in maximum power (2,453.33 to 2,460.00 horsepower per axle) reflects the small differences in the mass per axle for the mix of four- and six-axle locomotives used in the calculation.

The KINTOR segment would also be adhesion-limited, with the controlling grade within the segment. The 60 mph track speed limit (for freight trains) gives the same results as above.

---

[2] While available adhesion has been shown to decrease with increasing speed, this simple rule was consistent with the objectives of identifying a maximum bound.

TABLE 3

MAXIMUM USABLE POWER PER AXLE FOR $\mu = 0.25$

	Worst Case Conditions			
	Speed Limit (mph)	Grade (%)	Controlling Zone Gradient (%)	Maximum Power per Axle (hp)
1. ARTEDM				
Box West	60	0.9090	0.9090	2453.33
Bulk West	60	0.7310	0.7310	2460.00
TOFC East	60	0.4242	0.44	2460.00
2. KINTOR				
Box West	60	1.0776	0.0776	2456.00
Bulk East	60	1.1098	0.1098	2456.00
TOFC East	60	1.1003	0.1003	2460.00
3. MOJWAL				
Box West	55	0.6818	1.35	1531.25
Bulk West	55	0.6022	1.35	1356.96
TOFC East	55	0.6325	1.06	2061.31
4. SPYSAS				
Box West	60	0.5189	0.70	2453.33
Bulk West	60	0.5075	0.70	2429.29
TOFC East	60	0.4166	0.44	2460.00
5. MTLTOR				
Box West	65	0.7215	0.77	2665.00
Bulk East	50	1.0018	0.01	2076.49
	65	0.5492		
TOFC East	50	1.0208	1.01	2665.00
	65	0.7556		
6. BICSWN				
Box West	50	0.4564	0.52	2050.00
Bulk West	50	0.4564	0.52	2050.00
TOFC East	50	0.4393	0.49	2050.00
7. EDMBIC				
Box West	50	0.5000	0.52	2050.00
Bulk West	50	0.5000	0.52	2050.00
TOFC East	50	0.4753	0.49	2050.00
8. IGNKEN				
Box West	65	0.8125	1.05	2660.67
Bulk East	65	0.5321	0.56	2665.00
TOFC East	65	0.5113	0.56	2665.00

TABLE 3 (cont'd)

MAXIMUM USABLE POWER PER AXLE FOR $\mu = 0.25$

	Worst Case Conditions			
	Speed Limit (mph)	Grade (%)	Controlling Zone Gradient (%)	Maximum Power per Axle (hp)
9. CALSTE				
Box West	50	1.0018	1.01	2046.67
Bulk West	50	0.9943	1.01	2048.48
TOFC East	50	0.5340	2.28	805.00
10. GLDMTL				
Box West	60	0.9829	1.28	2335.11
Bulk East	60	0.8693	1.19	2202.23
TOFC East	60	0.9981	1.19	2460.00
11. NBNVAN				
Box West	25	0.9678	1.14	1088.96
	30	0.9034		
	45	0.4848		
	50	0.3503		
Bulk West	25	0.9583	1.14	1000.54
	30	0.8484		
	40	0.4545		
	45	0.4469		
	50	0.3484		
TOFC East	25	1.1609	2.40	719.76
	30	1.1193		
	40	0.7784		
	45	0.6231		
	50	0.4412		
12. STEGOL				
Box West	30	0.7196	1.01	980.13
Bulk West	30	0.5909	1.01	834.63
TOFC East	30	2.0132	2.28	1142.20
13. SUXWHT				
Box West	45	0.5606	0.70	1827.92
Bulk West	45	0.4640	0.62	1725.83
TOFC East	45	0.5492	0.62	1845.00
14. RPSVAN				
Box West	50	0.9810	0.84	2050.00
Bulk West	50	0.8276	0.84	2048.15
TOFC East	25	0.8541	0.8541	1806.68
	50	0.4659		
	60	0.2837		

The MOJWAL segment would not be adhesion-limited, since there is a substantial difference between the controlling grade within the segment and the controlling grade for the zone. The consequence is a substantial reduction in the power per axle that could be used on the segment.

Results similar to those for the ARTEDM segment were obtained for the SPYSAS and GLDMTL (eastward) segments.

The MTLTOR (westward) segment has a zone controlling grade only slightly greater than the segment controlling grade. The higher track speed results in a higher axle power, with the value being adhesion-limited. In the eastward direction, the zone grade is substantially greater than the segment grade. As a result, a heavy bulk train would not require full adhesion at track speed, and hence the maximum axle power could be reduced. However, the lighter and shorter express train would be adhesion-limited.

The BICSWN and EDMBIC segments have relatively low zone controlling grades, and hence would be adhesion-limited at track speed. However, with a track speed limit of 50 mph, the maximum axle power would be limited to 2,050 horsepower.

The IGNKEN segment would be marginally power-limited in the westward direction, but adhesion-limited in the eastward direction. The track speed limit is 65 mph.

Adhesion would limit axle power on the CALSTE (westward) segment, but the severe zone grade east-bound would limit the axle power to 805 horsepower.

Westward traffic on the GLDMTL segment would be power-limited, while the eastward traffic would face similar conditions to that on the MTLTOR segment. However, the lower track speed limit of 60 mph would reduce the maximum usable axle power.

The NBNVAN, STEGOL, SUXWHT (westward), and RPSVAN (eastward) segments would all be power-limited, with zone grades substantially larger than the segment grades. The SUXWHT (eastward) segment would be similar to the MTLTOR segment, with the lower track speed

limit (45 mph) limiting the maximum axle power, while the RPSVAN (westward) segment resembles the BICSWN segment.

To identify the importance of each level of axle power, traffic estimates for each segment were converted to the number of locomotive axles required to haul the traffic over the segment. The axle trips were then multiplied by the segment length (to obtain, in effect, locomotive-kilometres per year). The percentage of the total axle-kilometres for each axle power has been plotted in Figure 1 to illustrate the importance of each axle power level. An overload power rating in excess of 2,500 horsepower per axle would be required for

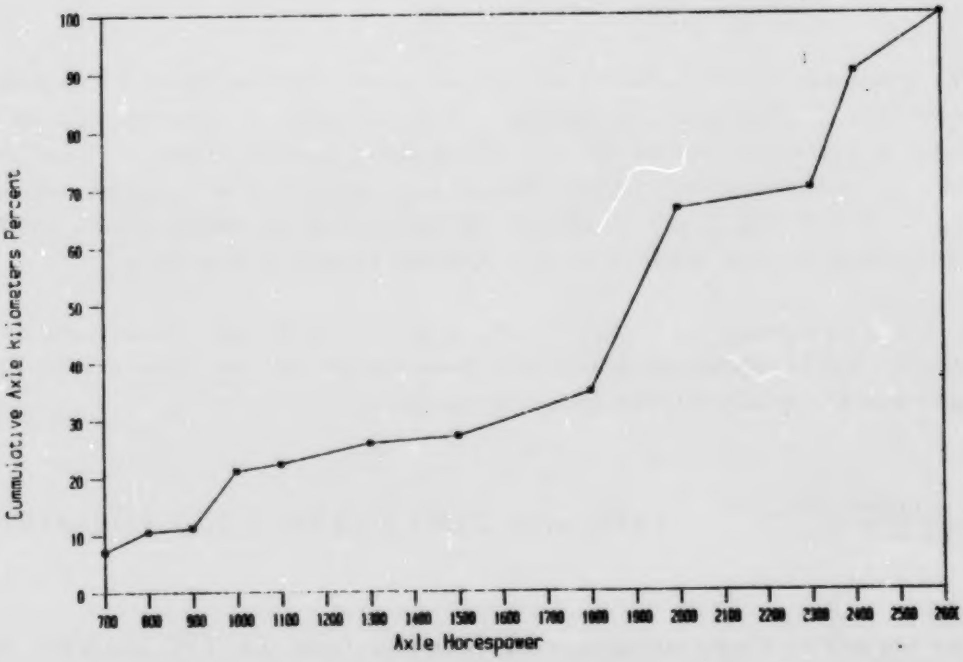

Note that the axle-km figure is a product of subdivision length and the maximum power that could be utilised at some point on that subdivision.

Figure 1 Per cent of axle-kilometres vs maximum axle power which might be used on the track segment

less than ten per cent of the service. On the other hand, for subdivisions requiring 55 per cent of the axle-kilometres, overload power levels of 2,000 to 2,500 horsepower per axle could be used at some point in the subdivision.

Essentially, Figure 1 indicates that the maximum usable short-term overload rating, for all practical applications, is 1,835 kilowatts (2,460 horsepower) per axle.[3]

Typically, the maximum track grade length is relatively short. Hence, the short-time rating may be in the order of seconds or minutes.

3.2 Continuous Power Defined by a Minimum Run Time Criterion

The previous section placed an upper bound on the short-term power requirement of a traction motor. The purpose of this section is to place a maximum bound on the continuous power rating. This was done by estimating the power required to achieve the minimum feasible run time for the track segment, as governed by track speed limits. The estimates were made with a simplified exponential model.

It was postulated that each track segment could be characterized to provide an estimate of train run time based on the power per unit mass for the train, in the following manner:

$$\left(\frac{\text{HORSEPOWER}}{\text{TRAIN TONS}}\right)^{1/x} \cdot (\text{TRAIN RUN TIME}) = (\text{TRACK TIME CONSTANT})$$

The train run time estimates were obtained from the TPC analysis, for two different power-per-ton ratios, and hence the value of the exponent, x, and the track time constant were identified for each train and segment set. Although the exponent varies to some extent with train type, the results of the initial analysis on three different

---

[3] Note that the axle power is directly related to adhesion. Therefore, if the useful adhesion at track speed is only 0.20, the overload power must be reduced proportionately (to 80 per cent of the above figures).

segments were sufficiently close to proceed further with the simple model for train run time.

The initial calculations revealed that better results were obtained if the TPC train times were corrected for start and stop delays, since the power per unit mass (which varied with train type) would significantly affect the start delay, in particular. The start delay for a number of different train configurations was examined to confirm the relationship between delay and power per ton.

The TPC simulations were completed for the balance of the fourteen segments, and exponents and run time constants were generated for each train and segment. It was necessary to reduce the locomotive power by the equivalent of the average power required to overcome the kinetic energy changes resulting from speed increases after speed restrictions. This modification eliminated the need to estimate the train delay involved in starting and stopping the train at the segment boundaries. The complexity of some of the speed restrictions (often with several occurring within a single train length) complicated the computation of the kinetic energy, and the associated train delay. In some segments, speed changes will require a substantial portion of the locomotive power, and will cause significant additional time delays. The time depends on train length, since train speed would not be increased until the full train cleared the speed restriction. In one case (MTLTOR), the additional track time caused by this speed change delay, for a train length of 6,524 feet, adds 25 minutes to the train run time (track time for operation at the track speed 100 per cent of the time is 396 minutes). Appendix C provides a summary of the train and track values, and some train details.

Using the exponential model and the track time with the additional delay caused by train length and speed changes, it was possible to compute a power-per-ton figure which would permit close approximation of the maximum track speed. The power-per-ton figure, in conjunction with train tons and locomotive axles, provided a target power per axle for each train. Some of the results are presented in Appendix D.

The projections vary to some extent with the power per ton used to develop them, and with train type. However, the projections provide a reasonable estimate of the maximum continuous axle power that might be used if economic and technical factors permitted. Axle power greater than the projections would provide little or no improvement in train speed. Appendix D presents only those cases identified as the limits for practical train configurations.

The target power values in Appendix D have been averaged to produce a simplified Table 4 illustrating the target values for each segment, by direction. Note that the target power for westward movement on the BICSWN segment matches that shown in Table 3 for the maximum value. This suggests that a locomotive overload capability for this segment direction would be of little value, and subsequent analysis confirms this to be the case. Locomotives on this segment are truly power-limited. The values of Table 4 for CALSTE (eastward), NBNVAN (both directions), STEGOL (both directions), and RPSVAN (westward) exceed the maximum values. A review of the train times shown in Appendix C for these segments reveals that train time is insensitive to axle power. For traffic in the eastward direction on the CALSTE segment, and for all traffic on the NBNVAN and STEGOL segments, increased axle power would provide little improvement in train time. This traffic represents 22 per cent of the total axle kilometers on the 14 segments investigated. The RPSVAN (eastward) movement represents 18 per cent of the total, and train time is relatively insensitive to axle power on this segment, as well. However, this results more from the substantial number of speed changes and severe speed restrictions on the many curves, than from the gradients. The maximum power value of 1,530 kilowatts (2,050 horsepower) shown in Table 3 indicates that higher-power locomotives would provide some benefit on this segment, although the benefit would be less than that for the remaining 60 per cent of the locomotive axle traffic.

3.2.1 Variability Within a Segment

Because the BICSWN segment was the shortest "average" segment being examined (the STEGOL segment has a 30 mph speed limit and steep grades), detailed evaluation of a number of factors was carried out for this segment. The effects of train meets and overtakes were examined using the STS computer program. To use the STS simulation effectively, it was necessary to compute the train delay at each siding, since some sidings have relatively steep grades. To reduce the

TABLE 4

MAXIMUM USABLE CONTINUOUS POWER PER AXLE

Segment	Westward kW	Westward hp	Eastward kW	Eastward hp
ARTEDM	1190	(1595)	1485	(1990)
KINTOR	1275	(1710)	1210	(1620)
MOJWAL	1105	(1480)	1435	(1925)
SPYSAS	1260	(1690)	1350	(1810)
MTLTOR	1245	(1670)	1285	(1725)
BICSWN	1530	(2050)	1360	(1825)
EDMBIC	1200	(1610)	1245	(1670)
IGNKEN	1285	(1725)	1180	(1580)
CALSTE	1080	(1450)	1250	(1675)
GLDMTL	1250	(1675)	1205	(1615)
NBNVAN†	2940	(3940)*	11890	(15940)
STEGOL†	1596275	(2139780)*	1045	(1400)*
SUXWGT	1165	(1560)	1120	(1500)
RPSVAN	1890	(2535)*	1115	(1495)
Average*	1235**		1272**	

† The very high predicted values reflect situations where train times are very insensitive to increasing power. These values are artifacts of the model used in the analysis. Warranted power levels would in fact be very low.

** Segment directions with values exceeding the maximums identified in Table 3 have been left out of the average.

number of train meets, the possibility of longer sidings, and hence longer trains (within the limits imposed by allowable locomotive drawbar forces), was examined.

In addition, the effects of different train complements, and the effect of using higher adhesion values (μ = 0.40, assuming that it could be achieved) were examined. Thus, a broad range of power:weight ratios was examined for this segment.

The data for the section has been collected into Table 5.

TABLE 5

VARIABILITY WITHIN A SEGMENT -- BICSWN

Train Type	No.	Axles	Train Tons	hp/ton	Cars	Predicted Maximum hp/Axle	Required Adhesion
Box West							
0.52%*	025	4	4,741	1.0968	62	0.2522	2,121.57
	123	4	4,667	1.1142	61	0.2483	2,096.06
	124	4	4,001	1.2997	52	0.2129	1,837.40
Bulk West							
0.52%	030	8	15,396	0.6755	126	0.4101	2,527.68
	155	8	14,916	0.6972	122	0.3973	2,472.22
	028	16	19,242	1.0810	156	0.2562	2,007.05
	026	12	14,319	1.0895	116	0.2542	2,033.96
	154	16	18,642	1.1158	151	0.2482	1,964.03
	125	12	13,959	1.1176	113	0.2479	1,992.18
	126	12	12,639	1.2343	102	0.2244	1,841.15
	029	16	15,762	1.3196	127	0.2099	1,733.05
Bulk East							
0.49%	162	12	14,679	1.0627	119	0.2487	1,853.13
	163	12	12,999	1.2001	105	0.2202	1,783.58
TOFC East							
0.49%	027	4	5,081	1.0234	88	0.2739	2,371.52
	127	4	4;577	1.1361	79	0.2467	1,982.19
	128	4	3,457	1.5042	59	0.1863	1,732.92

* controlling grade

Table 5 provides the computed adhesion required to maintain 20 km/h on the zone controlling grade. The adhesion required to maintain 80 km/h (50 mph) is greater for this segment. Hence, variations of resistance with velocity for different train configurations should affect train time, and, therefore, the target axle power. The number of samples is not sufficient to refine the model, but an assumption that the target axle power varies as the square root of the controlling adhesion was applied. The resulting predictions are shown in Column 5 of Table 6.

TABLE 6

PREDICTION ERROR WITHIN A SEGMENT -- BICSWN

Train Type	No.	hp/ton A	Adhesion B	hp/axle (adh.)	% Error*	hp/axle (power)	% Error†	AxB
Box West	025	1.0968	0.2522	1,974.63	-6.93	1,976.01	-6.86	0.2766
	123	1.1142	0.2483	1,959.30	-6.52	1,960.52	-6.47	0.2767
	124	1.2997	0.2129	1,814.27	-1.26	1,815.23	-1.21	0.2767
Bulk East	303	0.6755	0.4101	2,518.02	-0.38	2,517.91	-0.39	0.2770
	155	0.6972	0.3973	2,478.41	0.25	2,478.42	0.25	0.2770
	028	1.0810	0.2562	1,990.23	-0.84	1,990.40	-0.83	0.2770
	026	1,0895	0.2542	1,982.45	-2.53	1,982.62	-2.52	0.2770
	154	1.1158	0.2482	1,958.91	-0.26	1,959.12	-0.25	0.2769
	125	1.1176	0.2479	1,957.73	-1.73	1,957.54	-1.74	0.2771
	126	1.2343	0.2244	1.862.62	1.17	1,862.70	1.17	0.2770
	029	1.3196	0.2099	1,801.44	3.95	1,801.49	3.95	0.2770
TOFC East	162	1.0627	0.2487	1,960.88	5.81	2,007.47	8.33	0.2643
	163	1.2001	0.2202	1,845.11	3.45	1,889.06	5.91	0.2643
TOFC East	027	1.0234	0.2739	2,057.83	-13.23	2,045.65	-13.74	0.2803
	127	1.1361	0.2467	1,952.98	-1.47	1,941.53	-2.05	0.2803
	128	1.5042	0.1863	1,697.15	-2.06	1,687.33	-2.63	0.2802

* Prediction based on an adjustment for the square root of adhesion variations.

† Prediction based on an adjustment for the square root of hp/ton variations.

This simple correction method introduces a maximum deviation of 4.0 per cent for the bulk trains moving west. This set includes two high-adhesion (0.40) cases, and hence has the widest variation of required adhesion. Applying the same criterion to the box car train running west introduces a maximum error of 4.9 per cent. It is evident that the higher resistance per unit mass requires a target power roughly 4.8 per cent greater than that predicted by the simple approximation. For the movement east, the prediction is 4.7 per cent high for bulk trains, and 5.5 per cent low for the TOFC trains.

For a specific axle power and locomotive unit weight, there must be a relationship between the power per unit mass and the adhesion figure used above. For the bulk train movement west, the product of the horsepower per ton (1,300 hp/axle) and the adhesion is 0.2770. Thus, the use of the square root of the ratio of power per unit mass may be used in place of the adhesion correction factor to provide a reasonable estimate of the axle power without the additional data and calculations required to identify the adhesion value. However, as illustrated in Table 6, an additional error of up to 2.5 per cent is introduced by the use of the power per unit mass values for this segment.

In summary:

- the axle power predictions for minimum run times vary with the adhesion requirement, roughly as shown in Figure 2
- the predicted axle power is affected by track characteristics, with the power requirement for movement east on the BICSWN segment approximately 5.1 per cent greater than for movement west
- the target axle power varies with train characteristics, with a variation of 6.7 per cent noted on the BICSWN segment
- the combination of track and train variations introduced a maximum combined error in the prediction of 6.7 per cent, using the bulk train west as a reference.

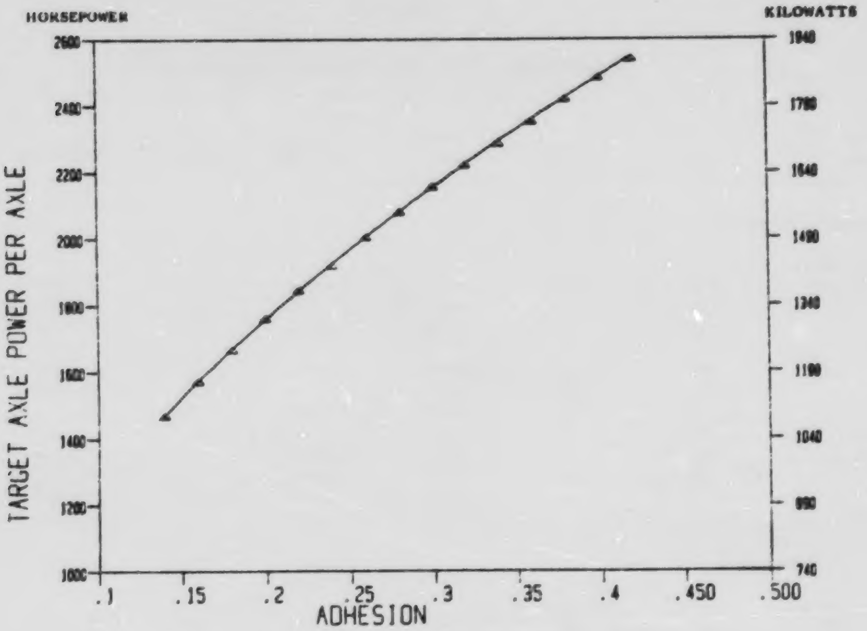

Figure 2 Estimated bound on axle power vs adhesion

3.2.2 Variability from Segment to Segment

Three segments -- EDMBIC, IGNKEN and CALSTE -- were evaluated in detail to determine the variability from segment to segment. Table 7 provides a summary of the computed data for these segments. More detailed analysis revealed that each segment had unique characteristics which had an impact on the axle power figures that were derived. For example, the higher track speed of the IGNKEN segment (65 mph versus 50 mph for the other two segments) resulted in a higher value for the maximum power (see Table 3). The zone controlling grade for the CALSTE (eastward) segment is substantially greater than the segment controlling grade, resulting in a low value for the maximum axle power within the segment.

The train time was relatively sensitive to the power per unit mass for traffic on the EDMBIC (westward), IGNKEN (eastward) and CALSTE (westward) segments. Because the type of train has some influence on the target axle power values, we might start by examining a single train type. The bulk train is common to the three segment directions. The EDMBIC (westward) segment predictions, based on both

TABLE 7

VARIABILITY BETWEEN SEGMENTS

Train Type	No.	Axles	Train Tons	hp/Ton	Cars	Adhesion	hp/axle
EDMBIC Segment							
Box West							
0.52%*	039	4	4741	1.0968	62	0.2522	1684.04
	129	4	4667	1.1176	61	0.2483	1674.00
	130	4	3779	1.3760	49	0.2011	1563.09
Bulk West							
0.52%	040	12	14319	1.0895	116	0.2542	1644.87
	131	12	13959	1.1176	113	0.2479	1633.95
	132	12	11919	1.3088	96	0.2116	1560.94
TOFC East							
0.49%	041	4	5081	1.0234	88	0.2739	1770.50
	133	4	4577	1.1361	79	0.2467	1720.72
	134	4	3289	1.5810	56	0.1772	1621.33
IGNKEN Segment							
Box West							
1.05%	042	10	5887	2.2083	75	0.2270	1711.52
Bulk West							
1.05%	164	24	15288	2.0408	121	0.2455	1738.03
Bulk East							
0.56%	043	12	13359	1.1678	108	0.2517	1563.70
	135	12	13119	1.1891	106	0.2472	1557.18
	136	12	10479	1.4887	84	0.1974	1511.19
TOFC East							
0.56%	044	4	4465	1.1646	77	0.2661	1842.26
	137	4	4129	1.2594	71	0.2460	1766.61
	138	4	2673	1.9454	45	0.1592	1487.97
CALSTE Segment							
Box West							
1.01%	139	10	6701	1.9400	86	0.2497	1459.43
	045	10	6183	2.1025	79	0.2304	1440.17
	140	10	5887	2.2083	75	0.2194	1432.21
Bulk West							
1.01%	142	22	14626	1.9554	116	0.2477	1448.91
	046	22	13546	2.1113	107	0.2294	1438.53
Bulk East							
2.23%	165	24	7488	4.1667	56	0.2451	3125.41
TOFC East							
2.28%	141	20	6245	4.1633	100	0.2488	919.95
	047	20	5461	4.7610	86	0.2175	981.24

* Controlling grade

adhesion and power per unit mass, are high by roughly 20 per cent (see Table 8). The predictions for the IGNKEN (eastward) segment are high by the same amount. However, for the CALSTE (westward) segment, there is a marked difference between the two predictions, with the power per unit mass providing an accurate prediction.

Examining the other bulk train traffic, the two predictions span the IGNKEN (westward) values, and are significantly in error on the CALSTE (eastward) movement. The other train types show similar prediction problems.

It appears that the predictions are acceptable only within a specific segment direction. Table 9 presents predictions based on individual segments. It must be concluded that a target power per axle must be identified for each segment direction. The variation with train type does not introduce sufficient error to justify the additional computations required to identify a target value for each train type. Also, the additional computation to identify the adhesion required is unnecessary.

3.3 Maximum Bounds for Continuous Power Ratings

Two sets of design bounds have been identified in the analysis -- the maximum or peak overload value, typically based on adhesion and controlling grade, and the continuous value, based on train time versus track time. A peak short-term overload rating of 2,460 hp was previously identified as meeting the requirements of 90 per cent of the traffic (Figure 1).

A similar analysis of target axle power against annual locomotive axle distance generated the results shown in Figure 3.

An axle power of 1,540 hp would be usable on all segments except MOJWAL, CALSTE, NBNVAN, STEGOL, SUXWHT (eastward), and RPSVAN (eastward). The traffic on these segments represents 40.3 per cent of the total axle distance. However, the target axle power values for SUXWHT (eastward) and RPSVAN (eastward) are only slightly less than 1,540 hp (3.8 per cent maximum), and hence a target axle power of 1,540 hp would essentially be usable for 67.5 per cent of the traffic.

TABLE 8

PREDICTION ERROR, SEGMENT TO SEGMENT

Train Type	No.	hp/Ton (A)	Adhesion (B)	hp/Axle (adh.)	Per Cent Error	hp/Axle (power)	Per Cent Error	(A)x(B)
EDMBIC Segment								
Box West	039	1.0968	0.2522	1974.63	17.26	1976.01	17.34	0.2766
	129	1.1176	0.2483	1959.30	17.04	1957.54	16.94	0.2775
	130	1.3760	0.2011	1763.27	12.81	1764.19	12.87	0.2767
Bulk West	040	1.0895	0.2542	1982.45	20.52	1982.62	20.53	0.2770
	131	1.1176	0.2479	1957.73	19.82	1957.54	19.80	0.2771
	132	1.3088	0.2116	1808.72	15.87	1808.91	15.89	0.2769
TOFC East	014	1.0234	0.2739	2057.83	16.23	2045.65	15.54	0.2803
	133	1.1361	0.2467	1952.98	13.50	1941.53	12.83	0.2803
	134	1.5810	0.1772	1655.18	2.09	1645.84	1.51	0.2802
IGNKEN Segment								
Box West	042	2.2083	0.2270	1873.38	9.46	1392.59	-18.63	0.5013
Bulk West	164	2.0408	0.2455	1948.23	12.09	1448.62	-16.65	0.5010
Bulk East	043	1.1678	0.2517	1972.67	26.15	1915.00	22.47	0.2939
	135	1.1891	0.2472	1954.96	25.54	1897.77	21.87	0.2939
	136	1.4887	0.1974	1746.98	15.60	1696.09	12.24	0.2939
TOFC East	044	1.1646	0.2661	2028.32	10.10	1917.63	4.09	0.3099
	137	1.2594	0.2460	1950.21	10.39	1844.05	4.38	0.3098
	138	1.9454	0.1592	1568.86	5.44	1483.71	-0.29	0.3097
CALSTE Segment								
Box West	139	1.9400	0.2497	1964.82	34.63	1485.77	1.81	0.4844
	045	2.1025	0.2304	1887.36	31.05	1427.20	-0.90	0.4844
	140	2.2083	0.2194	1841.75	28.60	1392.59	-2.77	0.4845
Bulk West	142	1.9554	0.2477	1956.94	35.06	1479.91	2.14	0.4844
	046	2.1113	0.2294	1883.26	30.92	1424.22	-0.99	0.4843
Bulk East	165	4.1667	0.2451	1946.64	-37.72	1013.81	-67.56	1.0213
TOFC East	141	4.1633	0.2488	1961.28	113.19	1014.23	10.25	1.0358
	047	4.7610	0.2175	1833.76	86.88	948.43	-3.34	1.0355

TABLE 9

PREDICTION ERROR, SEGMENT TO SEGMENT

Train Type	No.	hp/Ton (A)	Adhesion (B)	hp/Axle (adh.)	Per Cent Error	hp/Axle (power)	Per Cent Error	(A)x(B)
EDMBIC Segment								
Box West 1641*	039	1.0968	0.2522	1468.20	-2.13	1649.36	-2.06	0.2766
	129	1.1176	0.2483	1635.41	-2.31	1633.94	-2.39	0.2775
	130	1.3760	0.2011	1471.79	-5.84	1472.55	-5.79	0.2767
Bulk West 1641	040	1.0895	0.2542	1654.73	0.60	1654.87	0.61	0.2770
	131	1.1176	0.2479	1634.09	0.01	1633.94	0.00	0.2771
	132	1.3088	0.2116	1509.72	-3.28	1509.72	-3.28	0.2769
TOFC East 1641	014	1.0234	0.2739	1717.65	-2.99	1707.48	-3.56	0.2803
	133	1.1361	0.2467	1630.13	-5.26	1620.58	-5.82	0.2803
	134	1.5810	0.1772	1381.56	-14.79	1373.77	-15.27	0.2802
IGNKEN Segment								
Box West 1754* 2359†	042	2.2083	0.2270	1671.37	-2.35	1670.97	-2.37	0.5013
Bulk West 1754 2359	164	2.0408	0.2455	1738.14	0.01	1738.19	0.01	0.5010
Bulk East 1566*	043	1.1678	0.2517	1571.32	0.49	1571.16	0.48	0.2939
1613†	135	1.1891	0.2472	1557.21	0.00	1557.02	-0.01	0.2939
	136	1.4887	0.1974	1391.54	-7.92	1391.56	-7.92	0.2939
TOFC East 1566	044	1.1646	0.2661	1615.65	-12.30	1573.32	-14.60	0.3099
1613	137	1.2594	0.2460	1553.42	-12.07	1512.94	-14.36	0.3098
	138	1.9454	0.1592	1249.66	-16.02	1217.31	-18.19	0.3097
CALSTE Segment								
Box West 1456*	139	1.9400	0.2497	1455.13	-0.29	1454.79	-0.32	0.4844
1925†	045	2.1025	0.2304	1397.76	-2.94	1397.44	-2.97	0.4844
	140	2.2083	0.2194	1363.99	-4.76	1363.55	-4.79	0.4845
Bulk West 1456	142	1.9554	0.2477	1449.29	0.03	1449.05	0.01	0.4844
1925	046	2.1113	0.2294	1394.72	-3.05	1394.52	-3.06	0.4843
Bulk East 922* 1783†	165	4.1667	0.2451	912.92	-70.79	919.44	-70.58	1.0213
TOFC East 922	141	4.1633	0.2488	919.78	-0.02	919.82	-0.01	1.0358
1783	047	4.7610	0.2175	859.98	-12.36	860.15	-12.34	1.0355

* Base hp/axle for adhesion criterion.

† Base hp/axle for hp/ton criterion.

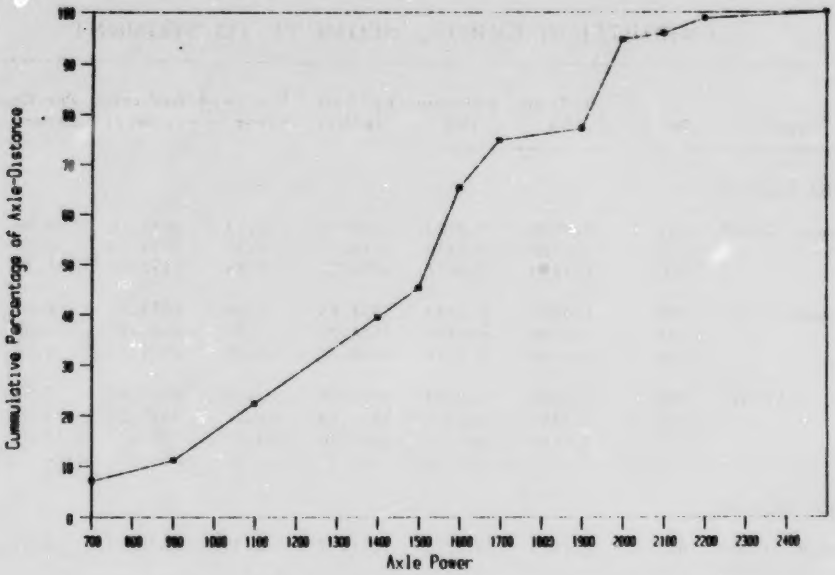

Figure 3 Maximum usable power estimates on a minimum-run-time criterion

Increasing the target axle power to 1,650 hp would reduce the percentage of traffic to 49.3. A further increase to 1,900 hp would reduce the percentage of traffic to 25.2. Thus, it appears that a target axle power of 1,540 to 1,650 hp would be a reasonable maximum. With the peak power requirement set to 2,460 hp, an overload capability (less than four minutes duration) of 50 to 60 per cent is indicated. However, it should be noted that the continuous power values were established on the basis of only two data points, with estimated values for most segments determined by extrapolation. Also, as discussed in the next section, an economic evaluation has not been performed to determine the "optimum" value.

The law of diminishing returns can be expected to prevail (the fact that the prediction model is an exponential one supports this expectation). Thus, one might achieve a significant proportion of the time savings with a lesser increase in power.

Also, the utilization of power decreases as greater power is made available. This is illustrated in the duty cycle experienced for the two power levels in the TPC simulations made. Figures 4(a) to 4(d)

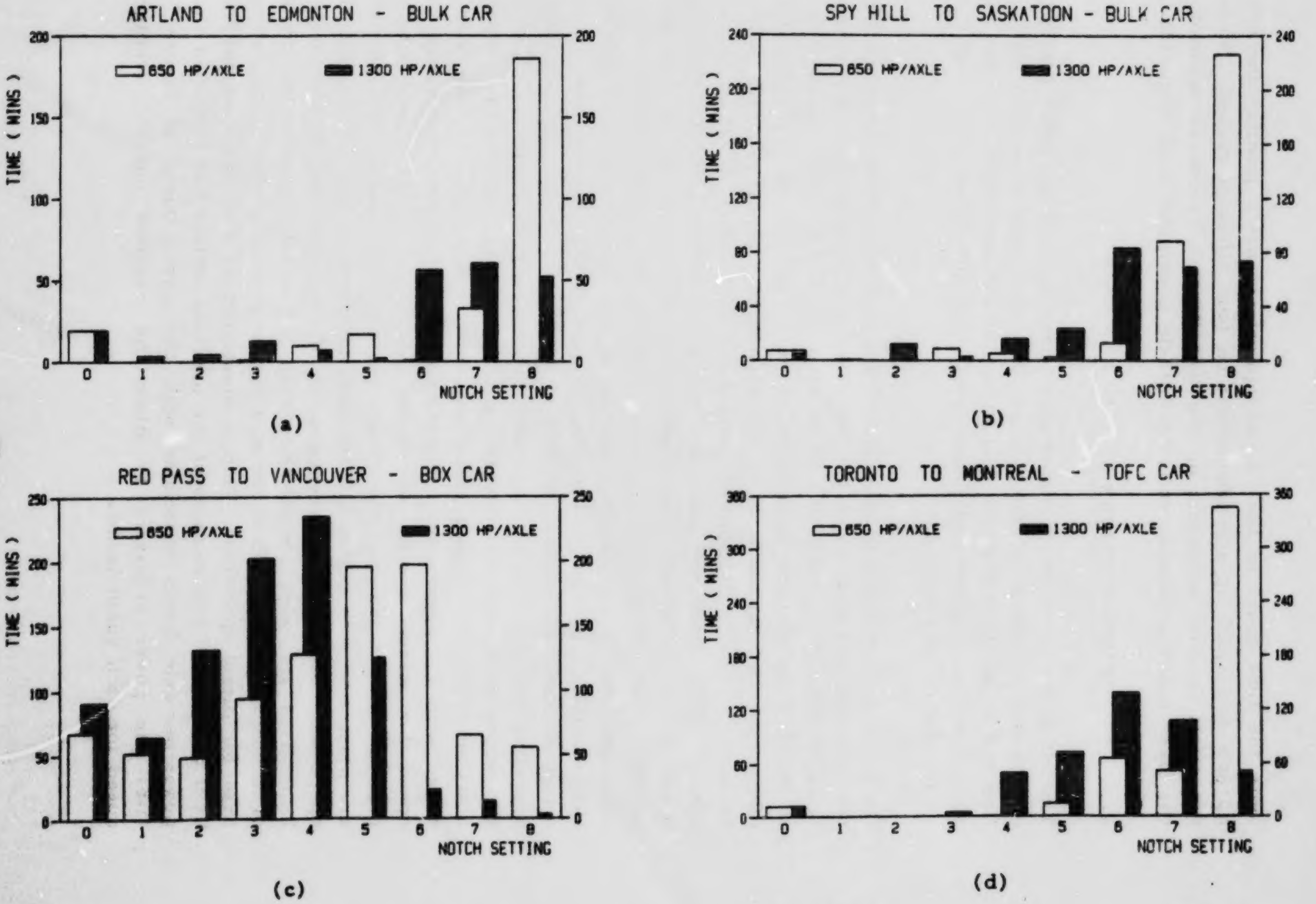

(a)

(b)

(c)

(d)

Figure 4 Time spent in "diesel-equivalent" notch setting

show the time spent in the "diesel-equivalent" notch position for 650 hp/axle and 1,300 hp/axle simulations on four different routes. While the effect is most noticeable on the Red Pass to Vancouver segment, the lower power utilization at 1,300 hp/axle is evident on all segments.

4. THE IMPLICATIONS OF THE ANALYSIS

The identification of the minimum-cost power level is beyond the scope of this study. However, the relevant cost trade-offs have been identified and it is clear that the cost structure under electric operation is such that the minimum-cost power level would be higher than it is for diesel-electric locomotives.

Once the power-conditioning unit and traction motors are designed for the current-carrying capacity necessary to achieve the low-speed tractive effort, the marginal cost of attaining power levels higher than those of diesel-electric locomotives is very low. However, there are other cost factors which must be considered. Energy, track maintenance and power distribution costs would increase. Offsetting these, track, rolling stock and locomotive utilization would increase, thereby lowering the investment costs associated with these items. If one assumes that the present operation reflects an overall minimum cost situation, then a significant reduction in the marginal cost of two of the variables (energy and motive power), while leaving the other marginal costs unchanged, must lead to a shift in the minimum-cost operating point. This is illustrated conceptually in Figure 5. Curve C2, which decreases with increasing train speeds, includes the capital costs of track and rolling stock and reflects the value of time associated with the commodity. These costs have the same sensitivity to speed for either electric or diesel operation. Those costs which increase with higher speeds (track maintenance, energy and power) are illustrated with curve CIE for electric operation and CID for diesel operation. Since the incremental costs of electricity and higher-power locomotives are lower for electrics than for diesel-electrics, the point of minimum total cost will occur at a higher speed for electric operation than for diesel operation. This is illustrated by the total cost curves TCD and TCE. The analysis of the previous section has identified the power-per-axle levels associated with the upper bound of Figure 5 (i.e. the power necessary to attain the maximum possible average speed for each subdivision).

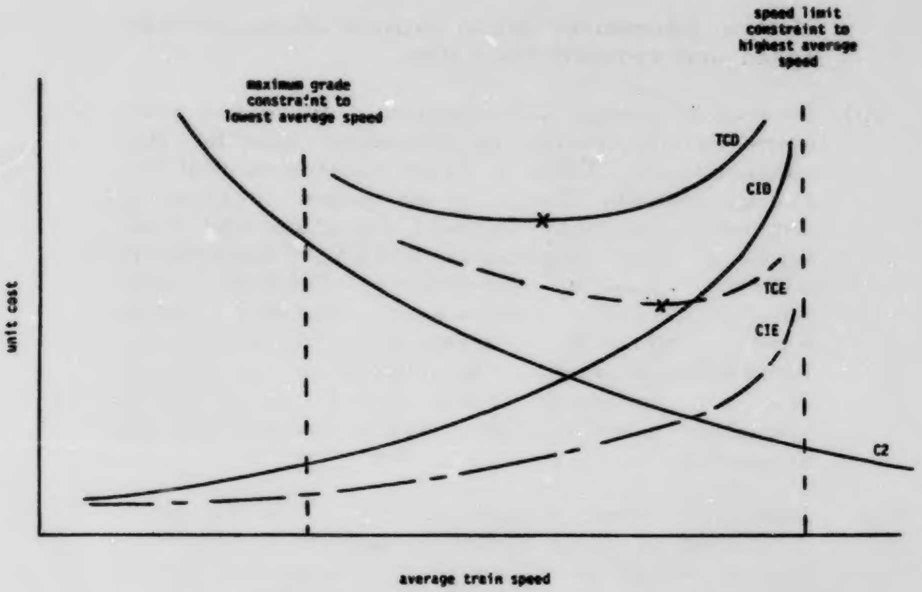

TCD = total locomotive cost with diesel operation
TCE = total locomotive cost with electric operation
CID = incremental maintenance, power and energy costs (diesel)
CIE = incremental maintenance, power and energy costs (electric)
C2 = cost of rolling stock and fixed infrastructure

Figure 5 Conceptual representation of optimal train speed

An "optimal" power level has not been determined. However, on the basis of the sampling of performance effects, the following observations can be made regarding each major effect:

(a) Increased speed. In all of the cases investigated, increasing the axle power to values greater than those currently available on diesel-electric six-axle locomotives would increase train speed and reduce train time. For seven per cent (see Figure 1) of the traffic (eastward movement on the NBNVAN segment), four-axle diesel-electric locomotives would have axle power in excess of the maximum that could be used. The four-axle diesel-electric locomotive, operating at a maximum adhesion of 0.19, would have excess power capacity for 11 per cent of the traffic. Thus, for 89 to 93 per cent of the traffic, higher axle power values available with electric locomotives would provide increased train speed and reduced train time.

(b) Increased energy consumption. Increased train speed would result in increased specific fuel consumption. Table 2 again illustrates that the energy penalty for a given speed increase is dependent on both segment direction and train type. For segments SPYSAS (eastward), BICSWN, EDMBIC (westward), IGNKEN (eastward), CALSTE (westward), GLDMTL (eastward), STEGOL (eastward), SUXWHT and RPSVAN (eastward), the penalty is not severe, and the increased train speed could prove attractive when evaluated for a specific service or market.

(c) Increased power supply costs. This factor is discussed in more detail in Section 9.4. Substation design is based on the combined probability of multiple train loads (i.e. power times probability). Since probability is inversely proportional to speed, the impact of power increases on substation costs would be small for the "low-speed train on steep gradient" case and significant for the "high-speed train on level track" case. In either case, the impact would be less than that of a change in kVA brought about by displacement factor changes.

(d) Increased line capacity. As axle power increases, the train time for different types of trains, and for different power per unit mass values, decreases and becomes more uniform. The uniformity in train speed significantly reduces train delays caused by train interference. The reduction in train time and the more uniform operation increases the effective track capacity. This impact on rail line capacity was a major factor in the decisions to electify some Russian and Western European railways. Capacity benefits also provided the impetus for CP Rail's 1972 evaluation of electrification for its main line through the Rockies west of Calgary. The value of being able to delay a major expansion program is signficant, both in direct monetary savings and also in terms of reducing the risk associated with uncertain traffic forecasts. The maximum potential improvements in line capacity that might be attributed to electification were assessed in the National

Impacts Study[4] for the western main lines as shown in Figure 6. The Prairie lines had the greatest potential, and the steep-gradient sections of the mountain lines the next highest. Whether these potentials can be realized is as yet uncertain, and the short-term disbenefits of service disruption during installation have not been quantified.

(e) In a number of segments, train dispatch trailing tons is established on the basis of power (speed) requirements, and not on the basis of adhesion on the controlling grade. On these segments, increased axle power would permit a reduction in the number of locomotives required, with consequent savings in maintenance and labour costs.

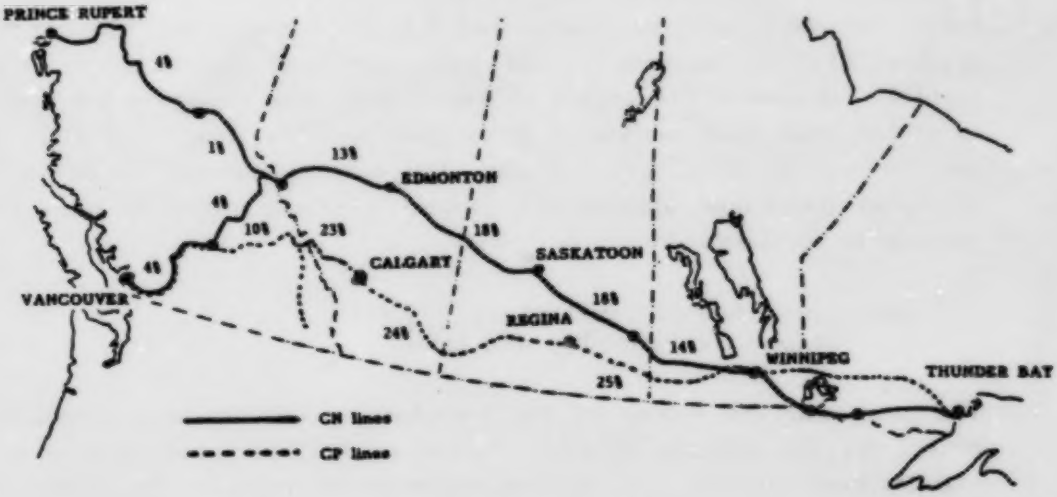

Source: National Impacts Study, op. cit.

Figure 6 Estimates of maximum potential capacity increase (in per cent) for western line segments

The provision of a short-term overload capability involves a different set of trade-offs. As long as track conditions are such that peak locomotive power is required for relatively short periods, the overload capacity can be useful. However, the electronic equipment used to control the electric current will not have an overload capability, and hence must be designed to handle the peak current values on a continuous basis. This will make the locomotive more expensive; a cost-benefit analysis will be required to determine if these changes are justified. An optimal value was not determined, but the following observations are offered:

---

[4] Empey, W.F., et al., op. cit.

(a) Overload Versus Train Performance.

Identification of the benefits of an overload capacity in an electric locomotive requires a fairly elaborate analysis. This analysis was completed for the BICSWN segment. On this segment, the controlling grades are modest but of substantial length, so that the locomotive would be required to operate in an overload condition for long periods of time. Consequently, locomotive overload capability would contribute little to train performance on this segment. On the other hand, the short but steep adverse grades and the many restrictive speed limits of the RPSVAN segment would make overload capability a useful feature. However, the degree of useful overload capacity could not be identified from this analysis. It is clear that overload capability will not be as important in Canadian freight applications as it is in European passenger applications (where overload power is used frequently to accelerate to cruise speeds).

(b) The Effect of Overload on Locomotive Reliability and Life.

The peak current values in the transformer and traction motors are limited by the heating effects. These electric machines have a substantial heat capacity. If the locomotive is not required to operate for long periods at full load, the machine components would be relatively cool, so that an overload situation could be tolerated for some time. Also, degradation of electrical insulation is a function of time and temperature. Operation for long periods at full load or in overload conditions will reduce the insulation life. Clearly, the life of some components in the traction system will be reduced by operation under overload conditions. The provision of overload capability will involve consideration of a complex series of design factors, and will affect both component reliability and component life.

(c) Overload Versus Efficiency

Inspection of a traction system efficiency curve (such as that shown in Figure 14(a)) reveals that there are a number of fixed losses which result in a low efficiency value at light loads. As the motor load increases, the motor efficiency rises, to a peak value of approximately 85 per cent at 80 to 100 per cent of full load. As the motor goes into the overload condition, electrical resistance losses become increasingly important, and the motor efficiency again drops off.

To achieve maximum energy efficiency, a locomotive should operate at a high load factor, using overload where necessary, rather than operate at a lower load factor without overload.

The efficiency of electronic control circuits complicates this conclusion to some extent. Control circuit efficiency depends on the specific power-conditioning unit and its characteristics. Various power-conditioning systems are discussed later in this report.

5. NUMBER OF AXLES PER UNIT

The 3,000 hp, six-axle locomotive is the principal power unit in North American mainline service. However, 3,000 hp on four axles is used in areas where adhesion is not a limiting factor, and a lesser number of 2,000 hp (and lower) power units are utilized in mixed freight service to more closely match available power to train tonnages. Standardization of motive power to reduce maintenance inventories and manpower training is an important factor in present motive power decisions.

A large proportion of the operations in western Canada involves very uniform and predictable train sizes -- fully loaded 100-ton bulk cars with 100 to 110 cars per train. In parts of Russia where similar bulk movements are handled with electric traction, the trend in motive power is to much larger unit powers. The USSR developed the 8,000 hp VL80R eight-axle locomotive in the last decade[5] and are now building a prototype 16,000 hp, twelve-axle locomotive using ac traction motors.[6] The economies of scale for such married-pair, six-axle units are restricted to the front-end transformer and rectifier equipment.

---

[5] Nekrasove, Potapov, Kabenin, "What Should Electric Locomotives be for the New Baikal-Amur Main Line," Elektrische and Teplovoznaya Tyaga, No. 5, May 1975, pp. 22-41.

Electric operations would introduce a different set of cost sensitivities to the motive power decision. Under diesel operation, the initial purchase cost and maintenance costs associated with traction motors are reduced by applying the 3,000 horsepower available power to four axles rather than six when adhesion is not a constraint. Under electric operation, where available power is not a constraint, economies of scale would be realized through purchase of a single unit with 50 per cent more power on six axles rather than a four-axle unit. The limiting factor in electric operation is the flexibility lost with the increasing size of individual power units. In areas of mixed freight operation, it may be desirable to forego some economies of scale and the maintenance advantages of unit standardization and standardize instead on the power per axle and the type of power-conditioning equipment used, while keeping both four- and six-axle units available. A mix of four- and six-axle units of the same power per axle would permit two-axle multiples of axle power (4-6-8-10-12-14-16 ... etc.), whereas six-axle units alone would permit only six-axle multiples (6-12-18 ... etc.). All else being equal, the higher the power per axle, the greater the (adverse) impact on flexibility.

In addition to flexibility and economy of scale considerations, the question concerning the number of axles per locomotive unit depends on the following technical factors:

- tractive effort and power required for trains
- power transmitted through a locomotive pantograph
- locomotive weight considerations
- locomotive reliability considerations.

---

[6] Personal discussions with the Electric Traction Department, Stromberg AB, Finland.

5.1 Adhesion Requirements

An analysis of the trains used for the TPC calculations (see Appendix B), together with projected traffic levels, provides some information concerning the importance of four- or six-axle units. It should be noted that train length and adhesion requirements were used to size the trains used in the calculations, and that the powered axles assigned to each train were in multiples of two.

For 10 per cent of the traffic, a single four-axle locomotive would be sufficient to haul the train, while a single six-axle locomotive would be sufficient for only 11 per cent of the traffic. With the criteria used to size the trains in this study, 22 per cent of the axle-distance would be generated by six-axle units, and 78 per cent by four-axle units. However, with minor modifications to train length, many trains would be hauled with equal effectiveness by either four- or six-axle locomotives. For 62 per cent of the traffic, there would be no significant advantage in having four- or six-axle locomotives for adhesion purposes, assuming that either unit could achieve the same adhesion value.

To examine the merits of an eight-axle locomotive, it was assumed that it could be used (without significant waste of its capability) whenever more than six axles were required for the train, except when the multiple number of axles differed by more than two (e.g. 8, 14, 16, 18, 22, 24, 26, 30 and 32 axles were acceptable, but not 12, 20 or 28 axles). An eight-axle locomotive, under these constraints, could haul 63 per cent of the traffic.

5.2 Power Transmitted Through a Locomotive Pantograph

A locomotive pantograph must maintain contact between the carbon contact strips of the pantograph and the overhead contact wire, with a minimum loss of contact from wire bounce, etc. Freight locomotive speeds are not considered high, and the identified track speed limits indicate that fairly heavy pantographs could be used. However, if multiple locomotives with individual pantographs are to be used, a minimum separation distance between each pair of pantographs must be maintained. This separation is dictated by the dynamic interactions between the pantographs and the contact wire. To minimize the required separation for the shorter four-axle locomotive, the pantograph must be as light as possible (i.e. a Faiveley type). As the locomotive length increases, the pantograph weight could be increased within limits, and use of additional contact strips would be possible.[7]

Typically, a Faiveley pantograph carries two contact strips, with a total current rating of 200 amperes if long life is required. A higher current rating (up to 200 amperes per contact strip) can be tolerated if reduced wear life is acceptable.

For a 50 kV nominal supply voltage, the locomotive should be able to produce full power at an actual supply voltage of 40 kV. Thus, a Faiveley pantograph could be rated at 8,000 kVA, or up to 16,000 kVA if reduced wear life is acceptable (as in overload).

The efficiency and power factor values for the locomotive will reduce the traction power to 6,480 kW continuous (efficiency x power factor = 0.81), or 8,686 hp. Thus, the Faiveley pantograph would easily meet the power requirements of a four-axle locomotive, and could meet the power requirements of a six-axle with a slight (probably negligible) degradation in wear life. For an eight-axle locomotive, a heavier pantograph assembly would be required, with at least three contact strips. However, the additional distance between pantographs for multiple units would help the contact dynamics situation.

The pantograph power capacity does not appear to be a constraint on the number of axles with a nominal 50 kV supply.

5.3 Locomotive Weight Considerations

With current technology, a 1,300 hp European locomotive, such as the ASEA RC-4,[8] will have an axle load of 21.5 tons per axle. Increasing the structural strength to meet North American standards has been accomplished without exceeding North American axle load limits, as with the Amtrak AEM-7. Discussions with manufacturers indicate that an electric locomotive with 6,160 to 6,560 hp on four axles could be built to North American standards if suitable traction motors could be obtained. The GM 10B electric locomotive, with a diesel rating of 10,000 hp, produces approximately 8,900 traction hp for six axles. Ballasting would be necessary to provide the required axle loads with six- or eight-axle units.

---

[7] Carbon Brushes and Electrical Machines, Morganite Electrical Carbon Limited, p. 271.

[8] Pamphlet 22-107E,, ASEA.

5.4 Reliability Considerations

Unit reliability will decrease as the number of components increases. Thus, an eight-axle locomotive would have a higher reliability than two four-axle locomotives providing the same tractive capacity. However, the impact of a unit failure on trains using a single locomotive are sufficiently severe that North American railways will rarely dispatch a train with less than two locomotives. A single eight-axle locomotive could handle 21 per cent of the traffic, as opposed to 10 to 11 per cent with four or six axles. This relatively high percentage of possible single locomotive trains suggests that the railways could favour four- or six-axle locomotives for "power security" reasons. A detailed cost-benefit analysis will be required if the concept of eight-axle locomotives is to be "sold" to the railways.

6. CONTROL PHILOSOPHY

Several options for locomotive power control are available. For example, acceleration to track speed could employ the maximum power permitted by the locomotive adhesion. Alternatively, the acceleration could be achieved using reduced power values.

The use of the maximum power permitted by the locomotive adhesion, including the use of overload ratings when appropriate, would result in the minimum train time -- the highest average train speed. Also, at low speed (e.g. less than 20 km/h), the locomotive power demand would be substantially below the continuous full power rating of a locomotive. For a constant tractive effort, the power demand increases proportionally with locomotive speed. Since the fixed plant equipment is designed for loads substantially greater than the low speed power demand, and the peak electrical demand is likely to be established by power requirements for operation at higher speeds, there should be no financial penalty in using the maximum tractive effort permitted by adhesion at low speeds.

However, continued operation at full tractive effort (as set by the available adhesion) will result in high electrical power demands as the locomotive speed increases. This operational philosophy may require increased electrical capacity in the fixed plant, and result in increased electric demand charges associated with energy use. Consequently, limiting the power demand of a locomotive at higher track speeds can result in substantial financial savings. These savings must be traded off against some increase in train time. The trade-off will be segment- and train-dependent. However, the simple model of train time, developed earlier in this report, can provide an indication of the significance of this trade-off.

Consideration of the control philosophy also affects other cost elements. If a number of trains are on an electrical segment simultaneously, there is the possibility of a high peak system demand created by simultaneous high power demands from several trains. A central control capability (either by radio link to the engineman, or carrier link to on-board control equipment) could substantially reduce peak system demands with a relatively slight impact on train performance. On most terrain types, peak locomotive power demand would be of relatively short duration. A reduction in power supplied to locomotives in non-critical areas of the segment would have little impact on train speed, and would often go unnoticed by train personnel. This ability to limit peak system demand would result in lower fixed plant costs and in lower electric demand charges. Such flexibility in load control could be used to obtain more advantageous electric rates, since the ability to reduce electric demand on the utility at critical times can be advantageous to the electric utility (load shedding and peak shaving).

The South African Railways reduced their peak power (and thus the demand charge) on their Sishen-Saldanha line from 53 MW to 42 MW while increasing the round trip performance (presumably cycle time) by only 1.3 per cent.[9] This was done by a combination of selective power restrictions, speed limits and departure delays on their scheduled operation. A demand monitoring system, which forecasts demand levels for each demand integrating period (10 to 30 minutes) and alerts the dispatcher if the target peak is to be exceeded, allows an immediate response to unscheduled operations.

7. GEAR RATIO CONSTRAINTS[10]

A specific traction motor can produce a specific full-load torque and a specific full-load power. These full-load values may be exceeded on a short-term basis. However, the overload capacity of a traction motor depends on motor and supply system details. The maximum values of torque and power do not necessarily occur at the same motor speed. The gear and wheel system translates the torque into a tractive effort, and the power into tractive power. Typically, the gear box reduces the motor rpm substantially, to a traction wheel rpm, while simultaneously increasing, by the same factor, the motor torque to an axle torque. The tractive effort is related to the axle torque simply by the traction wheel radius, or diameter. Except for a small efficiency loss from friction in the gears and bearings, the traction motor output power becomes the tractive power unless wheel slip occurs.

The following statements relate the various torques, tractive effort and power:

(1) AXLE TORQUE = MOTOR TORQUE x GEAR RATIO - GEAR TORQUE LOSS

(2) AXLE POWER = MOTOR OUTPUT POWER - GEAR LOSS

---

[9] A. Daniels, W.D. Weiss, "Design of Electrification for Heavy-Haul Railways: Its Contribution to Increased Tonnages," 2nd Heavy-Haul Conference, September 1982.

[10] Based on information contained in: Earle Buckingham, Manual of Gear Design, Section 2.

$$(3)\quad \text{TRACTION FORCE} = \frac{\text{AXLE TORQUE}}{\text{WHEEL RADIUS}} - \text{BEARING LOSS}$$

$$(4)\quad \text{TRACTION POWER} = \text{AXLE POWER} - \text{SLIP LOSS} - \text{BEARING LOSS}$$

$$(5)\quad \text{AXLE RPM} = \frac{\text{MOTOR RPM}}{\text{GEAR RATIO}}$$

$$(6)\quad \text{MOTOR POWER} = \text{MOTOR TORQUE} \times \text{MOTOR RPM}$$

From (1) and (3), the tractive force that a given traction motor can deliver is directly proportional to the gear ratio and inversely proportional to the wheel radius, if wheel slip does not occur. However, as the gear ratio is increased, the motor rpm must increase to provide the same track speed. Thus, the maximum motor rpm, the gear ratio, and the wheel diameter will establish the maximum track speed of the locomotive.

As an example, the electric locomotives for the BCR Tumbler Ridge unit coal train operation are designed for a top speed of 90 km/h (56 mph).[11] The selected gear ratio requires an adhesion of 28 per cent to fully utilize the continuous traction motor torque available at start-up. Since the allowable track speed on this line is only 56 km/h (35 mph), the possibility of using an even higher gear ratio to further increase the tractive force (assuming the required adhesion is available) should be investigated.

Gear design requires that the individual teeth have sufficient strength to withstand the dynamic loading as the gear teeth mesh and as track forces are transmitted through the drive assembly. The repetitive nature of this loading requires that the design be adequate to withstand fatigue effects. In addition, the tooth surface must tolerate the sliding contact as the teeth mesh, with sufficient resistance to surface wear to provide a reasonable gear set life. Surface wear will increase tooth clearances and reduce the structural strength of the tooth, increasing the probability of structural failure under dynamic loading.

---

[11] Proposal No. DDL 1214, "Technical Specifications of Tumbler Ridge Locomotives," July 8, 1982.

A high gear ratio requires a relatively small gear, with few teeth, on the traction motor shaft, and a relatively large gear on the locomotive axle. The traction wheel diameter limits the diameter of the gear mounted on the axle. Clearance between the rail head and the gear housing is essential if the locomotive is to traverse switches and cross-overs without damaging the gear housing. Additional clearance is required if rocks and other obstructions, which might fall on the track, are to be cleared by locomotive structural elements other than the gear housing.

The outside diameter of a standard cut gear is (N+2)/P, where N is the number of teeth in the gear, and P is the diametral pitch (the ratio of the number of teeth to the number of inches in the pitch diameter). Thus, a 77-tooth gear having a 2.25 diametral pitch will have an outside diameter of 35.111 inches. Allowing 5/16 inch for gear clearance and enclosure thickness, the diameter of the gear housing becomes 35.736 inches. A fully worn 42-in wheel (39 inch diameter) provides a clearance between the gear case and the rail head of only 1.632 inches. Anything less than this would not be considered adequate.

To improve wear characteristics, it is desirable that the number of teeth on each gear be an odd number. The next larger gear (79 teeth) would reduce the clearance to 1.188 inches.

The pinion gear, of small diameter, will have a relatively small number of teeth. Because each tooth will engage more frequently to carry the load, the wear and fatigue criteria for the pinion gear are more critical. Again, it is desirable to use an odd number of teeth in the pinion. On the Tumbler Ridge locomotive, a 17-tooth pinion was used to obtain the desired gear ratio for a 90 km/h maximum speed, resulting in a root diameter of 6.527 inches. Reducing the pinion to 15 teeth would reduce the root diameter to 5.638 inches, and would result in additional difficulties in mounting the pinion on the motor shaft. In addition, a 15-tooth pinion would have a wear life (in kilometres) only 48 per cent of that of a 17-tooth pinion, whereas a 19-tooth pinion would have a wear life twice as long as a 17-tooth pinion. However, using the 19-tooth pinion would increase the top speed to 101 km/h, and decrease the starting tractive effort by 10.5 per cent (μ = 25.1 per cent).

Increasing the wheel diameter without changing the gear ratio would modify the gear factors sufficiently to increase wear life by 10 per cent, while an increase in the diametral pitch, without changing the gear ratio or wheel diameter, would increase the wear life by 7.6 per cent. However, these modifications would necessitate a review of the structural strength of the gear teeth, since the wear criterion is the most critical constraint for modern designs.

An increase in gear face width can increase the contact wear area, thereby increasing wear life. However, an increased face width exacerbates problems of shaft deflection and hence uneven contact across the gear face. To accommodate higher gear loads imposed by more powerful traction motors, it has been necessary to install roller bearings on both the axle and the traction motor to reduce the bearing clearances, to more rigidly mount the bearings so as to maintain centre-to-centre distances, and to increase the stiffness of both the axle and the traction motor shaft to reduce deflection.

Increased face width also increases the problem of packaging the traction motor and gear assembly between the wheels of the locomotive.

An increase in gear quality can increase gear life. However, increased accuracy and improved surface finish would substantially increase the cost of gear production.

It is difficult to relate the wear life estimate (based on Buckingham) to the expected life in rail operation. Recorded instances of gear failure because of wear are relatively rare. Also, the wear life estimate increases exponentially with a reduction in load, and the wear life estimate varies with motor rpm under the same load. Thus, part-load operation would substantially increase the expected wear life of a gear set.

However, some conclusions may be drawn:

(1) As traction motor power output increases, the design and manufacture of the gear system will become more critical.

(2) For freight locomotives, wheel diameter and gear pinion life will limit the maximum tractive effort, and consequently maximum locomotive speed. The

Tumbler Ridge locomotives, which are geared to provide a top speed of 90 km/h, and to utilize an adhesion of 28 per cent (continuous, at start-up) would not likely experience a satisfactory gear life if used continuously, such as in pusher service on a steep grade. However, in applications where full-power operation is required for a relatively small portion of the run (such as on the Tumbler Ridge segment), the gear wear life is likely to be acceptable.

(3) Techniques are available to improve gear life through gear system modification. These techniques include an increase in traction wheel diameter, wider gear faces, and higher gear quality. In addition, a reduction in the transmission of shock loads through greater resiliency of the transmission system can insure an increase in gear life. However, even the combination of all techniques is unlikely to permit a doubling of the current power levels (735 kW) for a gear set meeting the between-wheel space constraints and required wear life criterion.

(4) A traction system designed to provide a maximum locomotive speed of not less than 110 km/h (65 mph) and a tractive effort capacity requiring an adhesion in excess of 30 per cent at North American axle loads, is unlikely to provide a satisfactory wear life.

8. ADHESION IMPLICATIONS

8.1 General Relationship Between Traction Coefficient and Wheel/Rail Wear

The relationship between tractive effort and wheel/rail wear is characterized by the wheel/rail contact stress and creepage (i.e. micro slip). Generally, tractive effort can be improved by increasing wheel load and/or creep, but this would increase wheel/rail wear due to the resulting higher contact stress and shear force respectively.

The relationship between wheel/rail contact load and wheel/rail wear is governed by the shakedown criteria. These criteria indicate whether a certain condition of contact stress and creep would cause plastic deformation (which constitutes failure according to the mechanical design convention) to a given type of wheel/rail steel.

Figure 7 shows the shakedown criteria compiled by Johnson.[12] Using the shakedown limit for line contact (top dotted line), a conservative estimate of the effect of a locomotive design on wheel/rail wear can be made. Below is a sample calculation:

> For a wheel load and diameter of 33 kips and 42 inches respectively, the Hertzian contact stress is about 138 kpsi. This stress is 1.84 times the yield strength of standard carbon rail (S = 75 kpsi) or 1.10 times that of heat-treated rail (S = 125 kpsi). The shakedown criteria in Figure 7 show that:
>
> a) For standard carbon rails, continuous plastic deformation would occur if the traction coefficient were greater than 20 per cent
>
> b) For heat-treated rails (which have a higher yield strength), continuous plastic deformation would not occur until the traction coefficient exceeds 50 per cent.
>
> The criteria further show that:
>
> a) To operate at a traction coefficient greater than 20 per cent on standard carbon rails, the contact stress must be reduced, either by reducing the wheel load, or by increasing the wheel diameter, or both. Figure 8 shows the required wheel load over a range of traction coefficient values for two wheel sizes. It should be noted that the reduction of wheel load to accommodate an increase in traction coefficient may compromise the overall objective of gaining more tractive effort. For example, the nominal tractive effort of a 42 inch wheel is:
>
> - at 33 kips wheel load and 20 per cent traction coefficient: 6.6 kips
> - at 24.5 kips wheel load and 30 per cent traction coefficient: 7.4 kips

---

[12] K.L. Johnson, "Inelastic Contact: Plastic Flow and Shakedown," International Symposium on Contact Mechanics and Wear of Rail/Wheel Systems, Vancouver, B.C., July 6-9, 1982, Preliminary Proceedings.

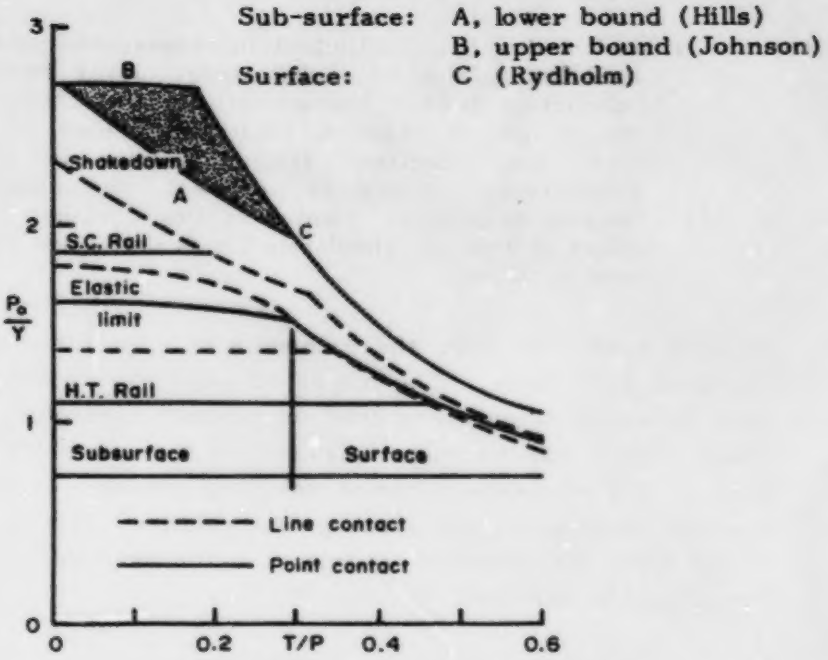

Source: K.L. Johnson, op. cit.

Figure 7 Elastic and shakedown limits in rolling contact

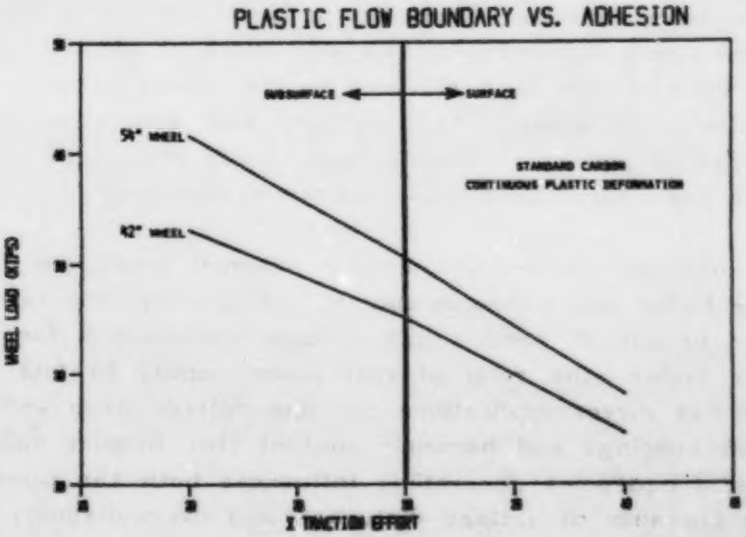

Figure 8 Required wheel load

- at 14.1 kips wheel load and 40 per cent traction coefficient: 5.6 kips

b) As the traction coefficient increases, the point of maximum octahedral shear stress moves from the subsurface toward the surface of wheel/rail. In the range of traction coefficient below 30 per cent, the wheel/rail fatigue damage is mainly subsurface. Above 30 per cent, the wheel/rail fatigue damage is mainly on the surface. The effect of this on wheel/rail life is discussed in the next section.

As with gear tooth life, the economics of high adhesion are tied to the expected duty cycle. The increased wear effects may be acceptable if peak adhesion is only required on a short controlling grade, whereas these effects may be unacceptable in a service which requires utilization of the available adhesion for long periods of time. A detailed economic evaluation considering the relative costs and relevant duty cycles would be required to determine the desirability of high adhesion for a specific service.

9. EFFECTS OF LOCOMOTIVE DESIGN ON ELECTRIFICATION FIXED COSTS

Unlike the diesel-electric locomotive, where the complete power plant is carried on board, the electric locomotive is only one small part of the power drive system. There are a large number of locomotive design factors which influence the wayside costs of electrification. Only a total systems viewpoint will lead to the lowest system cost method of operation. In addition to power per axle and power per locomotive, the type of power-conditioning unit (PCU) utilized on an electric locomotive has a significant impact on the system cost.

The principal factors influencing external costs are the efficiency, power factor and harmonic content. Efficiency (the ratio of input the power to output power) has obvious implications for energy costs; power factor (the ratio of real power input) to total volts-amperes input has direct implications for line voltage drop and thereby substation spacing; and harmonic content (the number and magnitude of higher frequencies generated) influences both the power distribution costs (because of voltage distortion and overvoltages), and the costs for immunization of wayside voice frequency communications lines.

The characteristics of a number of alternative PCUs were investigated, and comparisons made on the basis of the following measures of performance:

i) efficiency, E:

$$E = \frac{\text{POWER OUTPUT AT WHEELS}}{\text{POWER INPUT AT PANTOGRAPH}}$$

ii) input power factor, PF:

$$PF = \frac{\text{MEAN INPUT POWER}}{\text{RMS INPUT VOLT-AMPERES}}$$

iii) input displacement factor, DF:

$$DF = \cos \phi$$

where: ϕ = angle between the supply voltage and the fundamental component of the supply current.

iv) harmonic factor, HF:

$$HF = \frac{(I^2 - I_1^2)^{1/2}}{I_1}$$

where: I = total distorted rms input current

I_1 = rms value of input current at the fundamental frequency.

The actual measure used was truncated at the 80th harmonic, i.e.

$$HF_{80} = \frac{\left(\sum_{n=2}^{80} I_n^2\right)^{1/2}}{I_1}$$

v) telephone influence factor, TIF:

$$\mathrm{TIF} = \frac{\left[\sum_{f=0}^{\infty} (5\, f\, P_f\, I_f)^2 \right]^{1/3}}{\left[\sum I_f^{\,2} \right]^{1/2}}$$

where: f = frequency (Hz)

P_f = weighting factor which accentuates the voice frequency range

I_f = rms current at frequency f.

Again, for this evaluation the measure was truncated at the 80th harmonic (4,800 Hz).

vi) equivalent distributing current, I.T product:

$$\mathrm{I.T} = \mathrm{I.TIF}$$

While a number of these performance measures relate to the same factors, each is of unique interest. The displacement factor influences the voltage drop at the fundamental frequency, while power factor determines the total rms current (fundamental and harmonic) in the line. The harmonic factor illustrates the harmonic content and is a surrogate for voltage distortion on the feed line while the I.T product reflects the relative magnitude of inductive interference in the voice frequency range.

On the basis of these characteristics, the following five different PCUs were evaluated:

- a two-series bridge semi-converter with shunt traction motor
- a forced commutation variation of the above
- a three-series bridge semi-converter with series traction motor
- a pulse-width-modulated ac-dc converter

- a chopper control using a full-wave bridge rectifier on the front end and an L-C filter dc link.

It is the dc link of the ac/dc/dc chopper PCU which is the important element in external cost impacts. The measure of performance assessed would be very similar for any system which has a dc link isolating the ac feed system from the effects of the PCU. Thus, from the viewpoint of this assessment, the chopper PCU is representative of an ac/dc/ac PCU using ac traction motors.

A computer model was developed for each PCU. The analytic models prepared by John et al.[13] are discussed in detail in Appendix A. Further general discussion can be found in Sen.[14]

The PCU models were incorporated into an overall train simulation/ locomotive evaluation package. The modular layout of the program package is illustrated in Figure 9.

A rigorous assessment of an optimal locomotive is complicated by the trade-offs of on-board versus wayside filtering of harmonics; displacement factor improvement through forced commutation, on-board capacitors or series capacitors in the feed line; the development and materials costs associated with the alternatives; and the restrictions on space and weight for locomotive components. Detailed consideration of all of these parameters is beyond the scope of the present study. The trade-offs are for the most part dealt with qualitatively. In some cases preliminary estimates of the value of improving the locomotive measures of performance are made (e.g. displacement factor) but in no case is a optimum system design undertaken for a specific site.

9.1 The Costs of Low Displacement and Power Factors

A low power factor results in higher power feed line costs, while a low displacement factor increases the the number (and thus cost) of sub-

---

[13] John, V.I., P.C. Sen, G.E. Dawson, C. Namudiri, E. Ho, S. Burns, "Electric Locomotive Modelling of Harmonic Effects." CIGGT paper, March 1984.

[14] Sen, P.C., Thyristor DC Drives, John Wiley & Sons, 1981.

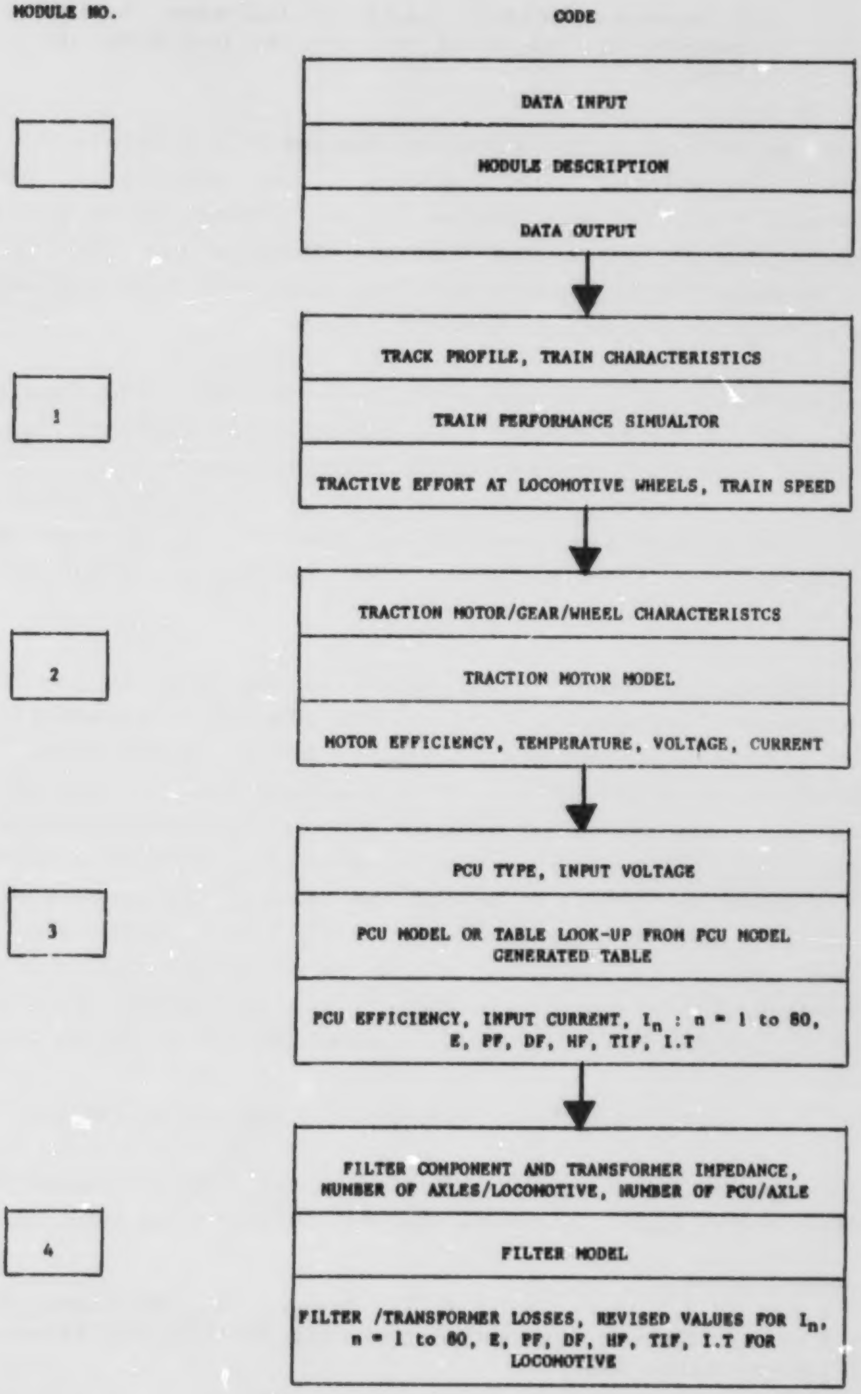
MODULE NO.
CODE
DATA INPUT
MODULE DESCRIPTION
DATA OUTPUT
1
TRACK PROFILE, TRAIN CHARACTERISTICS
TRAIN PERFORMANCE SIMUALTOR
TRACTIVE EFFORT AT LOCOMOTIVE WHEELS, TRAIN SPEED
2
TRACTION MOTOR/GEAR/WHEEL CHARACTERISTCS
TRACTION MOTOR MODEL
MOTOR EFFICIENCY, TEMPERATURE, VOLTAGE, CURRENT
3
PCU TYPE, INPUT VOLTAGE
PCU MODEL OR TABLE LOOK-UP FROM PCU MODEL GENERATED TABLE
PCU EFFICIENCY, INPUT CURRENT, I_n : n = 1 to 80, E, PF, DF, HF, TIF, I.T
4
FILTER COMPONENT AND TRANSFORMER IMPEDANCE, NUMBER OF AXLES/LOCOMOTIVE, NUMBER OF PCU/AXLE
FILTER MODEL
FILTER /TRANSFORMER LOSSES, REVISED VALUES FOR I_n, n = 1 to 80, E, PF, DF, HF, TIF, I.T FOR LOCOMOTIVE

Figure 9 Structure of the computer simulation package

stations and associated utility feed lines which must be built to supply an acceptable level of voltage to each locomotive on the line under expected operating conditions. Of the current which flows on a 60 Hz ac power line, only the current which is in phase with the 60 Hz supply voltage produces real power at the locomotive, where it is tranformed into mechanical torque and rotation at the wheels. The displacement factor measures the ratio of the 60 Hz current in phase with the supply voltage, to the total 60 Hz current flowing, while the power factor measures the ratio of the 60 Hz current in phase with the supply voltage to the total current flowing at all frequencies.

It is the total 60 Hz current which determines the fundamental voltage drop over the overhead contact system (OCS) between the supply point and the locomotive. An improvement in the ratio of the real to total 60 Hz current (the displacement factor) will thereby reduce voltage drop per unit length of OCS and thus permit greater substation spacings. A sensitivity evaluation was undertaken for estimated train load conditions in a Canadian mountain region to estimate the value of improving this ratio. The base case and methodology were extracted from the previous investigation of alternative voltages and frequencies for the Canadian railways.[15] At 50 kV, 60 Hz, the average substation spacing was estimated to be 78 km in the mountain region. This estimate was based on an average locomotive displacement factor of 0.8 lagging.

Using the same approach as that study, substation spacings were evaluated for locomotive displacement factors ranging from 0.7 lagging to 0.96 leading. The results are illustrated in Figure 10.

---

[15] G.W. English, E.R. Corneil, G.T. Fisher, Power Distribution Alternatives in Canadian Railway Electrification, CIGGT Report No. 81-10, January 1982.

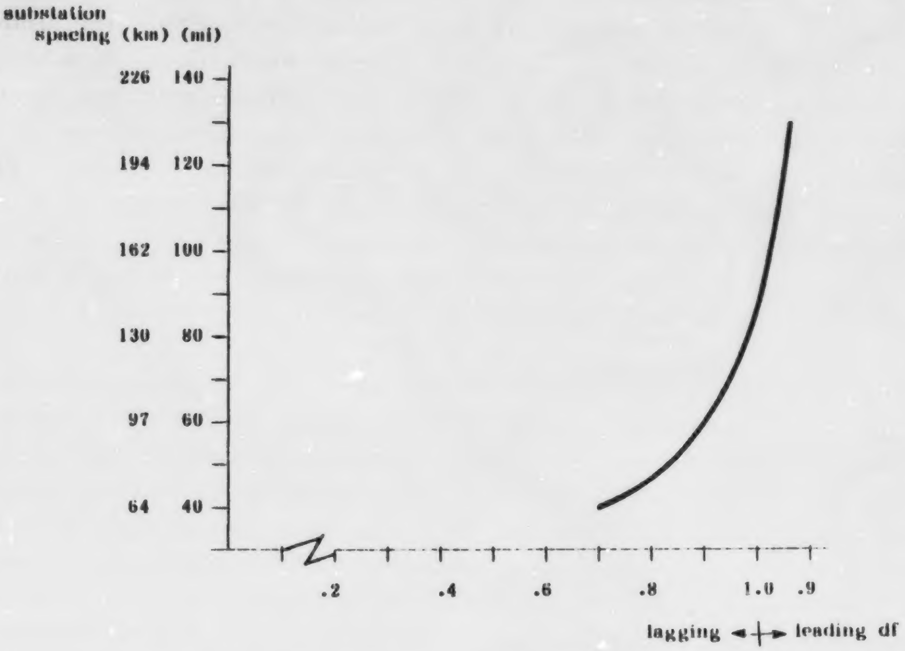

Figure 10 Substation spacing versus displacement factor

Investment in the locomotive to improve its displacement factor can generate savings in both the capital and operating costs of an electrified railway. The capital cost of substations and associated high-voltage feed lines would be reduced through a reduction in the number of feed points required. The operating cost saving would arise from a reduction in the "demand" charge which the utilities impose monthly for each substation on the basis of the highest volts-ampere power demand at that substation. The estimated cost reductions due to each of these factors were estimated for a mountain region using the same approach as outlined by English et al.[16] The cost savings are shown in Table 10.

---

[16] ibid

TABLE 10

COST IMPACTS OF LOCOMOTIVE DISPLACEMENT FACTOR ($000/km)

Displacement Factor	First Cost of Substations and Utility Feed Lines	Present Value of Demand Charge for First Thirty Operating Years kW billing (kVA billing)	Total
0.7	62.0	192/(275)	254.0/(337.0)
0.8	48.5	173/(216)	221.5/(264.5)
0.9	36.7	151/(168)	187.7/(204.7)
1.0	24.4	145/(145)	169.4/(169.4)
0.96 leading	18.0	128/(133)	146.0/(151.0)

The present value of improving the displacement factor from 0.8 to 0.9 lagging is $33,800/km ($11,800 in first cost and the remainder in present value for the first thirty years of operation). A shift to 0.96 leading is valued at $75,500/km.

On the basis of 216 electric locomotives, the estimated fleet requirement for 1,500 km of electrified territory in this region, the present value per locomotive for improvement in kW demand readings would be $241,000 for a 0.8 to 0.9 improvement, and $540,000 for a 0.8 to 0.96-leading improvement. These represent between 10 and 20 per cent of the present North American price for a 6,000 hp electric locomotive. While this is significant, it should be noted that the analysis did not evaluate the relative merit of using wayside power factor correction and line compensation through use of series and shunt capacitors.

These savings are dependent on the improved locomotive displacement factor being incorporated into the initial electrical distribution design. Nevertheless, there would be some savings from improvements on mature installations, since traffic growth exacerbates the problem of adequate voltage regulation. Typically, extra feed conductors are added to attempt to meet the added current-carrying requirements and eliminate train performance deterioration from reduced voltage. However, the SNCF has been investigating the effectiveness of on-board power factor correction in alleviating this problem.[17]

The problems of current-carrying capacity relate to total power factor rather than just the displacement factor. The first cost of supplying an extra 150 Amperes of capacity on the OCS has been estimated to be about $13,000 per km.[18] For a 50 kV feed line, a coincident load of 30 MW at the substation draws 600 Amperes. Locomotives which demonstrate a 0.73 pf, in comparison with locomotives which achieve a 0.9 pf, would require an additional 150 Amperes of reactive current and thus would incur incremental costs of $13,000 per km.

9.2 Cost of Harmonic Currents

Harmonic currents affects the costs of electrification in two areas -- the power distribution system and wayside communication systems.

Power distribution system problems arise from harmonics of higher magnitude (usually the 3rd, 5th and 7th harmonics). Because the feed line impedance is largely inductive, the impedance seen by higher harmonics increases with frequency. Thus, the voltage drop is not uniform, and the 60 Hz sin wave is further distorted.

Also, with longer feeding distances, the resonant frequency of the feed line decreases and the possibility of resonant voltage oscillations increases. Both forms of distortion lead to much higher peak voltages on the feed line, as illustrates in Figures 11 and 12 (from Morrison and Barlow[19]). This has implications for insulation requirements, air gap clearances required in tunnels and under bridges, and protection of the locomotive solid-state equipment.

---

[17] SNCF. Relèvement du facteur de puissance par filtrage des harmoniques de courant à bord des engins moteurs - Dispositifs expérimentés sur la BB 15016. SNCF Direction du Matériel, Research Report R' 33-40, September 1981.

[18] Shaw, P.L., Electrack Inc., Panel Discussion, "Railroad Energy Technology: The Alternatives," Memphis, Tenn., December 1982

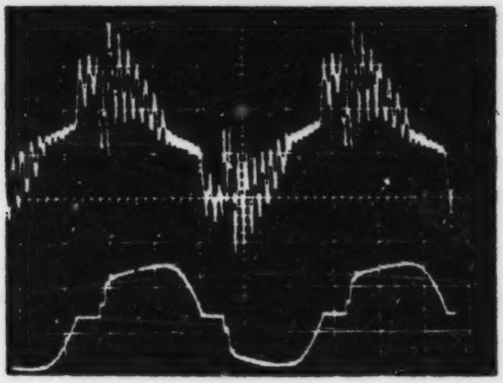

Source: Morrison & Barlow

Figure 11 Pantograph voltage and current waveform illustrating resonance effects

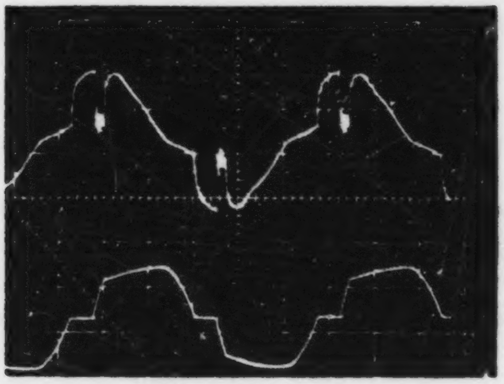

Source: Morrison & Barlow

Figure 12 Pantograph voltage and current waveform with filter connected

---

[19] Morrison, R.E., M.J. Barlow, Power Transmission Division, GEC Power Engineering Limited, Stafford, England, "Continuous Overvoltages on A.C. Traction Systems," IEEE Power Engineering Society, IEEE PES 1982 Summer Meeting, San Francisco, CA., July 18-23, 1982.

Many factors which would characterize Canadian railway electrification would accentuate these problems in comparison to European electrification. The use of 60 Hz versus 50 Hz or 16^2/3 Hz would shift the harmonic spectrum into a higher frequency range. The use of 50 kV would increase substation spacing significantly, which would lower the resonant frequency of the feed line. Problems requiring system modification were encountered on recent 50 kV lines. Installation of wayside filters was required on the Black Mesa[20] and BCR Tumbler Ridge lines, and locomotive filters were evaluated for South Africa's Sishen-Saldanka line.[21]

The utilities will not permit excessive harmonic distortion on their feed lines, so that the principal harmonics must be filtered out at, or before, the substation which connects the utility transmission system to the railway load. It has not yet been established whether it is more cost-effective to reduce harmonics on board the locomotive or through wayside filter installations.

Noise induction on voice frequency communications lines is another problem created by harmonic currents on the OCS. These problems arise principally from harmonics in the voice frequency range. Even harmonics of very small magnitudes can be a problem, because the effects are cumulative over a wide frequency range, and the signal strength on the affected conductors is usually low.

The cost of achieving compatibility with communications circuits has been estimated to range from $10,000 to $27,000 per km of electrification.[22] However, not all of these cost arise from the effects of voice frequency harmonics. Even if voice frequency harmonics are eliminated, there may still be electromagnetic compatibility costs associated with the 60 Hz current. The induced voltage from the fundamental current flow, if not controlled, can create safety hazards. Also, the addition of harmonics from separate sources is not arithmetic. Slight differences in the phase relationship of the fundamental frequency can significantly reduce the vector sum of higher harmonics.

---

[20] Burke, J.J., A.P. Engel, S.R. Gilligan, N.A. Mincer, "Increasing the power system capacity of the 50 kV Black Mesa and Lake Powell Railroad through harmonic filtering and series compensation." IEEE Transactions on Power Apparatus and Systems, Vol. PAS-98, No. 4, July/August 1979.

[21] Souch, D.J.W., J. Dowling, GEC Traction Limited, Manchester, England, "50 kV Locomotives for a Mineral Railway," Proc. Instn Mech Engrs, Vol. 195, 1981.

[22] See Table 3.12 in Empey et al., op. cit.

General Electric has found that even the 2° to 3° phase difference in PCUs on the same locomotive reduces the expected harmonic content at the pantograph.[23] Tests undertaken on a Swedish electrified rail line indicate that the average disturbing current for an "N" locomotive load is roughly $\sqrt{N}$ times that of a single locomotive. The measurements are illustrated in Figure 13.[24]

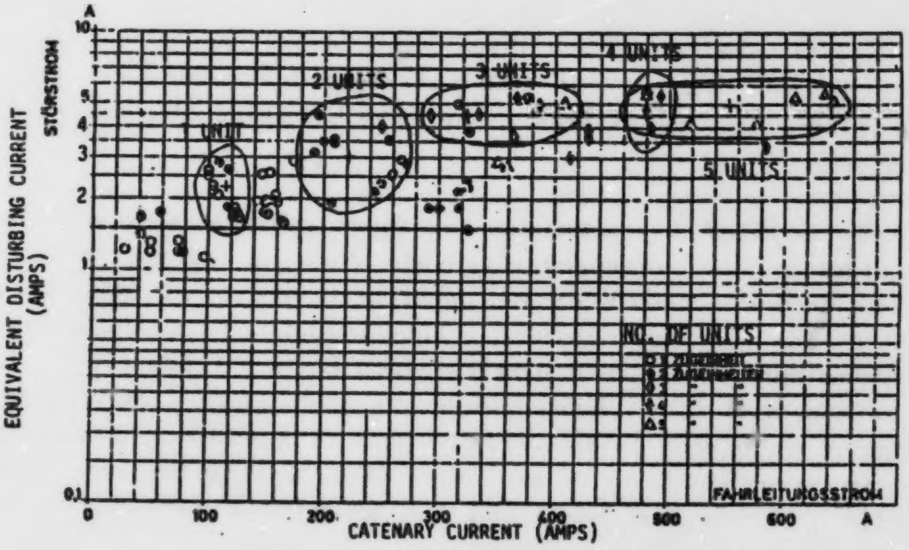

Source: Power Distribution Alternatives in Canadian Railway Electrification, op. cit.

Figure 13 Disturbing current for multiple locomotive loads

---

[23] Discussions with GE's Motive Power group in Erie, PA.

[24] Von G. Ingemanssen und S. Svensson, Blindleistungskompensation und Massnahmen zur Dampfung des Storinflusses durch Oberwellen beim Einsatz von Thyristorfahrzeugen, Stockholm.

9.3 Comparison of Power-Conditioning Units (PCU)

As noted previously, the characteristics of five different PCUs were predicted by computer simulation (see Appendix A). Of the five types investigated, the series phase-controlled PCUs would have the lowest development cost, and would use lower cost SCRs. The latter have a lower first cost, and are the dominant design in terms of present world market share. However, these produce a low, lagging displacement factor through much of the control range and have a considerable level of harmonic current. The displacement factor could be improved by connecting bridges in series so that one bridge is fully phase-advanced before the next one is brought into control. Present designs use two-series bridges for a shunt motor where both are fully advanced to full armature voltage part way through the speed range, beyond which point field weakening is used to increase motor speed. For a series motor, the PCU must control the terminal voltage over the complete speed range and three series bridges are used to improve the displacement factor. If high-power traction motors are required, it may be necessary to weaken the field by means of a switched bypass resistor.

The predicted characteristics of these PCUs at maximum continuous output for the full speed range are shown in Figures 14(a) to 14(e). The computer models do not incorporate the input inductance of the feed line and transformer. This inductance causes a lag in the commutation of the SCR bridges which limits the phase advance bridge to less than full. Thus, while the plots show a unity displacement factor when each bridge is fully phase-advanced, in reality the maximum value would be in the order of 0.9. For the same reason, the $(I)^2$ R losses are lower and the efficiencies somewhat higher than would be realized in service.

The phasing of each of the series bridges is clearly indicated in many of the plots. For the two-bridge/shunt motor, the first bridge is fully advanced at 14 mph and the second at 30 mph, after which speed control is achieved through field weakening. For a three-bridge/series motor, the first bridge is fully advanced at 11 mph and the second at 26 mph. At 32 mph, the motor shunting resistor is inserted, which reduces the input voltage requirement. The third bridge is phased back at this point, then advances with speed until full phase advance at 60 mph.

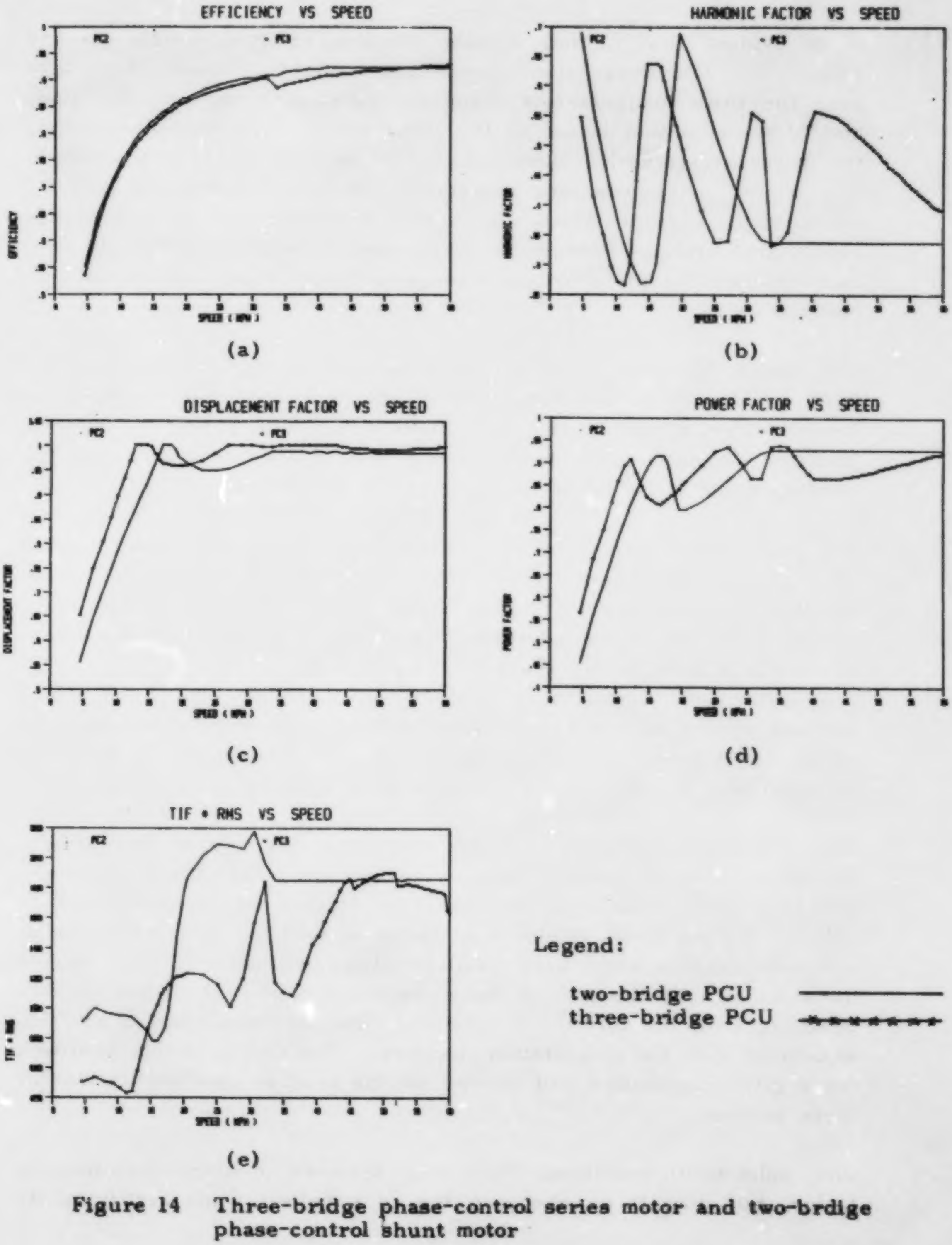

(a) (b) (c) (d) (e)

Figure 14 Three-bridge phase-control series motor and two-brdige phase-control shunt motor

It is evident that neither system offers a clear advantage in any area. The two-bridge/shunt motor has a slight efficiency advantage over the three-bridge/series motor arrangement because of the diode and SCR conduction losses of the third bridge. On the other hand, the three-bridge/series combination has an I.T product advantage. The higher harmonics are associated with the rate-of-rise in the commutation current which is directly proportional to the voltage across the bridge. Because it takes smaller voltage increments with each bridge, the three-bridge arrangement has reduced levels of high harmonics.

The actual harmonic content, as indicated by the harmonic factor (HF), is higher for the latter section of the speed range because the lower frequency harmonics have a higher magnitude when the bridge is partially advanced. The two-bridge system is fully advanced with the traction motor in field weakening over this range.

The two systems demonstrate a considerable variation in power factor over the speed range. The three-bridge/series system is not as desirable in the higher speed range where the two-bridge/shunt system is at full phase advance, but it has the advantage over segments of the lower speed range.

One can expect that any advantage one system has over the other in terms of the above characteristics will be quite site-specific. Each has different advantages over particular segments of the speed range.

The effect of employing forced commutation on one of the series-connected phase-controlled bridges to achieve a symmetrical current waveform (and thus a unity df) is illustrated in Figures 15(a) to 15(e). The improved displacement factor is achieved at the expense of harmonic content and, to a smaller extent, efficiency. The higher harmonic content arises from the sharp rates of change in line current resulting from the forced commutation. The additional losses are also associated with the commutation circuitry. The merits of this approach for a given application will depend on the relative cost implications of these factors.

The pulse-width-modulated PCU also achieves a unity displacement factor, but does it by chopping the ac waveform while rectifying it.

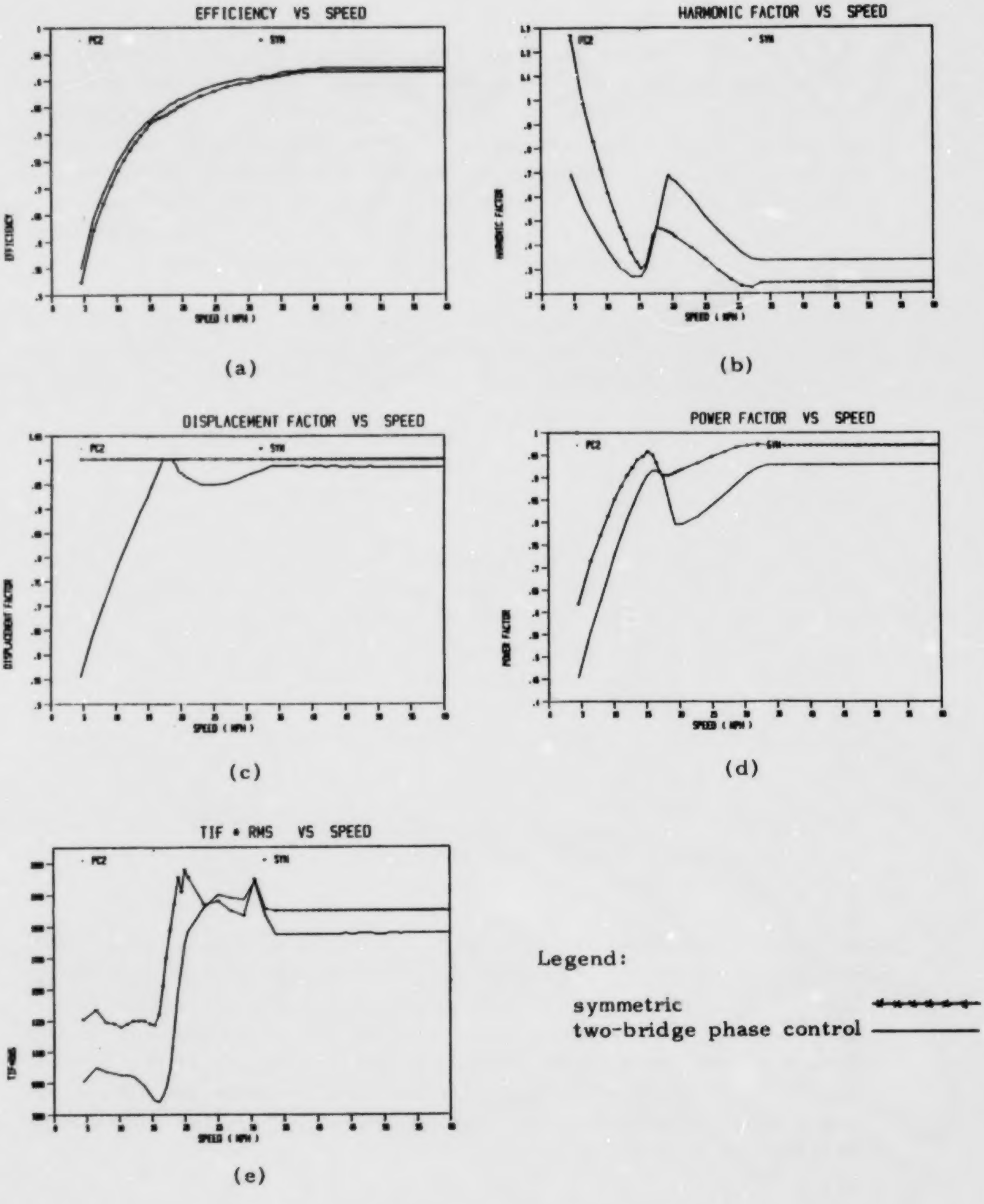

Figure 15 Two-phase control and symmetric control

The increased number of forced commutations per cycle increases the commutation losses and the harmonic content. However, this approach eliminates the lower-level harmonics,[25] while higher-frequency harmonics which remain can be more easily filtered. The performance measures for a 12 pulse/cycle PCU, with and without a front-end RC filter, are illustrated in Figures 16(a) to 16(e). The effectiveness of the filter in reducing the harmonics is evident, but a fixed filter creates a leading power factor and significantly higher losses.

The final PCU considered is the chopper with a front-end full-wave rectifier. Heavy filtering on the dc link is effective in reducing the chopper-induced harmonics. However, the lower frequency harmonics associated with the front-end rectifier remain, and, as with the PWM system, the filtering-out of these harmonics lowers efficiency and can create a low leading displacement factor. The performance measures for this PCU are illustrated in Figures 17(a) to 17(e).

Weighted average performance measures were generated for each of the PCUs in a computer simulation of a loaded bulk train traversing an 800 km mountain segment. The results are shown in Table 11. Each unit was simulated both with no filtering on the front end and with filtering. Fixed-value filters common to most existing electric locomotives were used. A broad-band RC filter was used for the PWM case, while tuned 3rd harmonic filters were used for all other filtered cases.

The particular line had speed restrictions which resulted in an average train speed of 51 km/h. The majority of the trip was spent at 50 km/h, while the maximum speed reached was 88 km/h.

The efficiency variations across PCUs, with the exception of the PWM, are not significant. The PWM unit has higher bridge commutation losses. The efficiency costs of constant filtering are evident in all applications. At the lower speed and low power requirement on this line, the fixed value filters overcompensate the lagging df of all PCUs, leading to a substantial drop in efficiencies. While the filters are effective in reducing harmonic content (HF and I*T), the VA/kW ratio increased in all cases.

---

[25] Sen, P.C., op. cit.

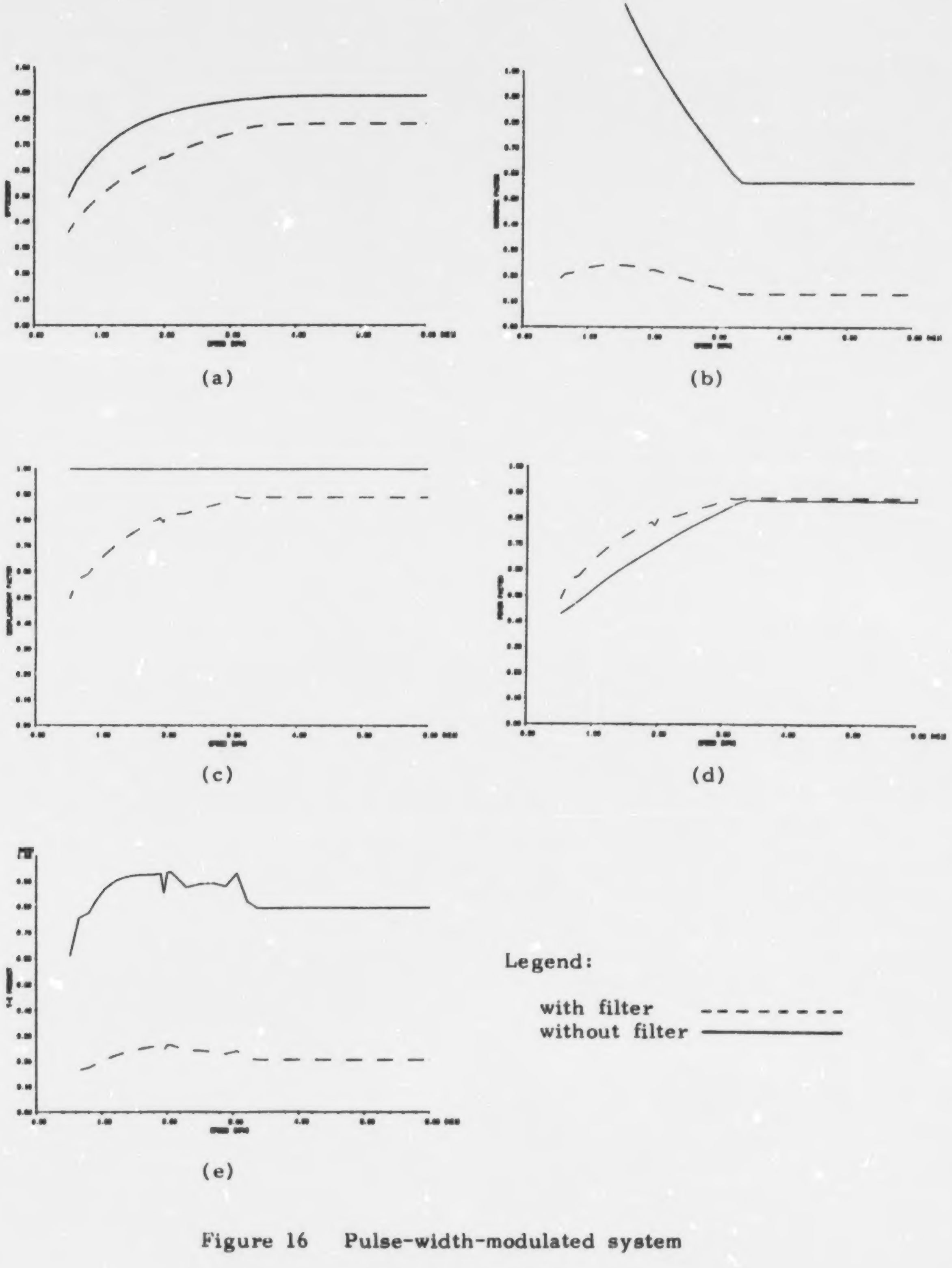

Figure 16 Pulse-width-modulated system

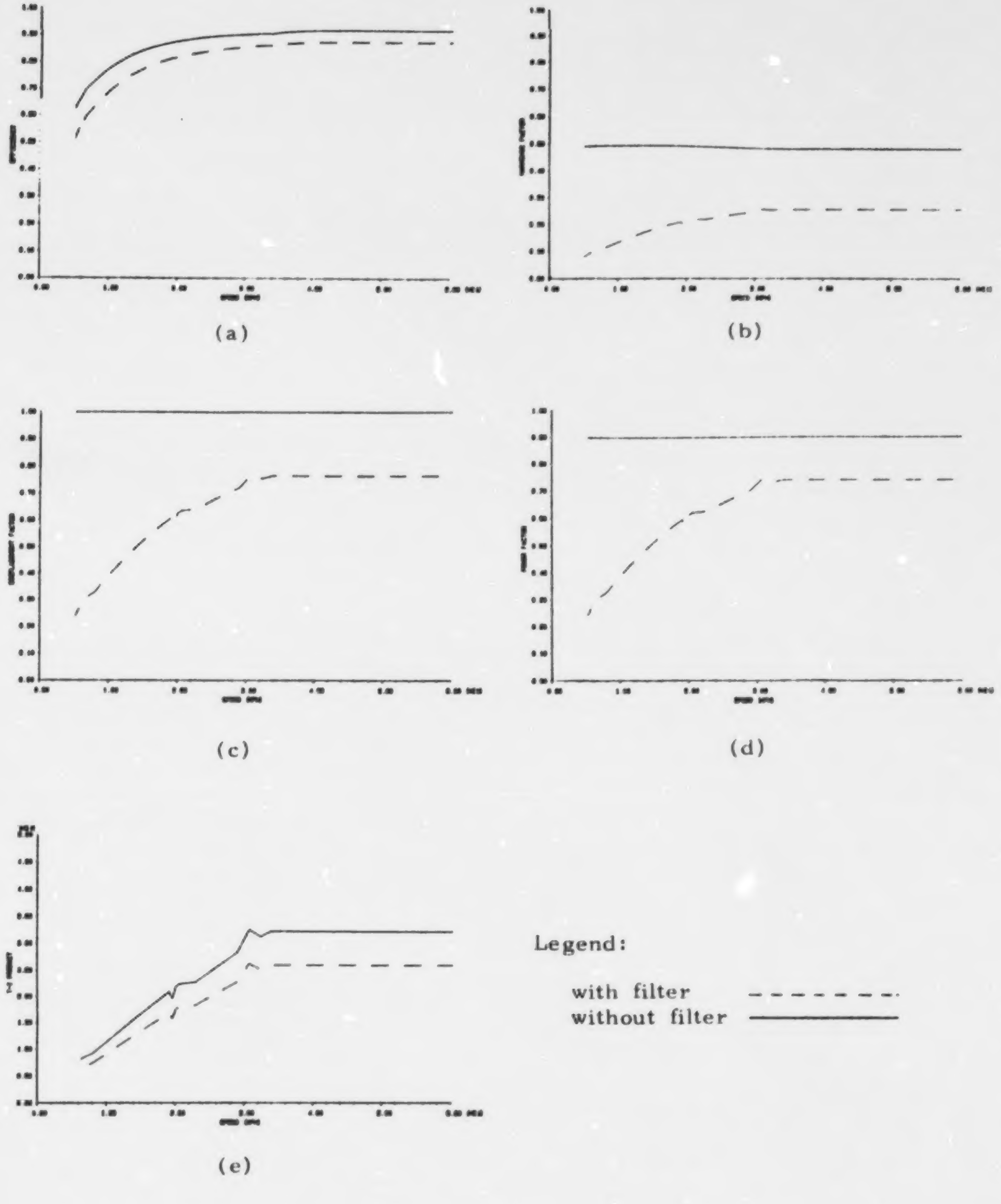

(a) (b)

(c) (d)

(e)

Figure 17 Chopper control

TABLE 11

AVERAGE PERFORMANCE RESULTS FOR AN 800 KM MOUNTAIN REGION TRAIN RUN

Type of PCU	Three-Bridge Phase Control		Two-Bridge Phase Control		Two-Bridge Symmetric Control		ac-dc Pulse-Width-Modulated (pwm)		ac-dc-dc Rectifier-Chopper	
Type of Motor	Series Motor		Shunt Motor		Shunt Motor		Shunt Motor		Shunt Motor	
Front-end filter	no	yes	no	yes	no	yes	no	yes	no	yes
Efficiency	.857	.73	.85	.74	.84	.73	.81	.66	.84	.74
TIF * I_{rms} (thousands)	35.5	29	41	33.6	40.3	33.5	187	49.2	59	47.4
kVA/kW (1/ph)	1.16	1.24	1.08	1.36	1.03	1.45	1.29	1.51	1.07	2.4
HF	.34	.153	.30	.12	.20	.07	.50	.06	.34	.08

This situation is particularly troublesome for the PWM unit which requires a large on-board capacitor to provide the commutating current for its fast switching SCRs. In the other units, a range of controlled filters could be used, so that a suitable level of 60 Hz compensation would be achieved. Harmonic reduction effectiveness would be reduced and additional space, complexity and first costs would be incurred, but df and efficiency should improve.

Some filter variations were simulated for the PWM and series phase-controlled cases. First was the effect of a simple on/off switching arrangement to cut out the filter below half load. While constant fixed-value filtering for the PWM case gave a 23 per cent reduction in the I*T product and a 100 per cent increase in losses, the switched filter gave a 50 per cent reduction in the I*T product and a 68 per cent increase in losses.

A variable filter was simulated for the phase-controlled bridge. The filter was cut out below one-third full load, was at half value between one-third and two-thirds full load, and was at full value above two-thirds full load. In this case the I*T product was reduced by 13 per cent (compared with 17 per cent for the fixed-filter case) and losses increased by 41 per cent (compared with 100 per cent for the fixed-filter case).

In terms of overall performance in this particular application, the unfiltered symmetrical control PCU may have some advantage. Its kVA/kW ratio and HF are both comparatively low. However, it demonstrates a slightly lower efficiency and a higher voice frequency harmonic content.

9.4 Effects of Power per Axle

The effects of increasing power per axle on the fixed cost of electrification is highly site-specific. It will only affect those areas where the increased on-board power can be utilized. These areas include high-gradient lines and level lines with high speed limits. Many areas would not be affected by increased power availability, and even in those areas where it could be utilized, there are many cost parameters related to the selection of how much power is desirable. This discussion is concerned only with the possible impacts on the cost of the electrical fixed installation. These impacts are similar to those of varying the displacement factor.

A higher power level creates higher current demand which influences the cost of OCS through current-carrying capacity, and the cost of substations through voltage regulation restrictions. However, the impacts of real power increases are less than those of displacement factor, which relates to imaginary power. The increase in real power leads to an increase in train speed. The faster the trains are moving, the lower the probability that they will be present on a substation feed segment in a fixed time interval. Consequently, the substation peak power requirement will be less than a direct multiple of the train power increment.

The degree of reduction will depend on the terrain. For high-speed passenger trains on level track, where aerodynamic drag is the principal resistance factor, the increase in speed will approximate the cube root of the increase in power. For low-speed bulk trains on steep gradient, where gradient is the principal resistance factor, the increase in speed will be almost directly proportional to the increase in power.

Substation design is based on the combined probability of multiple train loads (i.e. power times probability). Since probability is inversely proportional to speed, the impact of power increases on substation costs would be small for the "low-speed train on steep gradient case" and significant for the "high-speed train on level track" case. In either case, the impact would be less than that of a change in kVA brought about by displacement factor changes.

10. CONCLUSIONS

(1) A simple, relatively accurate model has been developed relating power per unit, train mass and train time. The relation is very sensitive to track features, making it necessary to calibrate the relation for each track segment. It is less sensitive to train characteristics, although errors of up to 6 per cent have been noted because of train variations. For the track segments sampled, a single locomotive with a short-term overload rating of 1,530 kW and continuous rating of 1,150 kW would satisfy the maximum performance demands of 66 per cent of the traffic.

(2) The overload capability for an electric locomotive can provide performance equivalent to a higher-powered unit if track characteristics permit. On some segments (e.g. BICSWN), overload capability will provide no benefit, while on others the benefit may be considerable.

(3) Careful design is necessary to provide an overload capability without serious consequences on locomotive reliability and life. This overload effect must be considered in the design of all components, from the pantograph down to the traction wheels.

(4) Adhesion levels have serious implications on wheel and rail wear and on gear design. Larger driving wheels permit higher adhesion levels. Reduced axle weight also permits higher adhesion levels, although the resulting drawbar force may not change appreciably.

(5) As axle power increases, gear wear is likely to become increasingly important. Envelope restrictions prevent physical modifications which could improve gear life. Gear design (single reduction) prohibits increasing the gear ratio to achieve high power and high adhesion.

(6) It is likely that railways will opt for a four- or six-axle locomotive, in preference to an eight-axle unit. The increased flexibility of dispatch, and the perceived improvement in train reliability achieved by the use of multiple locomotives is likely to outweigh arguments concerning reduced capital cost of the fleet, and possible improvements in unit reliability. The relatively small difference in the proportion of traffic which might be dispatched with a single locomotive, pantograph considerations, and unit/weight considerations is sufficiently indecisive that a clear choice between a four- or six-axle unit cannot be made.

(7) The analysis of power-conditioning units again presents no clear direction on the choice of system, since track characteristics will favour one type on one segment and another type on another segment. However, it is clear that active filtering is preferable to simpler forms, because of the wide range of operating conditions.

(8) A suitable choice of power-conditioning unit can provide substantial savings in the supply system. The benefits of reductions of the reactive power requirements of the locomotive are significant. A detailed economic evaluation of the relative costs and benefits of forced commutation, on-board filtering and wayside filtering and power factor correction should be undertaken.

APPENDIX A

ELECTRIC LOCOMOTIVE MODELLING, HARMONIC EFFECTS

V.I. John
P.C. Sen
G.E. Dawson
C. Namudiri
E. Ho

Department of Electrical Engineering
Queen's University at Kingston, Ontario

March 1984

APPENDIX A

ELECTRIC LOCOMOTIVE MODELLING, HARMONIC EFFECTS

The widespread use of solid-state converters in electric traction systems has increased the amount of harmonics injected into the power supply network. The most damaging frequencies to power devices and machines appear to be the lower frequencies, 5 kHz and under. Interference to wire communications, radio, video and digital data transmission from neighbouring power lines supplying traction systems has also increased. The presence of harmonic currents in the distribution lines also seriously distorts the pantograph voltages, especially when several trains are being fed from a long distribution line.

The following analyses examine the mechanism of harmonic generation due to four types of power converters commonly used in dc traction systems. Analytical expressions are derived for calculating the harmonic content in the source current for different operating conditions of the traction motor. Both series and separately-excited configurations for the motors are considered. In each case a computer program is used to calculate the input power factor, displacement factor, harmonic factor, losses and efficiency of the converter. The effect of introducing input filters to reduce particular harmonics in the supply lines is considered. In this context the concern is that improving the output waveform to reduce harmonic losses in the motors and other loads tends to shift the losses on to the supply power networks.

A.1 PHASE-CONTROLLED RECTIFIER

A.1.1 General

Phase-controlled rectifiers are by far the most common power-conditioning units used for dc motor drives. They are used extensively in traction systems. Two or three bridge converters are used with separately-excited and series-excited traction motors. Where regenerative braking is not used, only semiconverters are employed for economic reasons. In the normal converter firing angle, α, is varied to obtain the output voltage control. To improve the power factor and reduce the harmonic content, sector control with forced commutation is employed for either two-bridge or three-bridge configurations. In the following section these converters are examined in detail and computer programs are developed to calculate their performance for varying load conditions.

A.1.2 Two-Series Bridge Semiconverters

The actual connection diagram for this arrangement supplying a separately excited dc traction motor is given in Figure A.1.1. Figures A.1.2 and A.1.3 give the voltages and current wave forms for the two-bridge converters for $0 \leq E_a \leq 0.5$ pu and for $0.5 \leq E_a \leq 1.0$ pu. A list of symbols and the governing equation to compute the PCU performance is given in the next section.

A.1.3 Analysis of Two-Series Bridge Semiconverters

Table A.1.1 is a list of symbols and their definition.

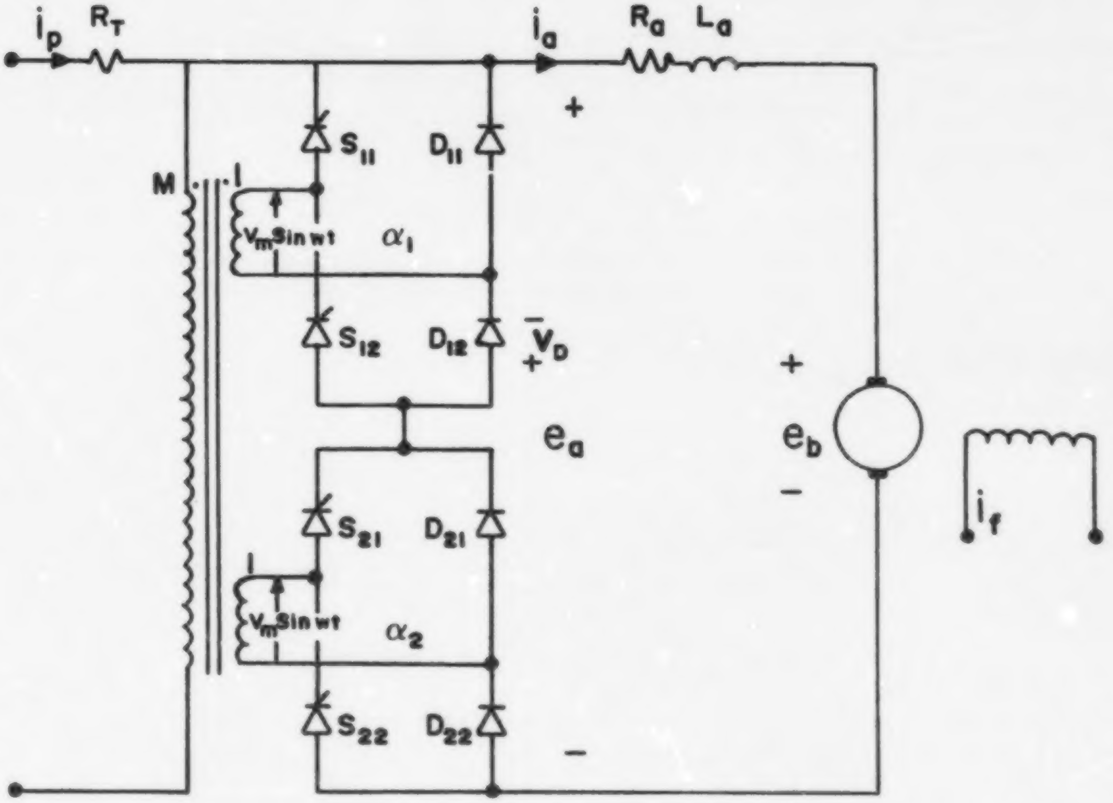

Figure A.1.1 Two-bridge phase-controlled semi-converters supplying a separately-excited dc motor

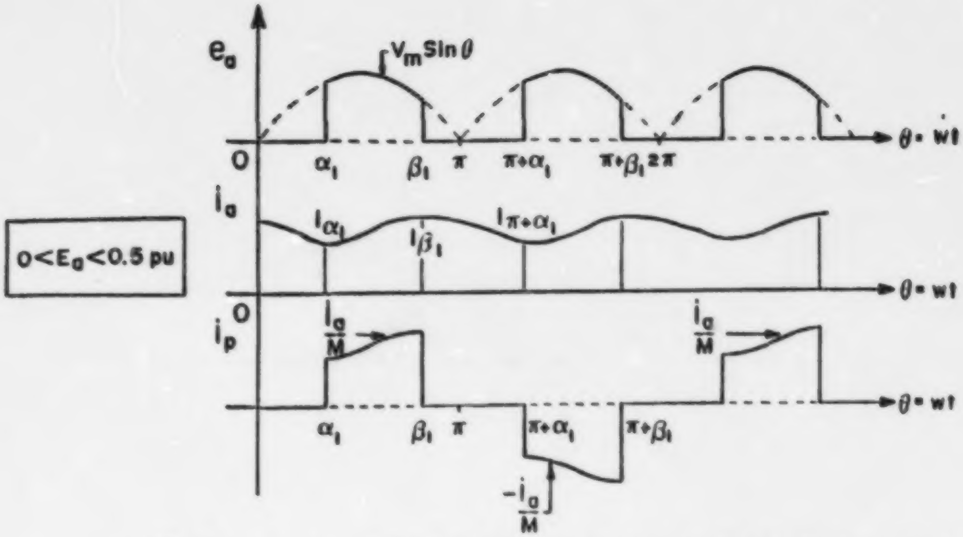

Figure A.1.2 Voltage and current waveforms for two-bridge phase-controlled semiconverter

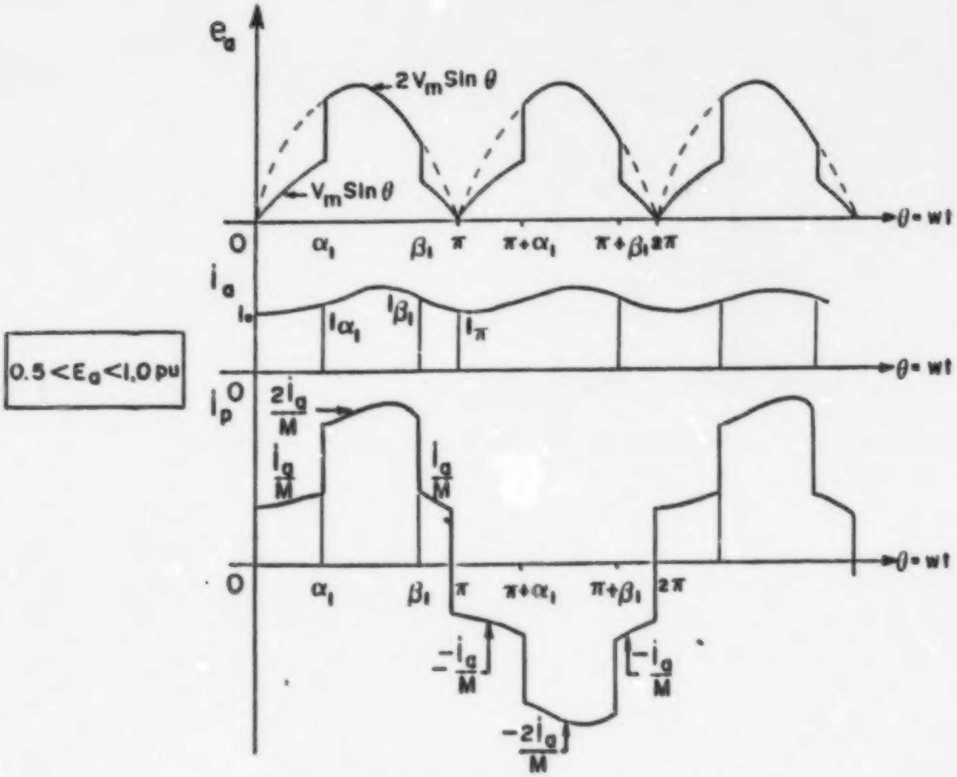

Figure A.1.3 Voltage and current waveforms for two-brdige phase-controlled semiconverter.

TABLE A.1.1

SYMBOLS AND DEFINITIONS

---

i_a = instantaneous armature current

i_p = instantaneous input current at primary of transformer

I = input rms current

I_{av} = motor average current

$I_{a_{rms}}$ = motor rms current

I_f = input fundamental rms current

I_n = input n^{th} harmonic rms current

E_a = average PCU output voltage

E_b = average motor back emf

V_m = peak value of sinusoidal input voltage to each converter

V_D = voltage drop across diode/thyristor while conducting

M = transformer turns ratio (between primary and each secondary)

x_n, y_n = Fourier coefficients for n^{th} harmonic

λ = input power factor

δ = input displacement factor

h = input harmonic factor

η = overall efficiency

P_L = converter/motor/transformer losses

α = firing angle

$$E_{max} = \frac{4Vm}{\pi} = 1.0 \text{ pu}$$

Case 1

$\boxed{0 < E_a < 0.5 \text{ pu}}$ $\quad 0 < \alpha_1 < \pi,\ \alpha_2 = \pi \quad$ $\boxed{\alpha_1 = \text{Cos}^{-1}\ (4\ E_a - 1)}$

$$i_a = a_1 \sin(\theta - \phi) + a_2 e^{-a_3 \theta} - a_4, \quad \alpha_1 < \theta \pi$$

$$= a_5 e^{-a_3 \theta} - a_4, \quad \frac{\pi < 0 < \pi + \alpha_1}{(\pi < \theta < \beta \text{ for discontinuous current})}$$

where: $\theta = \omega t$

$$a_1 = \frac{V_m}{Z}$$

$$a_2 = [I\alpha_1 + a_4 - a_1 \sin(\alpha_1 - \phi)] e^{a_3 \alpha_1}$$

$$a_3 = \frac{R_a}{\omega L_a}$$

$$a_4 = \frac{E_b}{R_a}$$

$$a_5 = (I\eta + a_4) e^{a_3 \pi}$$

$$Z = \sqrt{R_a^{\ 2} + (\omega L_a)^2}$$

$$\phi = \tan^{-1}\left(\frac{\omega L_a}{R_a}\right)$$

$$i_p = 0 \qquad , 0 \quad 0 \quad 1$$

$$= \frac{i_a}{M} = \frac{1}{m} [a_1 \sin (\theta-\phi) + a_2 e^{-a_3\theta} - a_4], \alpha_1 < \theta < \pi$$

Motor Average Current, I_{av}:

$$I_{av} = \frac{1}{\pi} [\int_{\alpha_1}^{\pi} i_a \, d0 + \int_{\pi}^{B} i_a \, d0]$$

$$I_{av} = \frac{1}{\pi} [a_1 (\cos \phi + \cos (\alpha_1-\phi) + \frac{a_2}{a_3} e^{-a_3\alpha} - \frac{a_5}{a_3} e^{-a_3\beta}$$

$$+ (a_3 - a_2) \frac{e^{-a_3\pi}}{a_3} - a_4(\beta-\alpha)]$$

Motor RMS Current, $I_{a_{rms}}$:

$$I_{a_{rms}} = \sqrt{\frac{1}{\pi} [\int_{\alpha_1}^{\pi} {i_a}^2 \, d\theta + \int_{\pi}^{\beta} {i_a}^2 \, d\theta}$$

$$= \sqrt{\frac{1}{\pi} [\frac{{a_1}^2}{2} (\pi-\alpha_1) + {a_4}^2 \pi + \frac{{a_1}^2}{4} [\sin 2\phi + \sin (2\alpha_1-2\phi)]}$$

$$+ \frac{{a_2}^2}{2a_3} (e^{-2a_3\alpha_1} - e^{-2a_3}) + \frac{2a_1a_2}{(1+{a_3}^2)} \left\{e^{-a_3\alpha_1} (a_3 \sin (\alpha_1-\phi)\right.$$

$$+ \cos(\alpha_1 - \phi)) - e^{-a_3\pi}(a_3 \sin\phi - \cos\phi)\Big\} - 2a_1 a_4 (\cos\phi +$$

$$\cos(\alpha_1 - \phi)) + \frac{2a_2 a_4}{a_3}(e^{-a_3\pi} - e^{-a_3\alpha_1}) + \frac{a_5^2}{2a_3}[e^{-2a_3\pi} - e^{-2a_3(\beta)}]$$

$$+ \frac{2a_4\ a_5}{a_3}[e^{-a_3(\beta)} - e^{-a_3\pi}]\ ]$$

Input RMS Current, I:

$$I = \frac{1}{M}\sqrt{\frac{1}{\pi}\int_{\alpha_1}^{\pi} i_a^2 \, d\theta}$$

$$= \frac{1}{M}\sqrt{\begin{aligned} &\frac{1}{\pi}\Big[\Big(\frac{a_1^2}{2} + a_4^2\Big)(\pi - \alpha_1) + \frac{a_1^2}{4}\big[(\sin 2\alpha_1 - s\phi) + \sin 2\phi\big] \\ &+ \frac{a_2^2}{2a_3}(e^{-2a_3\alpha_1} - e^{-2a_3\pi}) + \frac{2a_1 a_2}{1+a_3^2}\Big\{e^{-a_3\alpha_1}(a_3 \sin(\alpha_1 - \phi) + \\ &\cos(\alpha_1 - \phi)) - e^{-a_3\pi}(a_3 \sin\phi - \cos\phi)\Big\} - 2a_1 a_4 (\cos\phi + \\ &\cos(\alpha_1 - \phi)) + \frac{2a_2 a_4}{a_3}(e^{-a_3\pi} - e^{-a_3\alpha_1})\ \Big] \end{aligned}}$$

Input Harmonic Currents, I_n:

$$x_n = \frac{2}{M\pi}\int_{\alpha_1}^{\pi} i_a \sin n\theta \, d\theta$$

$$y_n = \frac{2}{M\pi} \int_{\alpha_1}^{\pi} i_a \cos n\theta \, d\theta$$

$$x_n = \frac{2}{M\pi} \left[\frac{a_1}{2} \left[\frac{\sin(\overline{n-1}\ \theta+\phi)}{(n-1)} - \frac{\sin(\overline{n+1}\ \theta-\phi)}{(n+1)} \right] + \frac{a_4}{n} \cos n\theta \right.$$

$$\left. - \frac{a_2 e^{-a_3\theta}}{(n^2+a_3^2)} [a_3 \sin n\theta + n \cos n\theta] \Big|_{\alpha_1}^{\pi} \right], \quad n \neq 1$$

$$y_n = \frac{2}{M\pi} \left[\frac{a_1}{2} \left[\frac{\cos(\overline{n-1}\ \theta+\phi)}{(n-1)} - \frac{\cos(\overline{n+1}\ \theta-\phi)}{(n+1)} \right] - \frac{a_4}{n} \sin n\theta \right.$$

$$\left. + \frac{a_2 e^{-a_3\theta}}{(n^2+a_3^2)} [n \sin n\theta - a_3 \cos n\,\theta] \Big|_{\alpha_1}^{\pi} \right], \quad n \neq 1$$

$$I_n = \sqrt{\frac{1}{2} (x_n^2 + y_n^2)}$$

Fundamental Input Current, I_1:

$$x_1 = \frac{2}{M\pi} \left[\frac{a_1}{2} \left[\theta \cos \phi - \frac{1}{2} \sin (2\theta-\phi)\right] - \frac{a_2 e^{-a_3\theta}}{(1+a_3^2)} \right.$$

$$\left. (a_3 \sin \theta + \cos \theta) + a_4 \cos \theta \Big|_{\alpha_1}^{\pi} \right]$$

$$y_1 = \frac{2}{M\pi} \left[\frac{a_1}{2} \left(- \theta \sin \phi - \frac{1}{2} \cos (2\theta - \phi)\right) + \frac{a_2 e^{-a_3 \theta}}{(1 + a_3 2)} \right.$$

$$\left. (\sin \theta - a_3 \cos \theta) + a_4 \cos \theta \, \Big|_{\alpha_1}^{\pi} \right]$$

$$y_1 = \frac{2}{M\pi} \left[\frac{a_1}{2} \left(- \phi \sin \phi - \frac{1}{2} \cos (2\theta - \phi)\right] + \frac{a_2 e^{-a_3 \theta}}{(1 + a_3^{\,2})} \right.$$

$$\left. (\sin \theta - a_3 \cos \theta) - a_4 \sin \theta \, \Big|_{\alpha_1}^{\pi} \right]$$

$$I_1 = \sqrt{\frac{1}{2} \left(x_1^{\,2} + y_1^{\,2}\right)}$$

Input Power Factor, λ:

$$\lambda = \frac{x_1}{\sqrt{2}\, I}$$

Input Displacement Factor, δ:

$$\delta = \frac{x_1}{\sqrt{x_1^{\,2} + y_1^{\,2}}} = \frac{x_1}{I_i \sqrt{2}} = \frac{x_1}{\sqrt{2}\, I} \; \frac{I}{I_1} = \lambda \frac{I}{I_1}$$

Input Harmonic Factor, h:

$$h = \sqrt{\left(\frac{I}{I_1}\right)^2 - 1}$$

losses in the motor armature: $I_{a_{rms}}^{\ 2} R_a = P_A$

losses in the converter: $4 V_D I_{av} = P_C$

losses in the transformer: $I^2 R_T = P_T$

total losses in the system: $P_L = P_A + P_C + P_T$

overall efficiency, η: $\eta = \dfrac{E_b I_{av}}{E_b I_{av} + P_L}$

Case 2

$\boxed{0.5 < E_a < 1.0 \text{ pu}}$ $\alpha_1 = 0 \ , \ 0 < \alpha_2 < \pi$ $\boxed{\alpha_2 = \cos^{-1} (4E_a - 3)}$

$$i_a = a_1 \sin(\theta - \phi) + a_6 e^{-a_3\theta} - a_4 \ , \ 0 < \theta < \alpha_2$$

$$= 2a_1 \sin(\theta - \phi) + a_7^{-a_3\theta} - a_4 \ , \alpha_2 < \theta < \pi$$

where: $a_6 = (I_0 + a_4 + a_1 \sin \phi)$

$$a_7 = (I\alpha_2 - a_4 \ \ 2a_1 \sin(\alpha_2 - \phi)) e^{a_3\alpha_2}$$

$$i_p = \frac{i_a}{M} = \frac{1}{M}[\ a_1 \sin(\theta-\phi) + a_6 e^{-a_3\theta} - a_4] \quad , 0 < \theta < \alpha_2$$

$$= \frac{2i_a}{M} = \frac{2}{M}[2a_1 \sin(\theta-\phi) + a_7 e^{-a_3 0} - a_4], \alpha_2 < \theta < \pi$$

Motor Average Current, I_{av}:

$$I_{av} = \frac{1}{\pi}[\int_0^{\alpha_2} i_a \, d\theta + \int_{\alpha_2}^{\pi} i_a \, d\theta\ ]$$

$$= \frac{1}{\pi}[\ a_1 [\cos(\alpha_2-\phi) + 3\cos\phi] + \frac{a_6}{a_3}(1-e^{-a_3\alpha_2})$$

$$+ \frac{a_7}{a_3}(e^{-a_3\alpha_2} - e^{-a_3\pi}) - a_4\pi\ ]$$

Motor RMS Current, I_{rms}:

$$I_{a_{rms}} = \sqrt{\frac{1}{\pi}[\ f_1(\alpha_2) - f_1(0) + g_1(\pi) - g_1(\alpha_2)\ ]}$$

where: $f_1(0) = [\ (\frac{a_1^2}{2} + a_4^2)\theta - \frac{a_1^2}{4}\sin(2\theta-2\phi) - \frac{a_6^2}{2a_3}e^{-2a_3\theta}$

$$- \frac{2a_1a_6}{1+a_3^2} e^{-a_3\theta} [\ a_3 \sin(\theta-\phi) + \cos(\theta-\phi)\ ]$$

$$+ 2\,a_1a_4\cos(\theta-\phi) + \frac{2a_6a_4}{a_3} e^{-a_3\theta}\ ]$$

$$g_1(\theta) = [\ (2a_1^{\ 2} + a_4^{\ 2})\ \theta - a_1^{\ 2} \sin (2\theta - 2\phi) - \frac{a_7^{\ 2}}{2a_3} e^{-2a_3\theta}$$

$$- \frac{4a_1a_7}{1+a_3^{\ 2}} e^{-a_3\theta} \ [a_3 \sin (\theta-\phi) + \cos (\theta - \phi)$$

$$+ 4a_1a_4 \cos (\theta-\phi) + \frac{2a_7a_4}{a_3} e^{-a_3\theta} \ ]$$

Input RMS Current, I:

$$I = \frac{1}{M} \sqrt{\frac{1}{\pi} [\int_0^{\alpha_2} i_a^{\ 2}\, d\theta + \int_{\alpha_2}^{\pi} 4i_a^{\ 2}\, d\theta\ ]}$$

$$\therefore\ I = \frac{1}{M} \sqrt{\frac{1}{\pi} [\ f_1(\alpha_2) - f_1(0) + 4[g_1(\pi) - g_1(\alpha_2)]\ ]}$$

Input Harmonic Currents, I_n:

$$x_n = \frac{2}{M\pi} [\int_0^{\alpha_2} i_a \sin n\theta + \int_{\alpha_2}^{\pi} 2i_a \sin n\theta\ ]\ d\theta$$

$$y_n = \frac{2}{M\pi} [\int_0^{\alpha_2} i_a (\cos n\theta + \int_{\alpha_2}^{\pi} 2i_a \cos n\theta\ ]\ d\theta$$

$$x_n = \frac{2}{M\pi} [\ f_2\ (\alpha_2) - f_2(0) + g_2(\pi) - g_2(\alpha_2)\ ],\quad n \neq 1$$

$$y_n = \frac{2}{M\pi} [{}_3f\ (\alpha_2) - f_3(0) + g_3(\pi) - g_3(\alpha_2) \quad ,\quad n \neq 1$$

where:

$$f_2(\theta) = \frac{a_1}{2}\left[\frac{\sin(\overline{n-1}\,\theta + \phi)}{(n-1)} - \frac{\sin(\overline{n+1}\,\theta - \phi)}{(n+1)}\right] - \frac{a_6\, e^{-a_3\theta}}{n^2 + a_3^2}$$

$$(a_3 \sin n\theta + n \cos n\theta) + \frac{a_4}{n} \cos n\theta$$

$$g_2(\theta) = 2a_1\left[\frac{\sin(\overline{n-1}\,\theta + \phi)}{(n-1)} - \frac{\sin(\overline{n+1}\,\theta - \phi)}{(n+1)}\right] - \frac{2a_7\, e^{-a_3\theta}}{n^2 + a_3^2}$$

$$(a_3 \sin n\theta + n \cos n\theta) + \frac{2a_4}{n} \cos n\theta$$

$$f_3(\theta) = \frac{a_1}{2}\left[\frac{\cos(\overline{n-1}\,\theta + \phi)}{(n-1)} - \frac{\cos(\overline{n+1}\,\theta - \phi)}{(n+1)}\right] + \frac{a_6\, e^{-a_3\theta}}{n^2 + a_3^2}$$

$$(n \sin n\theta + a_3 \cos n\theta) + \frac{2a_4}{n} \sin n\theta$$

$$g_3(\theta) = 2a_1\left[\frac{\sin(\overline{n-1}\,\theta + \phi)}{(n-1)} - \frac{\sin(\overline{n+1}\,\theta - \phi)}{(n+1)}\right] - \frac{a_7\, e^{-a_3\theta}}{n^2 + a_3^2}$$

$$(n \sin n\theta + a_3 \cos n\theta) + \frac{2a_4}{n} \sin n\theta$$

$$\therefore\ In = \sqrt{\frac{1}{2}\left(x_n^{\ 2} + y_n^{\ 2}\right)}$$

RMS Fundamental Input Current, I_1:

$$x_1 = \frac{2}{M\pi} [\ f_4\ (\alpha_2) = f_4(0) + g_4\ (\pi) - g_4\ (\alpha_2)\ ]$$

$$y_1 = \frac{2}{M\pi} [\ f_5\ (\alpha_2) = f_5(0) + g_5\ (\pi) - g_5\ (\alpha_2)\ ]$$

where: $$f_4(\theta) = \frac{a_1}{2} [\ \theta \cos \phi - \frac{1}{2} \sin (2\theta - \phi)\ ]\ \frac{a_6\ e^{-a_3\theta}}{1 + a_3^2}$$

$$(a_3 \sin \theta + \cos \theta) + a_4 \cos \theta$$

$$g_4(\theta) = 2a_1\ [\ \theta \cos \phi - \frac{1}{2} \sin (2\theta - \phi)\ ]\ \frac{a_7\ e^{-a_3\theta}}{1 + a_3^2}$$

$$(a_3 \sin \theta + \cos \theta) + 2a_4 \cos \theta$$

$$f_5(\theta) = \frac{a_1}{2} [- \theta \cos \phi - \frac{1}{2} \sin (2\theta - \phi)\ ] + \frac{a_6\ e^{-a_3\theta}}{1 + a_3^2}$$

$$(\sin \theta - a_3 \cos \theta) - a_4 \cos \theta$$

$$g_5(\theta) = 2a_1\ [- \theta \cos \phi - \frac{1}{2} \sin (2\theta - \phi)\ ] + \frac{a_7\ e^{-a_3\theta}}{1 + a_3^2}$$

$$(\sin \theta + a_3 \cos \theta) - 2a_4 \cos \theta$$

$$I_1 = \sqrt{\frac{1}{2}\left(x_1^{\,2} + y_1^{\,2}\right)}$$

Then compute λ, δ, h and η.

A.2 ANALYSIS OF THREE-SERIES BRIDGE PHASE-CONTROLLED SEMICONVERTERS SUPPYING A SERIES MOTOR

A.2.1 General

The connection diagram for a three-bridge converter supplying a series motor is given in Figure A.2.1. The voltage and current waveforms for the converter ouptut for the three cases:

case 1: $0 \leq E_a \leq 1/3$ pu

case 2: $1/3 \leq E_a \leq 2/3$ pu

case 3: $2/3 \leq E_a \leq 1.0$ pu

are given in Figures A.2.2, A.2.3 and A.2.4.

The symbols and computer flow chart are similar to those presented in Section A.1. The governing equations to compute the PCU performance are presented in this appendix.

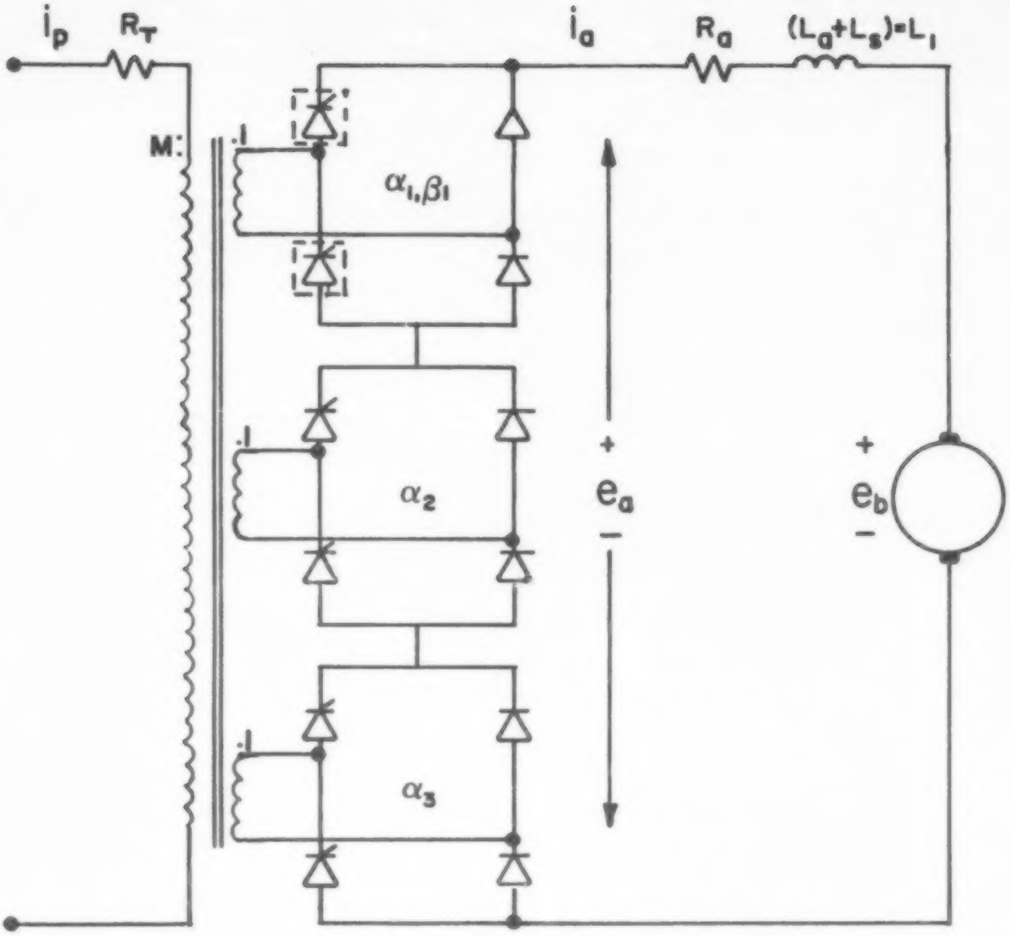

Figure A.2.1 Three-series bridge phase-controlled semiconverters supplying a dc series motor

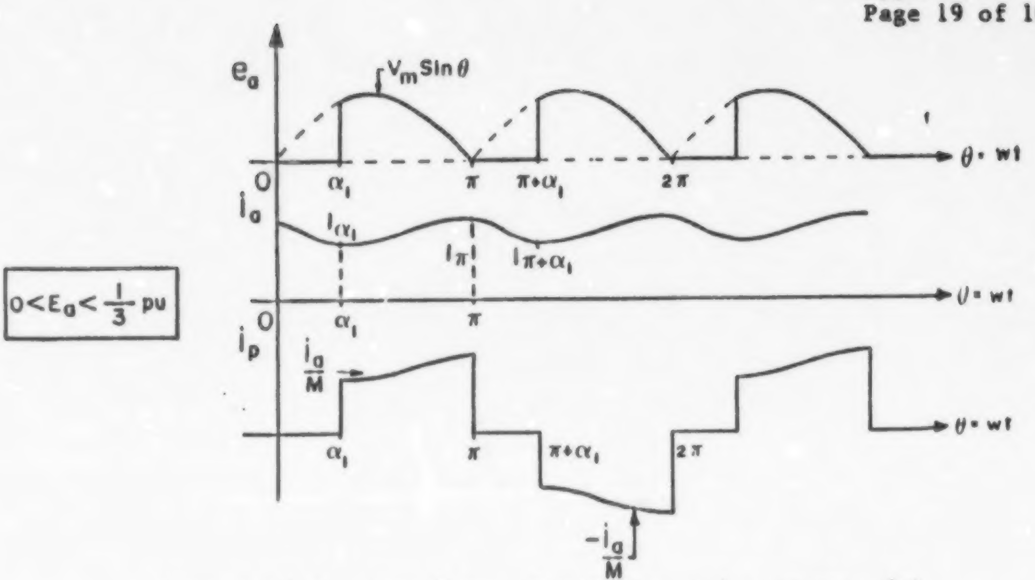

Figure A.2.2 Waveforms of voltages and currents with $0 \le E_a \le 1/3$ pu, phase control of one bridge with the other two bridges turned off

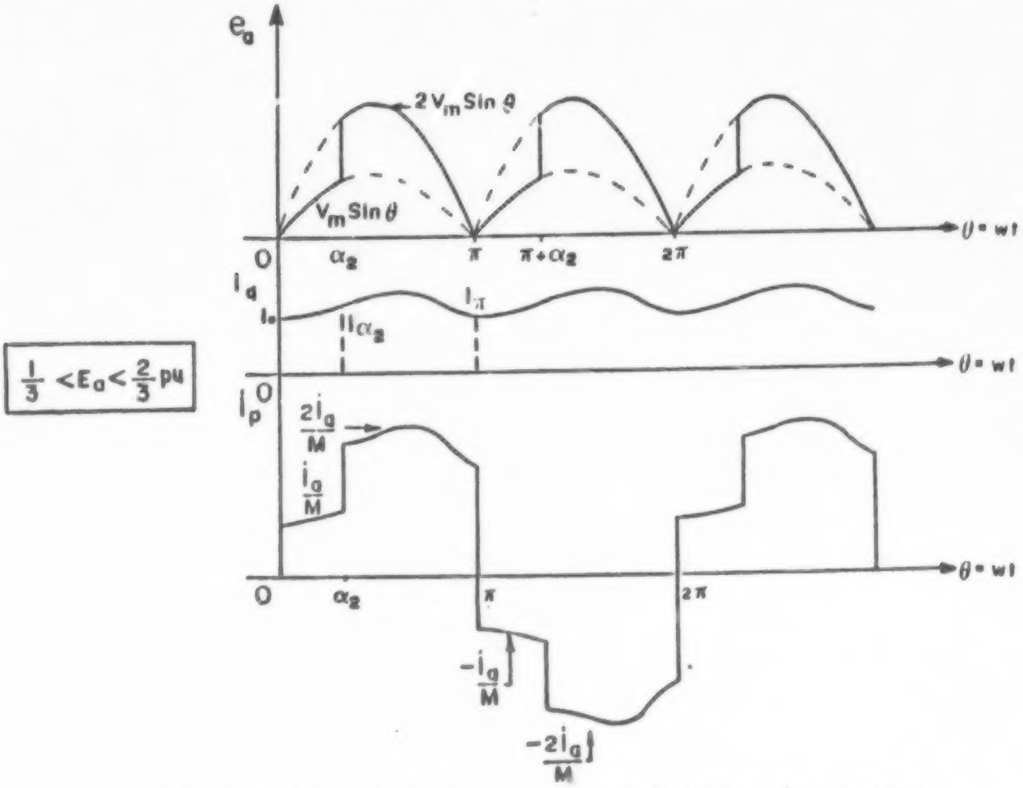

Figure A.2.3 Waveforms of the voltages and currents with 1/3 pu $\le E_a \le$ 2/3 pu, phase control of one bridge, with one bridge fully turned on and the other turned off

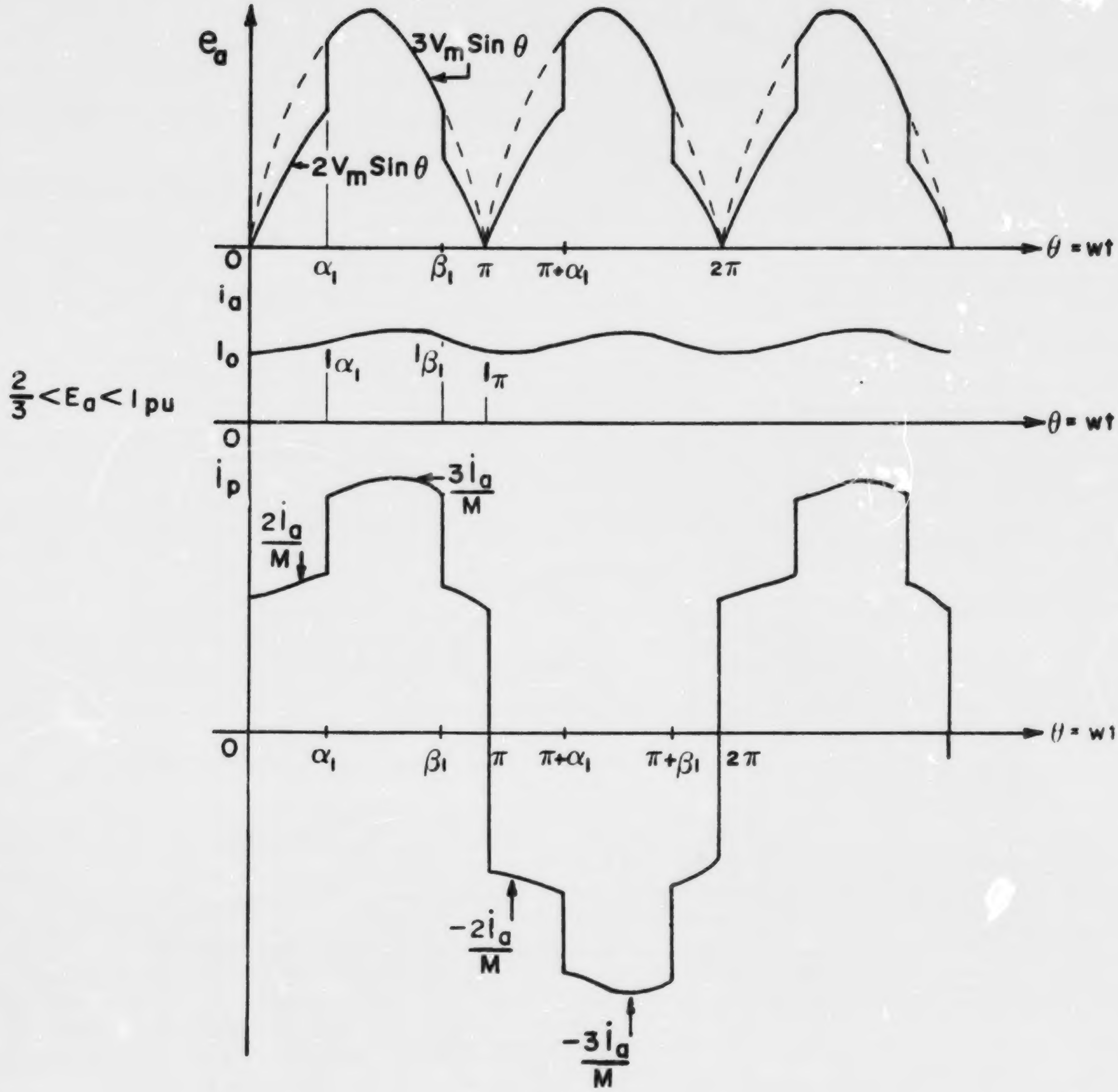

Figure A.2.4 Waveforms of voltages and currents with $2/3 \le E_a \le 1.0$ pu, phase control of one bridge, with two bridges fully turned on

A.2.2 Analysis

$$E_{max} = \frac{6v_m}{\pi} = 1.0 \text{ pu}$$

Case 1: Phase control of one bridge with the other two bridges turned off

$$\boxed{0 < E_a < \frac{1}{3} \text{ pu:}} \qquad \begin{array}{c} 0 < \alpha_1 < \pi \\ \alpha_2 = \alpha_3 = \pi \end{array} \qquad \boxed{\alpha_1 = \cos^{-1}(6E_a - 1)}$$

$$i_a = b_1 \sin(\theta - \phi) + b_2 e^{-b_3\theta} - b_4 \text{ , } \alpha_1 < \theta < \pi$$

$$= b_5 e^{-b_3\theta} - b_4 \qquad , \pi < \theta < \pi + \underbrace{\alpha_1}_{\beta \text{ for discontinuous current}}$$

where: $\theta = \omega t$

$$b_1 = \frac{V_m}{Z_1}$$

$$b_2 = [\, b_4 + I\alpha_1 - b_1 \sin(\alpha_1 - \theta) \,]\, e^{b_3\alpha_1}$$

$$b_3 = \frac{R_1}{\omega L_1}$$

$$b_4 = \frac{K_{res}N}{R_1}$$

$$b_5 = (I_\pi + b_4)\, e^{b_3\pi}$$

$R_1 = R_a + K_{af} N + R_s$

$L_1 = L_S + L_a$

$Z_1 = \sqrt{R_1^2 + (\omega L_1)^2}$

$\phi = \tan^{-1} (\omega L_1/R_1)$

N = motor speed

K_{res} = back emf constant due to residual flux

K_{af} = back emf constant due to series field

$i_p = 0 \quad , 0 < 0 < \alpha_1$

$= \frac{i_a}{M} , \alpha_1 < \theta < \pi$

Average Motor Current, I_{av}:

$$I_{av} = \frac{1}{\pi} \left[\int_{\alpha_1}^{\pi} i_a \, d\theta + \int_{\pi}^{\pi+\alpha_1} i_a \, d\theta \right]$$

$$= \frac{1}{\pi} [p_1(\pi) - p_1(\alpha_1) + q_1(\pi+\alpha_1) - q_1(\pi)$$

where: $p_1(\theta) = - b_1 \cos (\theta-\phi) - \frac{b_2}{b_3} e^{-b_3\theta} - b_4\theta$

$q_1(\theta) = - \frac{b_5}{b_3} e^{-b_3\theta} - b_4\theta$

RMS Motor Current, $I_{a_{rms}}$:

$$I_{a_{rms}} = \sqrt{\frac{1}{} \left[\int_{\alpha_1} i_a^2 \, d0 + \int_{\pi}^{\pi+\alpha_1} i_a^2 \, d\theta \right]}$$

$$= \sqrt{\frac{1}{\pi} \left[p_2(\pi) - p_2(\alpha_1) + q_2(\pi-\alpha_1) - q_2(\pi) \right]}$$

where: $$p_2(\theta) = \left(\frac{b_1^2}{2} + b_4^2\right) \theta - \frac{b_1^2}{4} \sin(2\theta - 2\phi) - \frac{b_2^2}{2b_3} e^{-2b_3\theta}$$

$$- \frac{2b_1b_2}{1+b_3^2} e^{-b_3\theta} \left[b_3 \sin(\theta-\phi) + \cos \theta-\phi \right]$$

$$+ 2b_1b_4 \cos(\theta-\phi) + \frac{2b_2b_4}{b_3} e^{-b_3\theta}$$

$$q_2(\theta) = -\frac{b_5^2}{2b_3} e^{-2b_3\theta} + b_4^2\theta + \frac{2b_4b_5}{b_3} e^{-b_3\theta}$$

Input RMS Current, I:

$$I = \frac{1}{M} \sqrt{\frac{1}{\pi} \int_{\alpha_1}^{\pi} i_a^2 \, d\theta}$$

$$= \frac{1}{M} \sqrt{\frac{1}{\pi} \left[p_2(\pi) - p_2(\alpha_1) \right]}$$

Input Harmonic Currents, I_n:

$$x_n = \frac{2}{\pi} \int_{\alpha_1}^{\pi} i_p \sin n\theta \, d\theta$$

$$y_n = \frac{2}{\pi} \int_{\alpha_1}^{\pi} i_p \cos n\theta \, d\theta$$

$$\therefore\ x_n = \frac{2}{M\pi} [\ p_3(\pi) - p_3(\alpha_1)\ ]$$

$$y_n = \frac{2}{M\pi} [\ q_3(\pi) - q_3(\alpha_1)\ ]$$

where: $$p_3(\theta) = \frac{b_1}{2} [\ \frac{\sin (\overline{n-1}\ \theta + \phi)}{(n-1)} - \frac{\sin (\overline{n+1}\ \theta - \phi)}{n+1}\ ] - \frac{b_2\ e^{-b_3\theta}}{(n^2+b_3{}^2)}$$

$$[\ b_3 \sin n\theta + n \cos n\theta\ ] + \frac{b_4}{n} \cos n\theta$$

$$q_3(\theta) = \frac{b_1}{2} [\ \frac{\cos (\overline{n-1}\ \theta + \phi)}{n-1} - \frac{\cos (\overline{n+1}\ \theta - \phi)}{n+1}\ ] + \frac{b_2\ e^{-b_3\theta}}{(b_3{}^2 + n^2)}$$

$$[\ n \sin n\theta - b_3 \cos n\theta\ ] + \frac{b_4}{n} \sin n\theta$$

$$I_n = \sqrt{\frac{1}{2} (x_n{}^2 + y_n{}^2)}\ ,\ n \neq 1$$

RMS Fundamental Input Current, I_1:

$$x_1 = \frac{2}{M\pi} [\ p_4\ (\pi) - p_4\ (\alpha_1)\ ]$$

$$y_1 = \frac{2}{M\pi} [\ q_4\ (\pi) - q_4\ (\alpha_1)\ ]$$

where: $$p_4(\theta) = \frac{b_1}{2} [\ \theta \cos \phi - \frac{1}{2} \sin (2\theta - \phi)\ ] - \frac{b_2\ e^{-b_3\theta}}{1 + b_3^2}$$

$$[\ b_3 \sin \theta + \cos \theta\ ] + b_4 \cos \theta$$

$$q_4(\theta) = \frac{b_1}{2} [\ -\theta \sin \phi - \frac{1}{2} \cos (2\theta - \phi)\ ] + \frac{b_2\ e^{-b_3\theta}}{1 + b_3^2}$$

$$[\ \sin \theta - b_3 \cos \theta\ ] - b_4 \sin \theta$$

$$\therefore\ I_1 = \sqrt{\frac{1}{2} (x_1^2 + y_1^2)}$$

Compute λ, δ, h and η as defined before in Appendix A.

Case 2: Phase control of one bridge with one bridge fully turned on and the other turned off.

$$\boxed{\frac{1}{3} < E_a < \frac{2}{3}\ \text{pu}} \qquad \begin{array}{l} \alpha_1 = 0\ \text{(on)}\ 0 < \alpha_2 < \pi \\ \alpha_3 = t\ \text{(off)} \end{array} \qquad \boxed{\alpha_2 = \cos^{-1}\ (6E_a - 3)}$$

$$i_a = b_1 \sin (\theta - \phi) + b_6\ e^{-b_3\theta} - b_4\ ,\ 0 < 0 < \alpha_2$$

$$= 2b_1 \sin (\theta - \phi) + b_7\ e^{-b_3\theta} - b_4, \alpha_2 < \theta < \pi$$

where: $b_6 = I_0 + b_4 + b_1 \sin \phi$

$$b_7 = [\ I\alpha_2 + b_4 - 2b_1 \sin (\alpha_2 - \phi)\ ]\ e^{b_3 \alpha_2}$$

$$i_p = \frac{i_a}{M} = \frac{1}{M} [\ b_1 \sin (\theta - \phi) + b_6\ e^{-b_3 \theta} - b_4\ ] \quad , 0 < \theta < \alpha_2$$

$$= \frac{2i_a}{M} = \frac{2}{M} [\ 2b_1 \sin (\theta - \phi) + b_7\ e^{-b_3 \theta} - b_4\ ] \ , \alpha_2 < \theta < \pi$$

Motor Average Current, I_{av}:

$$I_{av} = \frac{1}{\pi} [\int_0^{\alpha_2} i_a\ d\theta + \int_{\alpha_2}^{\pi} i_a\ d\theta\ ]$$

$$= \frac{1}{n} [\ p_5\ (\alpha_2) - p_5\ (0) + q_5\ (\pi) - q_5\ (\alpha_2)\ ]$$

where: $p_5(\theta) = -\ b_1 \cos (\theta - \phi) - \frac{b_6}{b_3}\ e^{-b_3 \theta} - b_4 \theta$

$$q_5(\theta) = -\ 2b_1 \cos (\theta - \phi) - \frac{b_7}{b_3}\ e^{-b_3 \theta} - b_4\ \theta$$

Motor RMS Current, $I_{a_{rms}}$:

$$I_{a_{rms}} = \sqrt{\frac{1}{\pi} [\int_0^{\alpha_2} {i_a}^2\ d\theta + \int_{\alpha_2} {i_a}^2\ d\theta\ ]}$$

$$= \sqrt{\frac{1}{\pi} [\ p_6(\alpha_2) - p_6(0) + q_6(\pi) - q_6(\alpha_2)\ ]}$$

where: $$p_6(\theta) = (\frac{b_1^{\ 2}}{2} + b_4^{\ 2})\ \theta - \frac{b_1^{\ 2}}{4} \sin(2\theta - 2\phi) - \frac{b_6^{\ 2}}{2b_3} e^{-2b_3\theta}$$

$$- \frac{2b_1b_6}{1+b_3^{\ 2}} e^{-b_3\theta} [\ b_3 \sin(\theta-\phi) + \cos(\theta-\phi)\ ]$$

$$+ 2b_1b_4 \cos(\theta-\phi) + \frac{2b_4b_6}{b_3} e^{-b_3\theta}$$

$$q_6(\theta) = (2b_1^{\ 2} + b_4^{\ 2})\ \theta - b_1^{\ 2} \sin(2\theta - 2\phi) - \frac{b_7^{\ 2}}{2b_3} e^{-2b_3\theta}$$

$$- \frac{4b_1b_7}{1+b_3^{\ 2}} e^{-b_3\theta} [\ b_3 \sin(\theta-\phi) + \cos(\theta-\phi)$$

$$+ 4b_1b_4 \cos(\theta-\phi) + \frac{2b_4b_7}{b_3} e^{-b_3\theta}$$

Input RMS Current, I:

$$I = \frac{1}{M} \sqrt{\frac{1}{\pi} [\int_0^{\alpha_2} i_a^{\ 2}\ d\theta + \int_{\alpha_2}^{\pi} 4\ i_a^{\ 2}\ d\theta\ ]}$$

$$\therefore\ I = \frac{1}{M} \sqrt{\frac{1}{\pi} [\ p_6(\alpha_2) - p_6(\theta) + r\ q_6(\pi) - 4\ q_6\ (\alpha_2)\ ]}$$

Input Harmonic Currents, I_n:

$$x_n = \frac{2}{M\pi} \left[\int_0^{\alpha_2} i_a \sin n\theta + \int_{\alpha_2}^{\pi} 2i_a \sin n\theta \right] d\theta$$

$$= \frac{2}{M\pi} \left[p_7(\alpha_2) - p_7(0) + q_7(\pi) - q_7(\alpha_2) \right]$$

$$y_n = \frac{2}{M\pi} \left[\int_0^{\alpha_2} i_a \cos n\theta + \int_{\alpha_2} 2i_a \cos n\theta \right] d\theta$$

$$= \frac{2}{M\pi} \left[p_8(\alpha_2) - p_8(0) + q_8(\pi) - q_8(\alpha_2) \right]$$

where: $$p_7(\theta) = \frac{b_1}{2} \left[\frac{\sin(\overline{n-1}\,\theta + \phi)}{(n-1)} - \frac{\sin(\overline{n+1}\,\theta - \phi)}{(n+1)} \right] - \frac{b_6\, e^{-b_3\theta}}{n^2 + b_3^2}$$

$$(b_3 \sin n\theta + n \cos n\theta) + \frac{b_4}{n} \cos n\theta$$

$$q_7(\theta) = 2b_1 \left[\frac{\sin(\overline{n-1}\,\theta + \phi)}{(n-1)} - \frac{\sin(\overline{n+1}\,\theta - \phi)}{(n+1)} \right] - \frac{2b_7\, e^{-b_3\theta}}{n^2 + b_3^2}$$

$$(b_3 \sin n\theta + n \cos n\theta) + \frac{2b_4}{n} \cos n\theta$$

$$p_8(\theta) = \frac{b_1}{2} \left[\frac{\cos(\overline{n-1}\,\theta + \phi)}{(n-1)} - \frac{\cos(\overline{n+1}\,\theta - \phi)}{(n+1)} \right] + \frac{b_6\, e^{-b_3\theta}}{n^2 + b_3^2}$$

$$(n \sin n\theta - b_3 \cos n\theta) - \frac{b_4}{n} \sin n\theta$$

$$q_8(\theta) = 2b_1 \left[\frac{\cos(\overline{n-1}\ \theta + \phi)}{(n-1)} - \frac{\cos(\overline{n+1}\ \theta - \phi)}{(n+1)} \right] + \frac{2b_7 e^{-b_3\theta}}{n^2 + b_3^2}$$

$$(n \sin n\theta - b_3 \cos n\theta) - \frac{2b_4}{n} \sin n\theta$$

$$\therefore\ I_n = \sqrt{\frac{1}{2}(x_n^2 + y_n^2)}$$

Fundamental Input RMS Current, I_1:

$$x_1 = \frac{2}{M\pi} [\ p_9(\alpha_2) - p_9(0) + q_9(\pi) - q_9(\alpha_2)\ ]$$

$$y_1 = \frac{2}{M\pi} [\ p_{10}(\alpha_2) - p_{10}(0) + q_{10}(\pi) = q_{10}(\alpha_2)$$

where: $$p_9(\theta) = \frac{b_1}{2} [\ \theta \cos \phi - \frac{1}{2} \sin(2\theta - \phi)\ ] - \frac{b_6 e^{-b_3\theta}}{1 + b_3^2}$$

$$(b_3 \sin \theta + \cos \theta) + b_4 \cos \theta$$

$$q_9(\theta) = 2b_1 [\ \theta \cos \phi - \frac{1}{2} \sin(2\theta - \phi) - \frac{2b_7 e^{-b_3\theta}}{1 + b_3^2}$$

$$(b_3 \sin \theta + \cos \theta) + 2b_4 \cos \theta$$

$$p_{10}(\theta) = \frac{b_1}{2} [\ -\theta \sin \phi - \frac{1}{2} \cos(2\theta - \phi)\ ] + \frac{b_6 e^{-b_3\theta}}{1 + b_3^2}$$

$$(\sin \theta - b_3 \cos \theta) - b_4 \sin \theta$$

$$q_{10}(\theta) = 2b_1 \left[\theta - \sin\phi - \frac{1}{2}\cos(2\theta-\phi) \right] + \frac{2b_7 e^{-b_3\theta}}{1+b_3^2}$$

$$(\sin\theta - b_3\cos\theta) - 2b_4 \sin\theta$$

$$I_1 = \sqrt{\frac{1}{2}(x_1^2 + y_1^2)}$$

Compute λ, δ, h and η.

Case 3: Phase control of one bridge with two bridges fully turned on.

$$\boxed{\frac{2}{3} < E_a < 1 \text{ pu:}} \quad \alpha_1 = \alpha_2 = 0,\ 0 < \alpha_3 < \pi \quad \boxed{\alpha_3 = \cos^{-1}(6E_a-5)}$$

$$i_a = 2b_1 \sin(\theta-\phi) + b_8 e^{-b_3\theta} - b_4,\ 0 < \theta < \alpha_3$$

$$= 3b_1 \sin(\theta-\phi) + b_9 e^{-b_3\theta} - b_4,\ \alpha_3 < \theta < \pi$$

where: $b_8 = I_0 + b_4 + 2b_1 \sin\phi$

$$b_9 = [\, I_{\alpha_3} + b_4 - 3b_1 \sin(\alpha_3 - 0) \,]\, e^{b_3\alpha_3}$$

$$i_p = \frac{2i_a}{M} = \frac{2}{M}[\, 2b_1 \sin(\theta-\phi) + b_8 e^{-b_3\theta} - b_4 \,],\ 0 < \theta < \alpha_3$$

$$= \frac{3i_a}{M} = \frac{3}{M}[\, 3b_1 \sin(\theta-\phi) + b_9 e^{-b_3\theta} - b_4 \,],\ \alpha_3 < \theta < \pi$$

Motor Average Current, I_{av}:

$$I_{av} = \frac{1}{\pi} [\, p_{11}(\alpha_3) - p_{11}(0) + q_{11}(\pi) - q_{11}(\alpha_3) \,]$$

$$p_{11}(\theta) = -\, 2b_1 \cos(\theta - \phi) - \frac{b_8}{b_3} e^{-b_3\theta} - b_4\theta$$

$$q_{11}(\theta) = -\, 3b_1 \cos(\theta - \phi) - \frac{b_9}{b_3} e^{-b_3\theta} - b_4\theta$$

Motor RMS Current, $I_{a_{rms}}$:

$$I_{a_{rms}} = \sqrt{\frac{1}{\pi} [\, p_{12}(\alpha_3) - p_{12}(0) + q_{12}(\pi) - q_{12}(\alpha_3) \,]}$$

$$p_{12}(\theta) = (2b_1^{\,2} + b_4^{\,2})\,\theta = b_1^{\,2} \sin(2\theta - 2\phi) - \frac{b_8^{\,2}}{2b_3} e^{-2b_3\theta} - \frac{4b_1 b_8}{1 + 6_3^{\,2}} e^{-b_3\theta}$$

$$[\, b_3 \sin(\theta - \phi) + \cos(\theta - \phi) + 4b_1 b_4 \cos(\theta - \phi) + \frac{2b_4 b_8}{b_3} e^{-b_3\theta}$$

$$q_{12}(\theta) = \frac{9}{2} b_1^{\,2} + b_4^{\,2})\,\theta - \frac{9}{4} b_1^{\,2} \sin(2\theta - 2\phi) - \frac{b_9^{\,2}}{2b_3} e^{-2b_3\theta} - \frac{6b_1 b_9}{1 + b_3^{\,2}} e^{-b_3\theta}$$

$$[\, b_3 \sin(\theta - \phi) + \cos(\theta - \phi) \,] + 6b_1 b_4 \cos(\theta - \phi) + \frac{2b_4 b_9}{b_3} e^{-b_3\theta}$$

Input RMS Current, I:

$$I = \frac{1}{M}\sqrt{\frac{1}{\pi}\left[\ 4\ (p_{12}(\alpha_3) - p_{12}(0)\ \right] + 9\ \left[\ q_{12}(\pi) - q_{12}(\alpha_3)\ \right]}$$

Input RMS Harmonic Currents, I_n ($n \neq 1$):

$$x_n = \frac{2}{M\pi}\left[\ p_{13}(\alpha_3) - p_{13}(0) - q_{13}(\pi) - q_{13}(\alpha_3)\ \right]$$

$$y_n = \frac{2}{M\pi}\left[\ p_{14}(\alpha_3) - p_{14}(0) - q_{14}(\pi) = q_{14}(\alpha_3)\ \right]$$

$$p_{13}(\theta) = 2b_1\ \left[\ \frac{\sin\ (\overline{n-1}\ \theta + \phi)}{(n-1)}\quad \frac{\sin\ (\overline{n+1}\ \theta - \phi)}{(n+1)}\ \right] - \frac{2b_8\ e^{-b_3\theta}}{n^2 + b_3{}^2}$$

$$(b_3\ \sin\ n\theta + n\ \cos\ n\theta) + \frac{3b_4}{n}\cos\ n\theta$$

$$q_{13}(\theta) = \frac{9b_1}{2}\ \left[\ \frac{\sin\ (\overline{n-1}\ \theta + \phi)}{(n-1)} - \frac{\sin\ (\overline{n+1}\ \theta - \phi)}{(n+1)}\ \right] - \frac{3b_9\ e^{-b_3\theta}}{n^2 + b_3{}^2}$$

$$(b_3\ \sin\ n\theta + n\ \cos\ n\theta) + \frac{3b_4}{n}\cos\ n\theta$$

$$p_{14}(\theta) = 2b_1\ \left[\ \frac{\cos\ (\overline{n-1}\ \theta - \phi)}{n-1}\quad \frac{\cos\ (\overline{n+1}\ \theta - \phi)}{n+1}\ \right] + \frac{2b_8\ e^{-b_3\theta}}{n^2 + b_3{}^2}$$

$$(n\ \sin\ n\theta - b_3\ \cos\ n\theta) - \frac{2b_4}{n}\sin\ n\theta$$

$$q_{14}(\theta) = \frac{9b_1}{2} \left[\frac{\cos(\overline{n-1}\,\theta + \phi)}{n-1} \quad \frac{\cos(\overline{n+1}\,\theta - \phi)}{n+1} \right] + \frac{3b_9\, e^{-b_3\theta}}{n^2 + b_3^2}$$

$$(n \sin n\theta - b_3 \cos n\theta) - \frac{3b_4}{n} \sin n\theta$$

Input RMS Fundamental Current, I_1:

$$x_1 = \frac{2}{M\pi} \left[p_{15}(\alpha_3) - p_{15}(0) + q_{15}(\pi) - q_{15}(\alpha_3) \right]$$

$$y_1 = \frac{2}{M\pi} \left[p_{16}(\alpha_3) - p_{16}(0) + q_{16}(\pi) - q_{16}(\alpha_3) \right]$$

$$p_{15}(\theta) = 2b_1 \left[0 \cos\phi - \frac{1}{2} \sin(2\theta - \phi) \right] - \frac{2b_8\, e^{-b_3\theta}}{1+b_3^2}$$

$$(b_3 \sin\theta + \cos\theta) + 2b_4 \cos\theta$$

$$q_{15}(\theta) = \frac{9b_1}{2} \left[\theta \cos\phi - \frac{1}{2} \sin(2\theta - \phi) \right] - \frac{3b_9\, e^{-b_3\theta}}{1+b_3^2}$$

$$(b_3 \sin\theta + \cos\theta) + 3b_4 \cos\theta$$

$$p_{16}(\theta) = 2b_1 \left[-\theta \sin\phi - \frac{1}{2} \cos(2\theta - \phi) \right] + \frac{2b_8 e^{-b_3\theta}}{1+b_3^2}$$

$$(\sin\theta - b_3 \cos\theta) - 2b_4 \sin\theta$$

$$q_{16}(0) = \frac{9b_1}{2} \left[- \theta \sin \phi - \frac{1}{2} \cos (2\theta - 2\phi) \right] + \frac{3b_3 \, e^{-b_3 \theta}}{1 + b_3^2}$$

$$(\sin \theta - b_3 \cos \theta) - 3b_4 \sin \theta$$

$$\therefore \; I_1 = \sqrt{\frac{1}{2} (x_1^2 + y_1^2}$$

Now compute λ, δ, h and η.

Losses: $P_e = 6V_D \, I_{av}$

A.3 ANALYSIS OF TWO-SERIES BRIDGE SEMICONVERTERS WITH SECTOR CONTROL SUPPLYING A SEPARATELY-EXCITED DC MOTOR

A.3.1 General

An improvement over the phase angle control scheme can be made to the input power factor through sector control of semiconverters. Symmetric angle controls is a special case of sector control.

The connector diagram for a two-bridge semiconverter with sector control supplying a separately-excited dc motor is given in Figure A.3.1. The voltage and current waveforms for the converter output for two cases:

Case 1: $0 \leq E_a \leq 0.5$ pu

Case 2: $0.5 \leq E_a \leq 1.0$ pu

are given in Figures A.3.2 and A.3.3. The symbols used are similar to those presented in Section A.1. In this appendix, the governing equations and the computer flow chart, Figure A.3.4, to compute the PCU performance are presented.

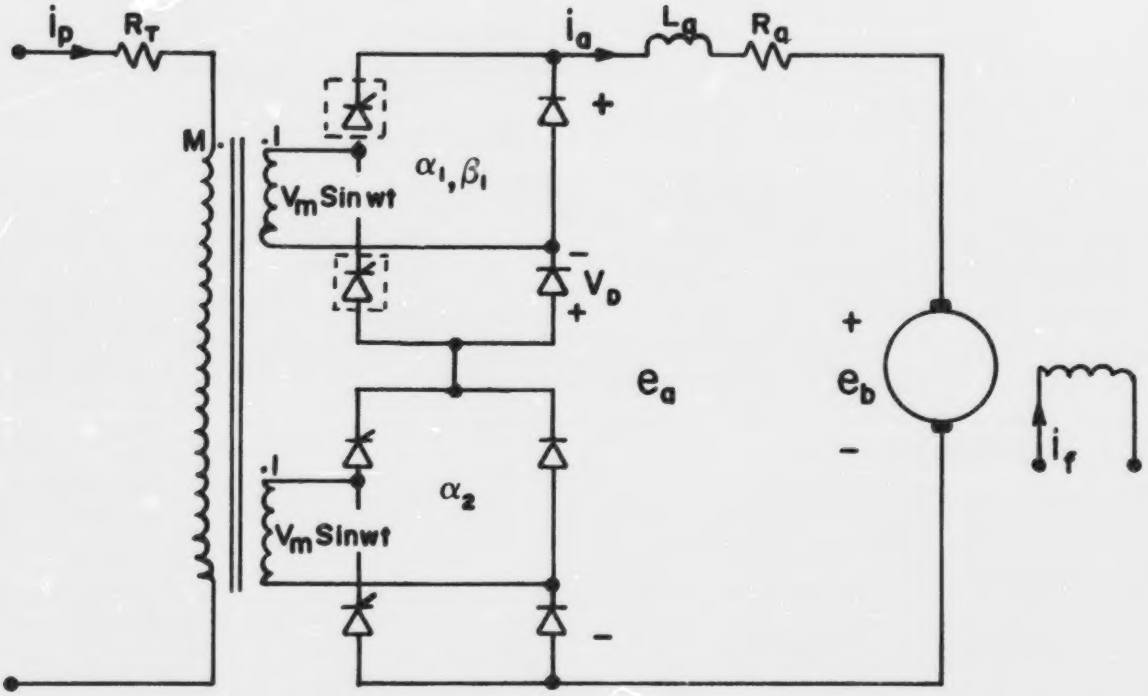

Figure A.3.1 Separately-excited dc Motor Supplied from Two-bridge Series Semiconverter

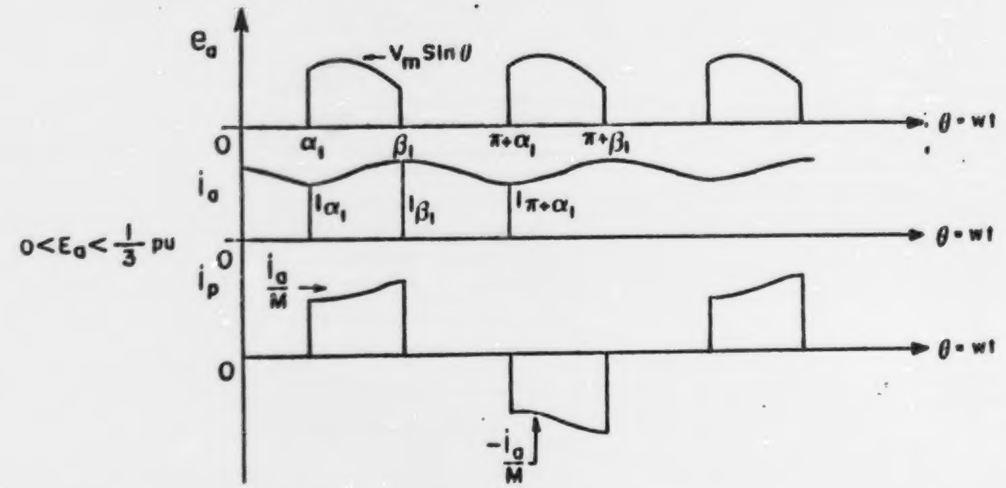

Figure A.3.2 Waveforms of Voltages and Currents with $0 \leq E_a \leq 0.5$ pu, sector control applied to one bridge with the other bridge turned off

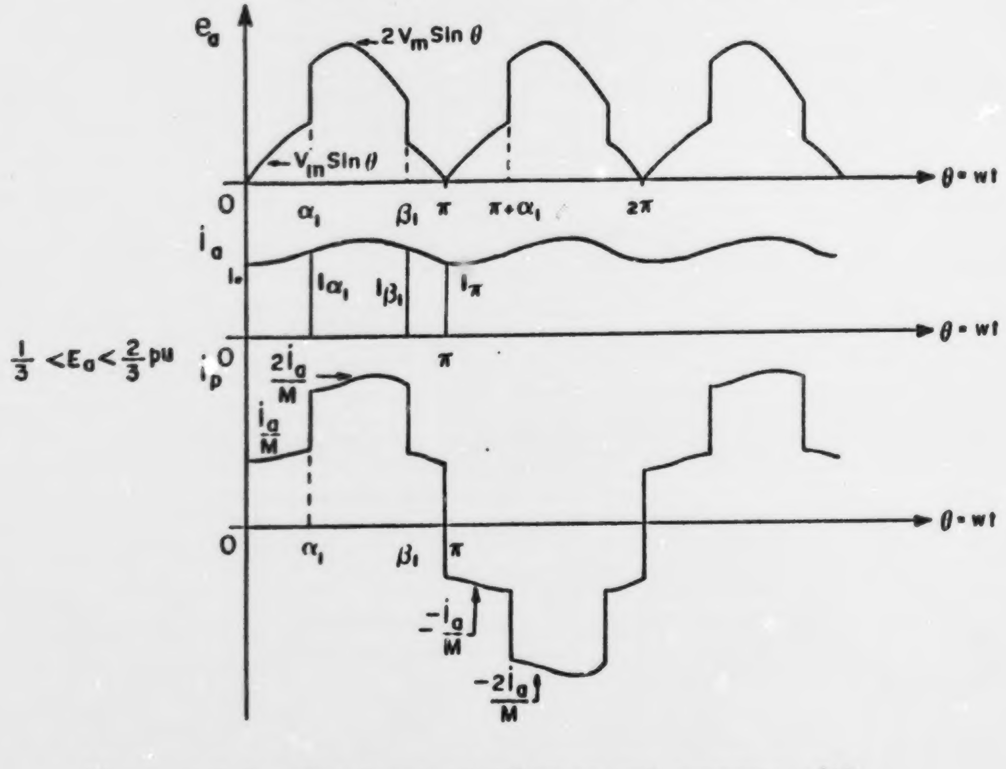

Figure A.3.3 Waveforms of voltages and currents with $0 \leq E_a \leq 0.5$ pu, sector control applied to one bridge with the other bridge fully turned on

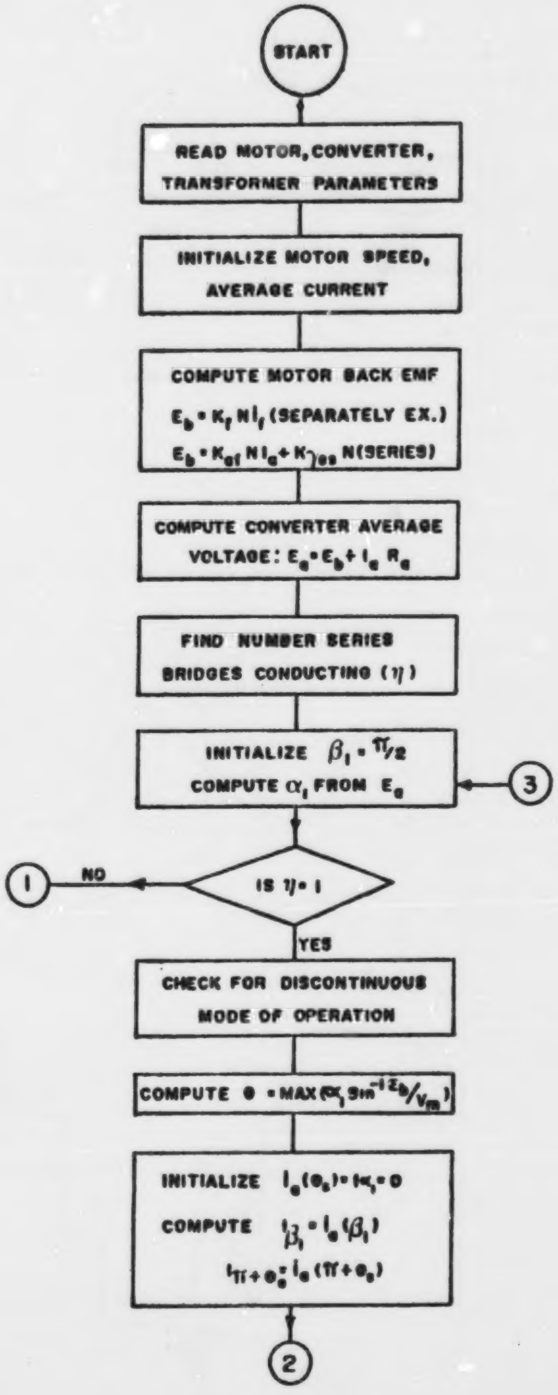
START
READ MOTOR, CONVERTER, TRANSFORMER PARAMETERS
INITIALIZE MOTOR SPEED, AVERAGE CURRENT
COMPUTE MOTOR BACK EMF
$E_b = K_f N I_f$ (SEPARATELY EX.)
$E_b = K_{af} N I_a + K_{res} N$ (SERIES)
COMPUTE CONVERTER AVERAGE VOLTAGE: $E_a = E_b + I_a R_a$
FIND NUMBER SERIES BRIDGES CONDUCTING (η)
INITIALIZE $\beta_1 = \pi/2$
COMPUTE α_1 FROM E_a
3
IS $\eta = 1$
NO
1
YES
CHECK FOR DISCONTINUOUS MODE OF OPERATION
COMPUTE $\theta = \mathrm{MAX}(\alpha_1, \sin^{-1} E_b/V_m)$
INITIALIZE $I_a(\theta_s) = i_{\alpha_1} = 0$
COMPUTE $i_{\beta_1} = I_a(\beta_1)$
$i_{\pi+\theta_s} = I_a(\pi+\theta_s)$
2

Figure A.3.4   Flowchart for Sector Control of Two-Bridge Semiconverter

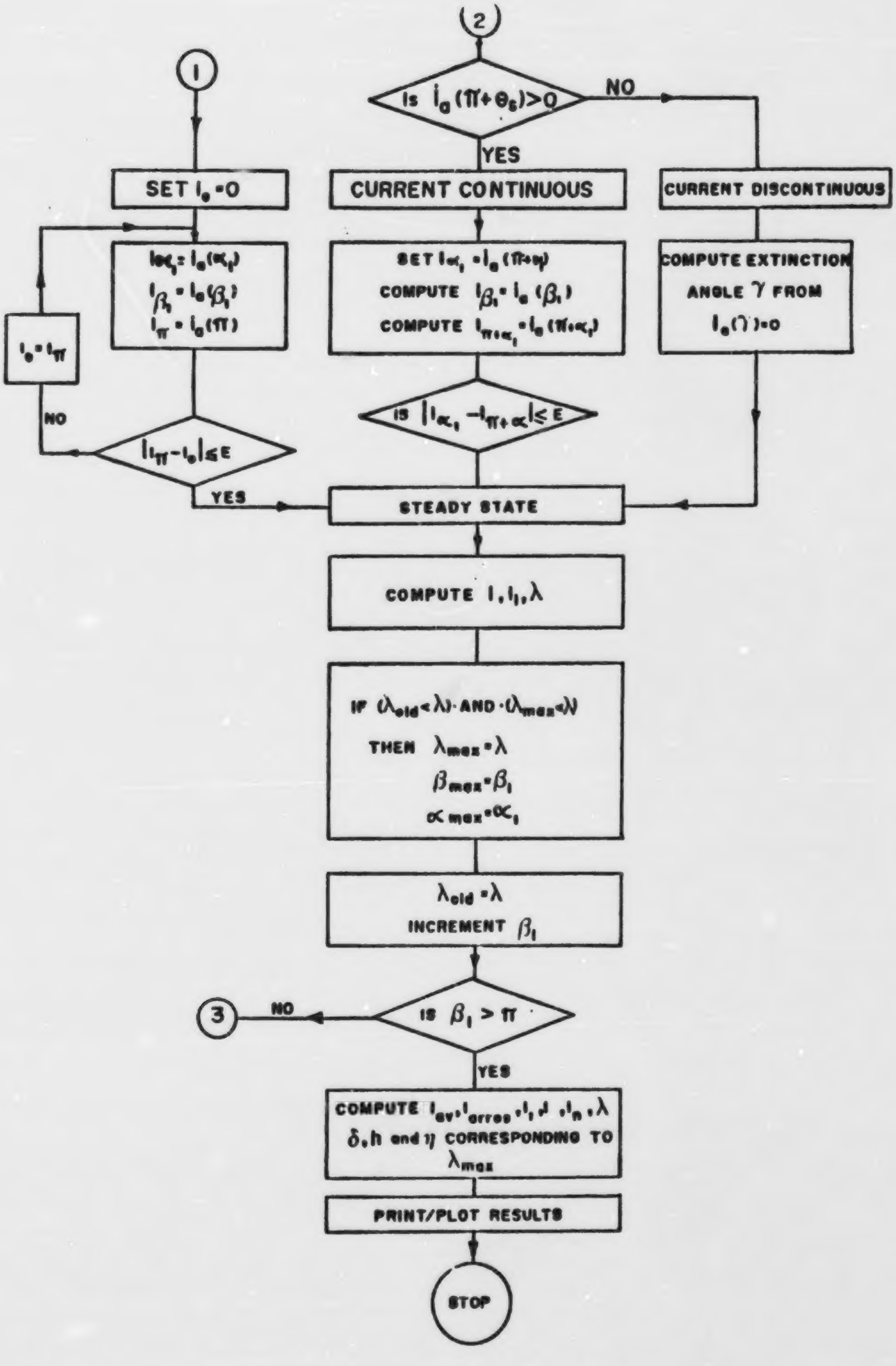
2
1
Is $i_a(\pi+\theta_s)>0$
NO
YES
SET $I_o=0$
CURRENT CONTINUOUS
CURRENT DISCONTINUOUS
$I_{\alpha_1}=i_a(\alpha_1)$
$I_{\beta_1}=i_a(\beta_1)$
$I_\pi=i_a(\pi)$
SET $I_{\alpha_1}=i_a(\pi+\alpha_1)$
COMPUTE $I_{\beta_1}=i_a(\beta_1)$
COMPUTE $I_{\pi+\alpha_1}=i_a(\pi+\alpha_1)$
COMPUTE EXTINCTION ANGLE γ FROM $i_a(\gamma)=0$
$I_o=I_\pi$
NO
$|I_\pi-I_o|\le E$
IS $|I_{\alpha_1}-I_{\pi+\alpha}|\le E$
YES
STEADY STATE
COMPUTE I, I_1, λ
IF $(\lambda_{old}<\lambda)$ .AND. $(\lambda_{max}<\lambda)$
THEN $\lambda_{max}=\lambda$
$\beta_{max}=\beta_1$
$\alpha_{max}=\alpha_1$
$\lambda_{old}=\lambda$
INCREMENT β_1
3
NO
IS $\beta_1>\pi$
YES
COMPUTE $I_{av}, I_{arms}, I_1, \phi, I_n, \lambda$ δ, h and η CORRESPONDING TO λ_{max}
PRINT/PLOT RESULTS
STOP

Figure A.3.4 (cont'd)

C.2 ANALYSIS

$$E_{max} = \frac{4V_m}{\pi} = 1.0 \text{ pu}$$

Case 1:

$$\boxed{0 < E_a < 0.5 \text{ pu:}} \qquad 0 < \alpha_1 < \frac{\pi}{2} < \beta_1 < \pi, \; \alpha_2 = \pi$$

$$E_a = \frac{1}{4} (\cos \alpha_1 - \cos \alpha_1) \text{ pu} \qquad \boxed{\alpha_1 = \cos^{-1} [\, 4 E_a + \cos \beta_1}$$

$$i_a = c_1 \sin (\theta - \phi) + c_2 e^{-c_3\theta} - c_4 \;, \; \alpha_1 < \theta < \beta_1$$

$$\left.\begin{aligned} &= c_5 c^{-c_3\theta} - c_4 && , \; \beta_1 < \theta < \pi + \alpha_1 \\ &= 0 && , \; \gamma < \theta < \pi + \alpha_1 \end{aligned}\right\} \text{for discontinuous current}$$

where: $\theta = \omega t$

$$c_1 = \frac{V_m}{z}$$

$$c_2 = [\, I\alpha_1 + c_4 - c_1 \sin (\alpha_1 - \phi) \,]\, e^{c_3\alpha_1}$$

$$c_3 = \frac{R_a}{\omega L_a}$$

$$c_4 = \frac{E_b}{R_a}$$

$$c_5 = (I\beta_1 + \frac{E_b}{R_a})\, e^{c_3\beta_1}$$

$$Z = \sqrt{R_a^{\ 2} + (\omega L_a)^2}$$

$$\phi = \tan^{-1} \frac{\omega L_a}{R_a}$$

$$I\alpha_1 = i_a\ (\theta=\alpha_1)$$

$$I\beta_1 = i_a\ (\theta=\beta_1)$$

In steady state, $I\alpha_1 = I\pi+\alpha_1$

Motor Average Current, I_{av}:

$$I_{av} = \frac{1}{\pi}\ [\ \int_{\alpha_1}^{\beta_1} i_a\ d0 + \int_{\beta_1}^{\pi+\alpha_1} i_a\ d\theta\ ]$$

$$\therefore\quad I_{av} = \frac{1}{\pi}\ [\ u_1(\beta_1) - u_1(\alpha_1) + v_1\ (\pi+\alpha_1) - v_1(\beta_1)$$

$$u_1(\theta) = c_1\ \cos\ (\theta-\phi) - \frac{c_2}{c_3}\, e^{-c_3\theta} - c_4\ \theta$$

$$v_1(\theta) = \frac{c_5}{c_5}\, e^{-c_3\theta} - c_4\ \theta$$

Motor RMS Current, $I_{a_{rms}}$:

$$I_{a_{rms}} = \sqrt{\frac{1}{\pi}\left[\int_{\alpha_1}^{\beta_1} i_a^{2}\,d\theta + \int_{\beta_1}^{\pi+\alpha_1} i_a^{2}\,d\theta\right]}$$

$$= \sqrt{\frac{1}{\pi}\left[u_2(\beta_1) - u_2(\alpha_1) + u_2(\pi+\alpha_1) - v_2(\beta_1)\right]}$$

$$u_2(\theta) = \left(\frac{c_1^{2}}{2} + c_4^{2}\right)\theta - \frac{c_1^{2}}{4}\sin(2\theta-2\phi) - \frac{c_2^{2}}{2c_3}e^{-2c_3\theta} - \frac{2c_1c_2}{1+c_3^{2}}e^{-c_3\theta}$$

$$(c_3\sin(\theta-\phi) + \cos(\theta-\phi) + 2ac_4\cos(\theta-\phi) + \frac{2c_2c_4}{c_3}e^{-c_3\theta}$$

$$v_2(\theta) = -\frac{c_5^{2}}{2c_3}e^{-2c_3\theta} + c_4^{2}\theta + \frac{2c_5c_4}{c_3}e^{-c_3\theta}$$

Transformer Primary Current, i_p:

$$i_p = \frac{i_a}{M} = \frac{1}{M}\left(c_1\sin(\theta-\phi) + c_2e^{-c_3\theta} - c_4\right), \quad \alpha_1 < \theta < \beta_1$$

$$= 0, \quad \beta_1 < \theta < \pi + \alpha_1$$

Input RMS Current, I:

$$I = \sqrt{\frac{1}{\ }\int_{\alpha_1}^{\beta_1} i_p^{2}\,d\theta}$$

$$= \frac{1}{M} \sqrt{\frac{1}{\pi} [\ u_2(\beta_1) - u_2(\alpha_1)\ ]}$$

Input Harmonic Currents, I_n:

$$x_n = \frac{2}{M\pi} \int_{\alpha_1}^{\beta_1} i_a \sin n\theta \, d\theta$$

$$y_n = \frac{2}{M\pi} \int_{\alpha_1}^{\beta_1} i_a \sin n\theta \, d\theta$$

$$x_n = \frac{2}{M\pi} [\ u_3(\beta_1) - u_3(\alpha_1)\ ]$$

$$y_n = \frac{2}{M\pi} [\ v_3(\beta_1) - v_3(\alpha_1)\ ]$$

$$u_3(\theta) = \frac{c_1}{2} \left[\frac{\sin(\overline{n-1}\ \theta + \phi)}{n-1} - \frac{\sin(\overline{n+1}\ \theta - \phi)}{n+1} \right] - \frac{c_2 e^{-c_3\theta}}{(n^2 + c_3{}^2)}$$

$$[\ c_3 \sin n\theta + n \cos n\theta\ ] + \frac{c_4}{n} \cos n\theta$$

$$v_3(\theta) = \frac{c_1}{2} \left[\frac{\cos(\overline{n-1}\ \theta + \phi)}{n-1} - \frac{\cos(\overline{n+1}\ \theta - \phi)}{n+1} \right] + \frac{c_2 e^{-c_3\theta}}{(n^2 + c_3{}^2)}$$

$$[\ n \sin n\theta - c_3 \cos n\theta\ ] - \frac{c_4}{n} \sin n\theta$$

$$I_n = \sqrt{\frac{1}{2} (x_n{}^2 + y_n{}^2)}\ , \ n \neq 1,\ n = 3,5,7,\ldots$$

RMS Fundamental Input Current, I_1:

$$x_1 = \frac{2}{M\pi} [\ u_4(\beta_1) - u_4(\alpha_1)\ ]$$

$$y_1 = \frac{2}{M\pi} [\ v_4(\beta_1) - v_4(\alpha_1)\ ]$$

$$v_4(\theta) = \frac{c_1}{2} [\ \theta \cos \phi - \frac{1}{2} \sin (2\theta - \phi)\ ] - \frac{c_2\ e^{-c_3\theta}}{1 + c_3^2}$$

$$[\ c_3 \sin \theta + \cos \theta\ ] + c_4 \cos \theta$$

$$v_4(\theta) = \frac{c_1}{2} [\ - \theta \sin \phi - \frac{1}{2} \cos (2\theta - \phi)\ ] + \frac{c_2\ e^{-c_3\theta}}{1 + c_3^2}$$

$$[\ \sin \theta - c_3 \cos \theta\ ] - c_4 \sin \theta$$

$$I_1 = \sqrt{\frac{1}{2} (x_1^2 + y_1^2)}$$

Compute:

$$\lambda = \frac{x_1}{\sqrt{2}\ I} = \text{power factor}$$

$$\delta = \frac{x_1}{\sqrt{x_1^2 + y_1^2}} = \text{displacement factor}$$

$$h = \sqrt{(\frac{I}{I_1})^2 - 1} = \text{harmonic factor}$$

Overall Efficiency, η:

Losses: $P_L = P_A + P_C + P_Q + P_T$

where: armature copper loss: $P_A = I_{a_{rms}}^2 R_a$

converter conduction losses: $P_C = 4\ I_{av}\ V_D$

commutation losses: $P_Q = 2\ (V_m \sin \beta_1) \cdot I\beta_i \cdot \frac{t_q}{T}$

transformer copper loss: $P_T = I^2 R_T$

efficiency: $\eta = \frac{E_6\ I_{av}}{E_b\ I_{av} + P_L}$

Case 2:

$\boxed{0.5 < E_a < 1.0 \text{ pu}}$ $\quad 0 < \alpha_1 < \frac{\pi}{2} < \beta_1 < \pi, \quad \alpha_2 = 0$

$E_a = \frac{1}{4}\ [2 + \cos \alpha_1 - \cos \beta_1],$ $\quad \boxed{\alpha_1 = \cos^{-1} (4E_a - 2 + \cos \beta_1)}$

$$i_a = c_1 \sin (\theta-\phi) + c_6 e^{-c_3\theta} - c_4\ ,\ 0 < \theta < \alpha_1$$

$$= 2c_1 \sin (\theta-\phi) + c_7 e^{-c_3\theta} - c_4\ ,\ \alpha_1 < \theta < \beta_1$$

$$= c_1 \sin (\theta-\phi) + c_8 e^{-c_3\theta} - c_4\ ,\ \beta_1 < \theta < \pi$$

where: $c_6 = I_0 + c_4 + c_1 \sin \phi$

$$c_7 = [\ I\alpha_1 + c_4\ 2c_1 \sin (\alpha_1 - \phi)\ ]\ e^{c_3 \alpha_1}$$

$$c_8 = [\ I\beta_1 + c_4\ c_1 \sin (\beta_1 - \phi)\ ]\ e^{c_3 \beta_1}$$

Motor Average Current, I_{av}:

$$I_{av} = \frac{1}{\pi} [\ \int_0^{\alpha_1} i_a \, d\theta + \int_{\alpha_1}^{\beta_1} i_a \, d\theta + \int_{\beta_1}^{\pi} i_a \, d\theta$$

$$= \frac{1}{\pi} [\ u_5(\alpha_1) - u_5(\theta) + u_6(\beta_1) - u_6(\alpha_1) + u_7(\pi) - u_7(\beta_1)\ ]$$

$$u_5(\theta) = - c_1 \cos (\theta - \phi) - \frac{c_6}{c_3} e^{-c_3 \theta} - c_4 \theta$$

$$u_6(\theta) = - 2c_1 \cos (\theta - \phi) - \frac{c_7}{c_3} e^{-c_3 \theta} - c_4 \theta$$

$$u_7(\theta) = - c_1 \cos (\theta - \phi) - \frac{c_8}{c_3} e^{-c_3 \theta} - c_4 \theta$$

Motor RMS Current, $I_{a_{rms}}$:

$$I_{a_{rms}} = \frac{1}{\pi} [\ v_5(\alpha_1) - v_5(0) + v_6(\beta_1) - v_6(\alpha_1) + v_7(\pi) - v_7(\beta_1)\ ]$$

$$v_5(\theta) = (\frac{c_1^2}{2} + c_4)\,\theta - \frac{c_1^2}{4} \sin(2\theta - 2\phi) - \frac{c_6^2}{2c_3} e^{-2v_3\theta} - \frac{2c_1c_6}{1 + c_3^2} e^{-c_3\theta}$$

$$[\, c_3 \sin(\theta - \phi) + \cos(\theta - \phi) \,] + 2c_1c_4 \cos(\theta - \phi) + \frac{2c_6c_4}{c_3} e^{-c_3\theta}$$

$$v_6(\theta) = (2c_1^2 + c_4^2)\,\theta - c_1^2 (2\theta - 2\phi) - \frac{c_7^2}{2c_3} e^{-2c_3\theta} - \frac{4c_1c_7}{1 + c_3^2} e^{-c_3\theta}$$

$$[\, c_3 \sin(\theta - \phi) + \cos(\theta - \phi) \,] + 4c_1c_4 \cos(\theta - \phi) + \frac{2c_4c_7}{c_3} e^{-c_3\theta}$$

$$v_7(\theta) = (\frac{c_1^2}{2} + c_4^2)\,\theta - \frac{c_1^2}{4} \sin(2\theta - 2\phi) - \frac{c_8^2}{2c_3} e^{-2c_3\theta} - \frac{2c_1c_8}{1 + c_3^2} e^{-c_3\theta}$$

$$[c_3 \sin(\theta - \phi) + \cos(\theta - \phi) \,] + 2c_1c_4 \cos(\theta - \phi) + \frac{2c_4c_8}{c_3} e^{-c_3\theta}$$

Input Current, i_p:

$$i_p = \frac{i_a}{M\pi} = \frac{1}{M} [\, c_1 \sin(\theta - \phi) + c_6 e^{-c_3\theta} - c_4 \,] \quad , \; 0 < \theta < \alpha_1$$

$$= \frac{2i_a}{M\pi} = \frac{2}{M} [\, 2c_1 \sin(\theta - \phi) + c_7 e^{-c_3\theta} - c_4] \; , \; \alpha_1 < \theta < \beta_1$$

$$= \frac{i_a}{M\pi} = \frac{1}{M} [\, c_1 \sin(\theta - \phi) + c_8 e^{-c_3\theta} - c_4] \quad , \; \beta_1 < \theta < \pi$$

Input RMS Current, I:

$$I = \frac{1}{M} \sqrt{\frac{1}{\pi} [\, v_5(\alpha_1) - v_5(0) + 4 [\, v_6(\beta_1) - v_6(\alpha_1) \,] + v_7(\pi) - v_7(\beta_1) \,]}$$

Input Harmonic Currents, I_n ($n \neq 1$):

$$x_n = \frac{2}{M\pi} \left[\int_0^{\alpha_1} i_a \sin n\theta + \int_{\alpha_1}^{\beta_1} 2i_a \sin n\theta + \int_{\beta_1} i_a \sin n\theta \right] d\theta$$

$$y_n = \frac{2}{M\pi} \left[\int_0^{\alpha_1} i_a \cos n\theta + \int_{\alpha_1}^{\beta_1} 2i_a \cos n\theta + \int_{\beta_1} i_a \cos n\theta \right] d\theta$$

$$x_n = \frac{2}{M\pi} [\, u_8(\alpha_1) - u_8(0) + u_9(\beta_1) - u_9(\alpha_1) + u_{10}(\pi) - u_{10}(\beta_1) \,]$$

$$y_n = \frac{2}{M\pi} [\, v_8(\alpha_1) - v_8(0) + v_9(\beta_1) - v_9(\alpha_1) + v_{10}(\pi) - v_{10}(\beta_1) \,]$$

$$u_8(\theta) = \frac{c_1}{2} \left[\frac{\sin(\overline{n-1}\;\theta + \phi)}{(n-1)} - \frac{\sin\overline{(n+1)}\;\theta - \phi)}{(n+1)} \right] - \frac{c_6\, e^{-c_3\theta}}{n^2 + c_3^2}$$

$$[\, c_3 \sin n\theta + n \cos n\theta \,] + \frac{c_4}{n} \cos n\theta$$

$$u_9(\theta) = 2c_1 \left[\frac{\sin(\overline{n-1}\;\theta + \phi)}{n-1} - \frac{\sin(\overline{n+1}\;\theta - \phi)}{n+1} \right] - \frac{2c_7\, e^{-c_3\theta}}{n^2 + c_3^2}$$

$$[\, c_3 \sin n\theta + n \cos n\theta \,] + \frac{2c_4}{n} \cos n\theta$$

$$u_{10}(\theta) = \frac{c_1}{2} \left[\frac{\sin(\overline{n-1}\;\theta + \phi)}{n-1} - \frac{\sin(\overline{n+1}\;\theta - \phi)}{n+1} \right] - \frac{c_8\, e^{-c_8\theta}}{n^2 + c_3^2}$$

$$[\, c_3 \sin n\theta + n \cos n\theta \,] + \frac{c_4}{n} \cos n\theta$$

$$v_8(\theta) = \frac{c_1}{2}\left[\frac{\cos(\overline{n-1}\,\theta + \phi)}{n-1} - \frac{\cos(\overline{n+1}\,\theta - \phi)}{n+1}\right] + \frac{c_6\, e^{-c_3\theta}}{n^2 + c_3^{\,2}}$$

$$[\, n \sin n\theta - c_3 \cos n\theta \,] - \frac{c_4}{n} \sin n\theta$$

$$v_9(\theta) = 2c_1\left[\frac{\cos(\overline{n-1}\,\theta + \phi)}{n-1} - \frac{\cos(\overline{n+1}\,\theta - \phi)}{n+1}\right] + \frac{2c_7\, e^{-c_3\theta}}{n^2 + c_3^{\,2}}$$

$$[\, n \sin n\theta - c_3 \cos n\theta \,] - \frac{2c_4}{n} \sin n\theta$$

$$v_{10}(\theta) = \frac{c_1}{2}\left[\frac{\cos(\overline{n-1}\,\theta + \phi)}{n-1} \quad \frac{\cos(\overline{n+1}\,\theta - \phi)}{n+1}\right] + \frac{c_8\, e^{-c_3\theta}}{n^2 + c_3^{\,2}}$$

$$[\, n \sin n\theta - c_3 \cos n\theta \,] - \frac{c_4}{n} \sin n\theta$$

$$I_n = \sqrt{\frac{1}{2}\left(x_n^{\,2} + y_n^{\,2}\right)}$$

RMS Input Fundamental Current, I_1:

$$x_1 = \frac{2}{M\pi}\left[\, u_{11}(\alpha_1) - u_{11}(\theta) + u_{12}(\beta_1) - u_{12}(\alpha_1) + u_{13}(\pi) - u_{13}(\beta_1) \,\right]$$

$$y_1 = \frac{2}{M\pi}\left[\, v_{11}(\alpha_1) - v_{11}(\theta) + v_{12}(\beta_1) - v_{12}(\alpha_1) + v_{13}(\pi) - v_{13}(\beta_1) \,\right]$$

$$u_{11}(\theta) = \frac{c_1}{2}\left[\, \theta \cos\phi - \frac{1}{2}\sin(2\theta - \phi) \,\right] - \frac{c_6\, e^{-c_3\theta}}{1 + c_3^{\,2}}\left(c_3 \sin\theta + \cos\theta\right)$$

$$+\, c_4 \cos\theta$$

$$u_{12}(\theta) = 2c_1 \; [\theta \cos \phi - \frac{1}{2} \sin (2\theta-\phi) \;] - \frac{2c_7 \, e^{-c_3\theta}}{1 + c_3^{\,2}} (c_3 \sin \theta + \cos \theta)$$

$$+ \; 2c_4 \cos \theta$$

$$u_{13}(\theta) = \frac{c_1}{2} \; (\theta \cos \phi - \frac{1}{2} \sin (2\theta-\phi) \;] - \frac{c_8 \, e^{-c_3\theta}}{1 + c_3^{\,2}} (c_3 \sin \theta + \cos \theta)$$

$$+ \; c_4 \cos \theta$$

$$v_{11}(\theta) = \frac{c_1}{2} \; [\; - \theta \sin \phi - \frac{1}{2} \cos (2\theta-\phi) \;] + \frac{c_6 \, e^{-c_3\theta}}{1 + c_3^{\,2}} (\sin \theta - c_3 \cos \theta)$$

$$+ \; c_4 \sin \theta$$

$$v_{12}(\theta) = 2c_1 \; [\; - \theta \sin \phi - \frac{1}{2} \cos (\theta-\phi)] + \frac{2c_7 \, e^{-c_3\theta}}{1 + c_3^{\,2}} (\sin \theta - c_3 \cos \theta)$$

$$- \; 2c_4 \sin \theta$$

$$v_{13}(\theta) = \frac{c_1}{2} \; [\; - \theta \sin \phi - \frac{1}{2} \cos (\theta-\phi) \;] + \frac{c_8 \, e^{-c_3\theta}}{1 + c_3^{\,2}} (\sin \theta - c_3 \cos \theta)$$

$$- \; c_4 \sin \theta$$

$$\therefore \; I_1 = \sqrt{\frac{1}{2} (x_1^{\,2} + y_1^{\,2})}$$

Compute:

$$\lambda = \sqrt{\frac{x_1}{\sqrt{2}\ I}} = \text{pf}$$

$$\zeta = \frac{x_1}{\sqrt{x_1^2 + y_1^2}} = \text{df}$$

$$h = \sqrt{\left(\frac{I}{I_1}\right)^2 - 1} = \text{hf}$$

$$\eta = \frac{E_b I_{av}}{(E_b I_{av} + I_{a_{rms}}^2 R_a + 4V_D I_{av} + 2\ V_m \sin \beta_1 \cdot I\beta_1 \cdot \frac{tq}{T} + I^2 R_T)}$$

= efficiency

A.4 ANALYSIS OF THREE-SERIES BRIDGE SECTOR-CONTROLLED SEMICONVERTERS SUPPLYING A DC SERIES MOTOR

A.4.1 General

The governing equations to compute the PCU performance are presented in this appendix.

The connection diagram for three-series bridge sector-controlled semiconverters supplying a series motor is given in Figure A.4.1. The voltage and current waveforms for the semi-converter output for the three cases:

Case 1: $0 \leq E_a \leq 1/3$ pu

Case 2: $1/3 \leq E_a \leq 2/3$ pu

Case 3: $2/3 \leq E_a \leq 1.0$ pu

are given in Figures A.4.2, A.4.3 and A.4.4. The symbols are similar to those presented in Section A.1 and the computer flow chart is similar to that presented in Figure A.3.4.

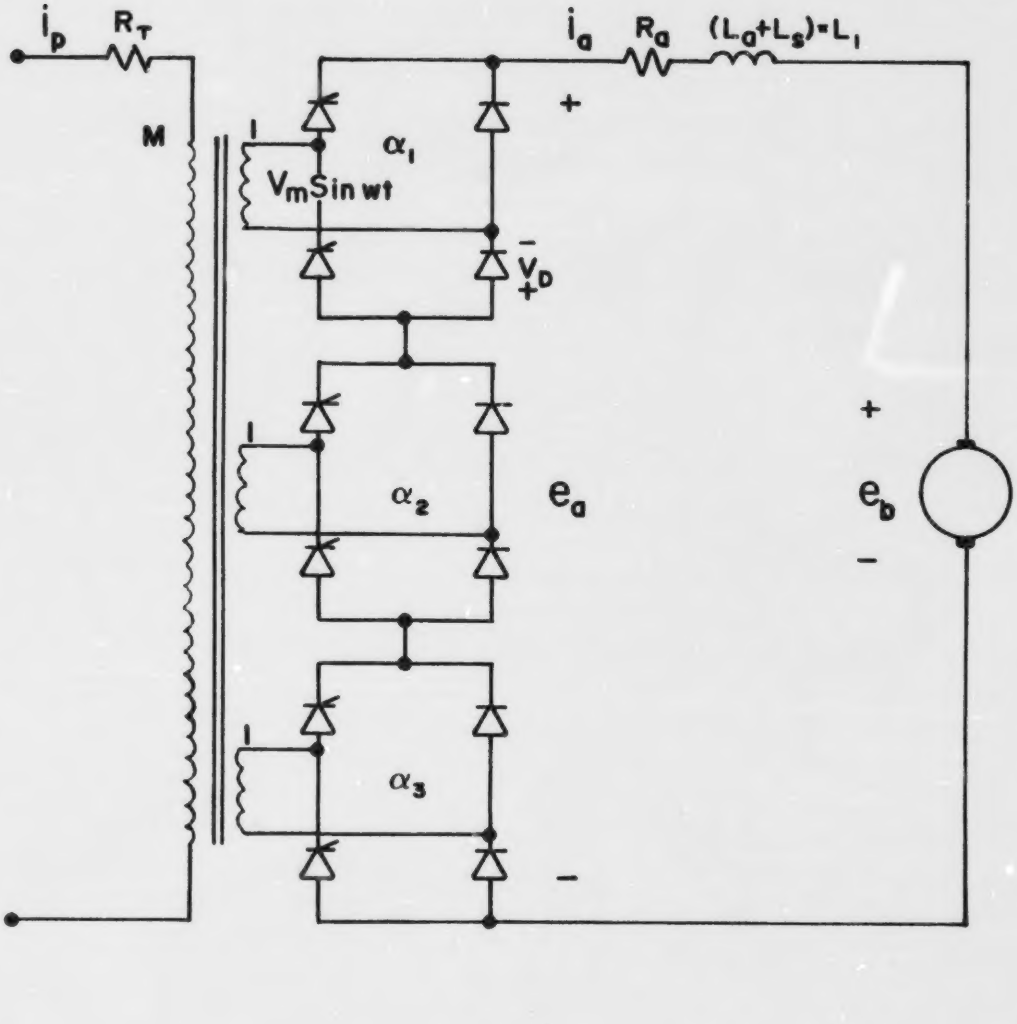

Figure A.4.1 Three-Series Bridge Sector-Controlled Semiconverters Supplying a dc Series Motor

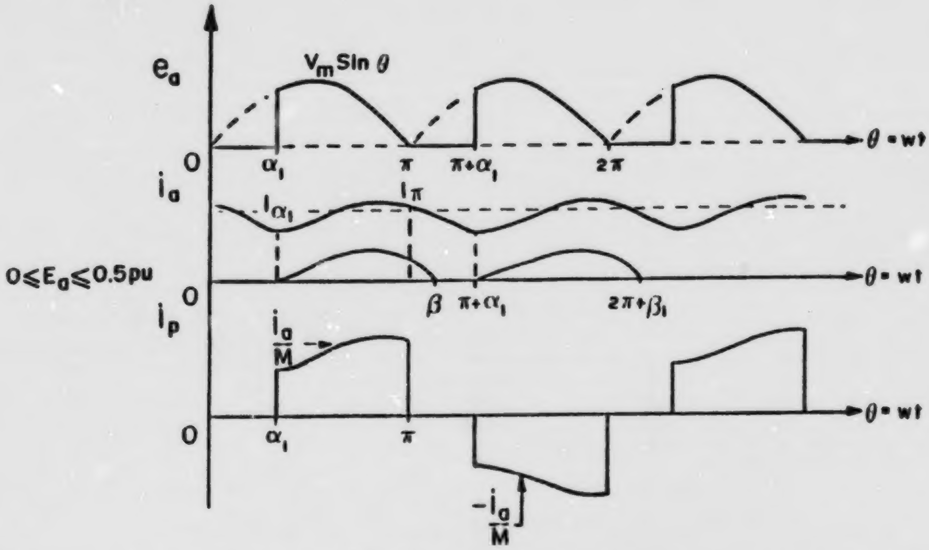

Figure A.4.2 Waveforms of Voltages and Currents with $0 \leq E_a \leq 1/3$ pu, sector control of one bridge with the other two bridges turned off

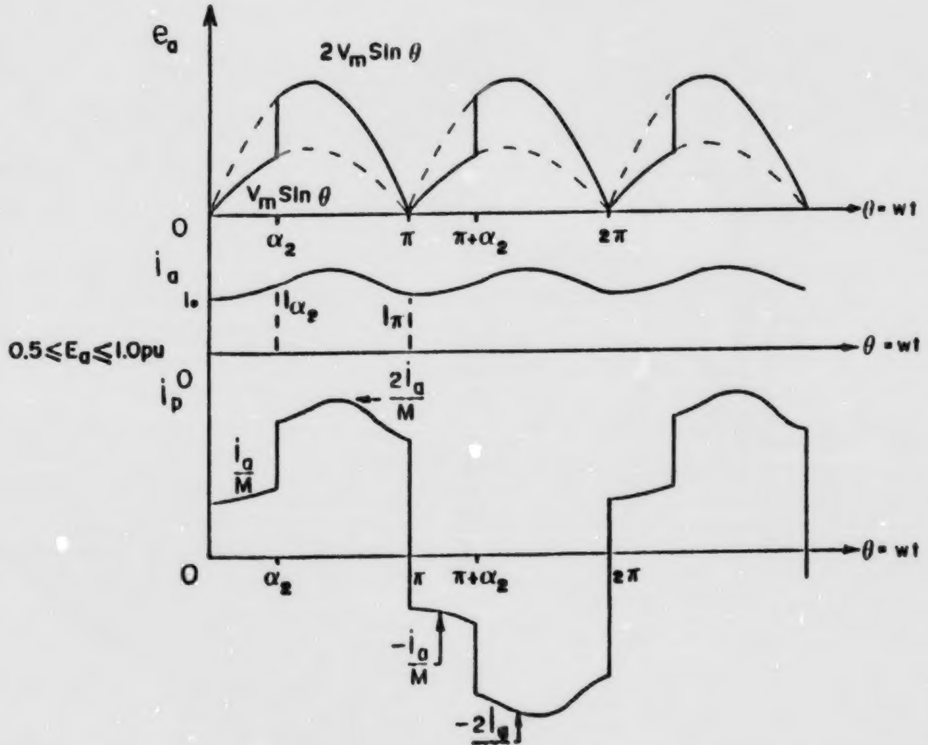

Figure A.4.3 Waveforms of Voltages and Currents with $1/3 \leq E_a \leq 2/3$ pu, sector control of one bridge with one bridge fully turned on and the other turned off

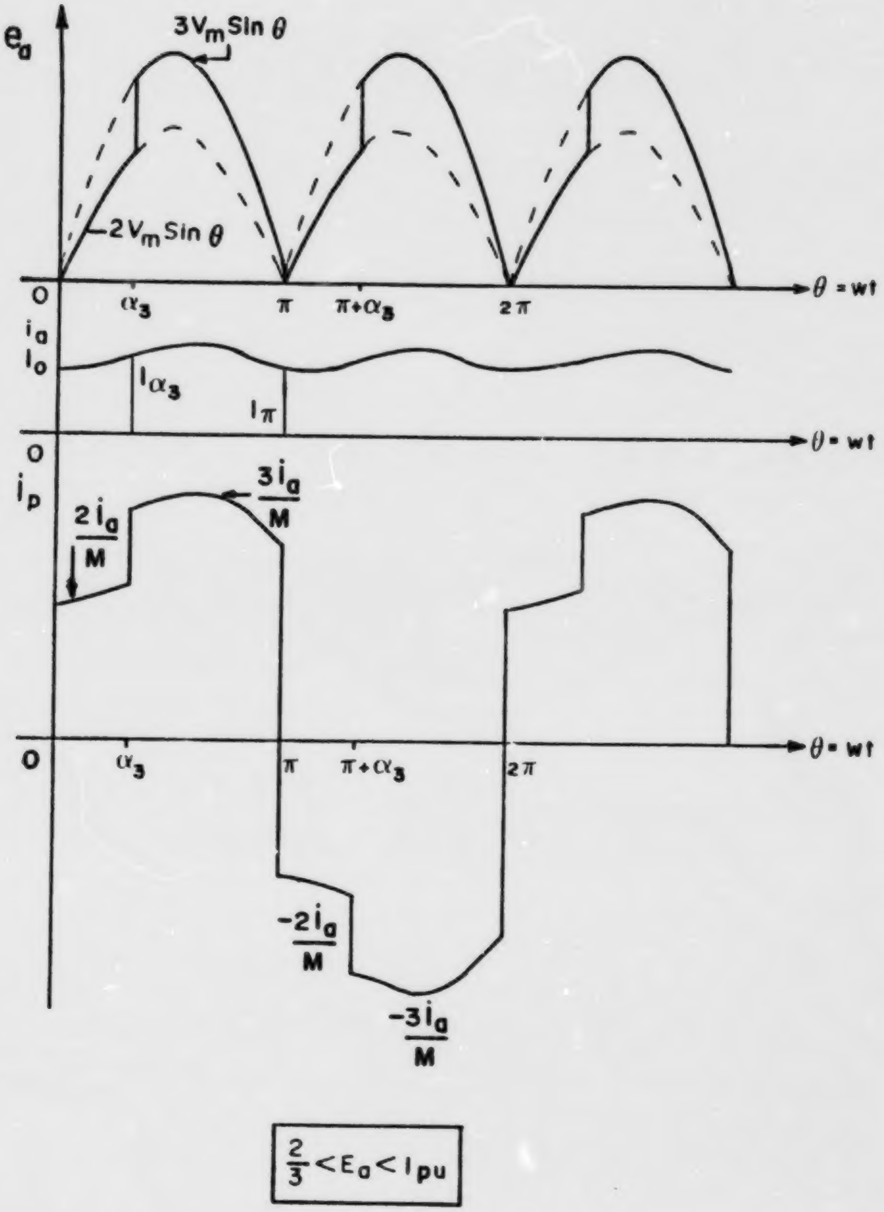

Figure A.4.4 Waveforms of Voltages and Currents with $2/3 \leq E_a \leq 1$ pu, Sector Control of One Bridge with Two Bridges Fully Turned On

D.2 ANALYSIS

$$E_{max} = \frac{6V_m}{\pi} = 1.0 \text{ pu}$$

Case 1:

$$\boxed{0 < E_a < \frac{1}{3} \text{ pu:}} \qquad 0 < \alpha_1 < \frac{\pi}{2} < \beta_1 < \pi, \quad \alpha_2 = \alpha_3 = \pi$$

$$E_a = \frac{1}{6} (\cos \alpha_1 - \cos \beta_1) \text{ pu} \qquad \boxed{\alpha_1 = \cos^{-1} (6E_a + \cos \beta_1)}$$

$$i_a = d_1 \sin (\theta-\phi) + d_2 e^{-d_3\theta} - d_4 , \ \alpha_1 < \theta < \beta_1$$

$$\left.\begin{array}{ll} = d_5 e^{-d_3\theta} - d_4 & , \ \beta_1 < \theta < \pi + \alpha_1 \\ = 0 & , \ \gamma < \theta < \pi + \alpha_1 \end{array}\right\} \text{for discontinuous conduction}$$

where: $d_1 = \frac{V_m}{Z_1}$

$$d_2 = [\ d_4 + I\alpha_1 - d_1 \sin (\alpha_1-\phi)\ ]\ e^{d_3\alpha_1}$$

$$d_3 = \frac{R_1}{\omega L_1}$$

$$d_4 = \frac{K_{res}N}{R_1}$$

$$d_5 = (I_{\beta_1} + d_4)\, e^{e_3\beta_1}$$

$$R_1 = R_a + R_s + K_{af}N$$

$$L_1 = L_a + L_s$$

$$Z_1 = \sqrt{R_1^{\,2} + (\omega L_1)^2}$$

$$\phi = \tan^{-1}\left(\frac{\omega L_1}{R_1}\right)$$

N = motor speed

$$\begin{aligned} i_p &= 0, & 0 < \theta < \alpha_1 \\ &= \frac{i_a}{M} = \frac{1}{M}\left[\, d_1 \sin(\theta-\phi) + d_2\, e^{-d_3\theta} - d_4 \,\right], & \alpha_1 < \theta < \beta_1 \\ &= 0 & \beta_1 < \theta < \pi \end{aligned}$$

Average Motor Current, I_{av}:

$$I_{av} = \frac{1}{\pi}\left[\, w_1(\beta_1) - w_1(\alpha_1) + z_1(\pi+\alpha_1) - z_1(\beta_1) \,\right]$$

$$w_1(\theta) = -\,d_1 \cos(\theta-\phi) - \frac{d_1}{d_3}\, e^{-d_3\theta} - d_4\theta$$

$$z_1(\theta) = -\frac{d_5}{d_3} e^{-d_3\theta} - d_4\theta$$

RMS Motor Current, $I_{a_{rms}}$:

$$I_{a_{rms}} = \sqrt{\frac{1}{\pi} [\ w_2(\beta_1) - w_2(\alpha_1) + z_2(\pi+\alpha_1) - z_2(\beta_1)\ ]}$$

$$w_2(\theta) = (\frac{d_1^{\ 2}}{2} + d_4^{\ 2})\ \theta = \frac{d_1^{\ 2}}{4} \sin(2\theta-2\phi) - \frac{d_2^{\ 2}}{2d_3} e^{-2d_3\theta} - \frac{2d_1d_2}{1+d_3^{\ 2}}$$

$$[\ d_3 \sin(\theta-\phi) + \cos(\theta-\phi)\ ] + 2d_1d_4 \cos(\theta-\phi)$$

$$+ \frac{2d_2d_4}{d_3} - e^{-d_3\theta}$$

$$z_2(\theta) = -\frac{d_5^{\ 2}}{2d_3} e^{-2d_3\theta} + d_4^{\ 2} + \frac{2d_4d_5}{d_3} e^{-d_3\theta}$$

Input RMS Current, I:

$$I = \frac{1}{M} \sqrt{\frac{1}{\pi} [\ w_2(\beta_1) - w_2(\alpha_1)\ ]}$$

Input Harmonic Currents, I_n ($n \neq 1$):

$$x_n = \frac{2}{M\pi} [\ w_3(\beta_1) - w_3(\alpha_1)\ ]$$

$$y_n = \frac{2}{M\pi} [\ z_3(\beta_1) - z_3(\alpha_1)$$

$$w_3(\theta) = \frac{d_1}{2} \left[\frac{\sin(\overline{n-1}\,\theta + \phi)}{n-1} - \frac{\sin(\overline{n+1}\,\theta - \phi)}{n+1} \right] - \frac{d_2\, e^{-d_3\theta}}{n^2 + d_3^{\,2}}$$

$$\left[d_3 \sin n\theta + n \cos n\theta \right] - \frac{d_4}{n} \cos n\theta$$

$$z_3(\theta) = \frac{d_1}{2} \left[\frac{\cos(\overline{n-1}\,\theta + \phi)}{n-1} \quad \frac{\cos(\overline{n+1}\,\theta - \phi)}{n+1} \right] + \frac{d_2\, e^{-d_3\theta}}{n^2 + d_3^{\,2}}$$

$$\left[n \sin n\theta - d_3 \cos n\theta \right] - \frac{d_4}{n} \sin n\theta$$

$$I_n = \sqrt{\frac{1}{2} (x_n^{\,2} + y_n^{\,2})}\ ,\ n \neq 1$$

Input RMS Fundamental Current, I_1:

$$x_1 = \frac{2}{M\pi} \left[w_4(\gamma_1) - w_4(\alpha_1) \right]$$

$$y_1 = \frac{2}{M\pi} \left[z_4(\gamma_1) - z_4(\alpha_1) \right)$$

$$w_4(\theta) = \frac{d_1}{2} \left[\theta \cos \phi - \frac{1}{2} \sin(2\theta - \phi) \right] - \frac{d_2\, e^{-d_3\theta}}{1 + d_3^{\,2}} \left[d_3 \sin \theta + \cos \theta \right]$$

$$+ d_4 \cos \theta$$

$$z_4(\theta) = \frac{d_1}{2} \left[-\theta \cos \phi - \frac{1}{2} \cos(2\theta - \phi) \right] + \frac{d_3\, e^{-d_3\theta}}{1 + d_3^{\,2}} \left[\sin \theta - d_3 \cos \theta \right]$$

$$- d_4 \sin \theta$$

$$I_1 = \sqrt{\frac{1}{2}\left(x_1^{\,2} + y_1^{\,2}\right)}$$

Now compute λ, δ and h as defined before.

The converter conduction losses are now $P_D = 6\, I_{av}\, V_D$.

Using this, calcualte the efficiency, η.

Case 2:

$$\boxed{\frac{1}{3} < E_a < \frac{2}{3} \text{ pu:}} \qquad \alpha_2 = 0\ ,\ 0 < \alpha_1 < \frac{\pi}{2} < \beta_1 < \pi,\ \alpha_3 = \pi$$

$$E_a = \frac{1}{6}\left[\,2 + \cos\alpha_1 - \cos\beta_1\,\right] \text{ pu} \qquad \boxed{\alpha_1 = \cos^{-1}\left[\,6E_a - 2 + \cos\beta_1\right]}$$

$$i_a = d_1 \sin(\theta-\phi) + d_6\, e^{-d_3\theta} - d_4\ ,\quad 0 < \theta < \alpha_1$$

$$= 2d_1 \sin(\theta-\phi) + d_7\, e^{-d_3\theta} - d_4\ ,\quad \alpha_1 < \theta < \beta_1$$

$$= d_1 \sin(\theta-\phi) + d_8\, e^{-d_3\theta} - d_4\ ,\quad \beta_1 < \theta < \pi.$$

$$d_6 = I_0 + d_4 + d_1 \sin\phi$$

$$d_7 = \left[\ I\alpha_1 + d_4 - 2d_1 \sin(\alpha_1-\phi)\ \right] d^{\,d_3\alpha_1}$$

$$d_8 = \left[\ I\beta_1 + d_4 - d_1 \sin(\beta_1-\theta)\ \right] d^{\,d_3\beta_1}$$

$$i_p = \frac{i_a}{M} \quad , \; 0 < \theta < \alpha_1$$

$$= \frac{2i_a}{M} \; , \; \alpha_1 < \theta < \beta_1$$

$$= \frac{i_a}{M} \quad , \; \beta_1 < \theta < \pi$$

Motor Average Current, I_{av}:

$$I_{av} = \frac{1}{\pi} [\; w_5(\alpha_1) - w_5(0) + w_6(\beta_1) - w_6(\alpha_1) + w_7(\pi) - w_7(\beta_1) \;]$$

$$w_5(\theta) = -\, d_1 \cos(\theta - \phi) - \frac{d_6}{d_3} e^{-d_3\theta} - d_4\theta$$

$$w_6(\theta) = -2d_1 \cos(\theta - \phi) - \frac{d_7}{d_3} e^{-d_3\theta} - d_4\theta$$

$$w_7(\theta) = -\, d_1 \cos(\theta - \phi) - \frac{d_8}{d_3} e^{-d_3\theta} - d_4\theta$$

Motor RMS Current $I_{a_{rms}}$:

$$I_{a_{rms}} = \sqrt{\frac{1}{\pi} [\; z_5(\alpha_1) - z_5(0) + z_6(\beta_1) - z_6(\alpha_1) + z_7(\pi) - z_7(\beta_1) \;]}$$

$$\begin{aligned} z_5(\theta) = {} & \left(\frac{d_1^2}{2} + d_4^2\right)\theta - \frac{d_1^2}{4} \sin(2\theta - 2\phi) - \frac{d_6^2}{2d_3} e^{-2d_3\theta} - \frac{2d_1d_6}{1+d_3^2} e^{-d_3\theta} \\ & [\; d_3 \sin(\theta - \phi) + \cos(\theta - \phi) \;] + 2d_1d_4 \cos(\theta - \phi) + \frac{2d_4d_6}{d_3} e^{-d_3\theta} \end{aligned}$$

$$z_6(\theta) = (2d_1^{\,2} + d_4^{\,2})\,\theta - d_1^{\,2}\sin(2\theta-2\phi) - \frac{d_7^{\,2}}{2d_3}\,e^{-2d_3\theta} - \frac{4d_1d_7}{1+d_3^{\,2}}\,e^{-d_3\theta}$$

$$[\,d_3\sin(\theta-\phi) + \cos(\theta-\phi)\,] + 4d_1d_4\cos(\theta-\phi) + \frac{2d_4d_7}{d_3}\,e^{-d_3\theta}$$

$$z_7(\theta) = \left(\frac{d_1^{\,2}}{2}\right)\theta - \frac{d_1^{\,2}}{4}\sin(2\theta-2\phi) - \frac{d_8^{\,2}}{2d_3}\,e^{-2d_3\theta} - \frac{2d_1d_8}{1+d_3^{\,2}}\,e^{-d_3\theta}$$

$$[\,d_3\sin(\theta-\phi) + \cos(\theta-\phi)\,] + 2d_1d_4\cos(\theta-\phi) + \frac{2d_4d_8}{d_3}\,e^{-d_3\theta}$$

Input RMS Current, I:

$$I = \sqrt{\frac{1}{\pi}\,[\,z_5(\alpha_1) - z_5(0) + 4\,[\,z_6(\beta_1) - z_6(\alpha_1)\,] + z_7(\pi) - z_7(\beta_1)\,]}$$

Input Harmonic Currents, I_n ($n \neq 1$):

$$x_n = \frac{2}{M\pi}\,[\,w_8(\alpha_1) - w_8(0) + w_9(\beta_1) - w_9(\alpha_1) + w_{10}(\pi) - w_{10}(\beta_1)$$

$$y_n = \frac{2}{M\pi}\,[\,z_8(\alpha_1) - z_8(0) + z_9(\beta_1) - z_9(\alpha_1) - z_{10}(\pi) - z_{10}(\beta_1)$$

$$w_8(\theta) = \frac{d_1}{2}\left[\,\frac{\sin(\overline{n-1}\,\theta + \phi)}{n-1} - \frac{\sin(\overline{n+1}\,\theta - \phi)}{n+1}\,\right] - \frac{d_6\,e^{-d_3\theta}}{n^2 + d_3^{\,2}}$$

$$(d_3\sin n\theta + n\cos n\theta) + \frac{d_4}{n}\cos n\theta$$

$$w_9(\theta) = 2d_1 \left[\frac{\sin (\overline{n-1}\,\theta + \phi)}{n-1} - \frac{\sin (\overline{n+1}\,\theta - \phi)}{n+1} \right] - \frac{2d_7\, e^{-d_3\theta}}{n^2 + d_3^2}$$

$$(d_3 \sin n\theta + n \cos n\theta) + \frac{2d_4}{n} \cos n\theta$$

$$w_{10}(\theta) = \frac{d_1}{2} \left[\frac{\sin (\overline{n-1}\,\theta + \phi)}{n-1} - \frac{\sin (\overline{n+1}\,\theta - \phi)}{n+1} \right] - \frac{d_8\, e^{-d_3\theta}}{n^2 + d_3^2}$$

$$(d_3 \sin n\theta + n \cos n\theta) + \frac{d_4}{n} \cos n\theta$$

$$z_8(\theta) = \frac{d_1}{2} \left[\frac{\cos (\overline{n-1}\,\theta + \phi)}{n-1} - \frac{\cos (\overline{n+1}\,\theta - \phi)}{n+1} \right] + \frac{d_6\, e^{-d_3\theta}}{1 + d_3^2}$$

$$(n \sin n\theta - d_3 \cos n\theta) - \frac{d_4}{n} \sin n\theta$$

$$z_9(\theta) = 2d_1 \left[\frac{\cos (\overline{n-1}\,\theta + \phi)}{n-1} - \frac{(\cos (\overline{n+1}\,\theta - \phi)}{n+1} \right] + \frac{2d_7\, e^{-d_3\theta}}{1 + d_3^2}$$

$$(n \sin n\theta - d_3 \cos n\theta\ ) - \frac{2d_4}{n} \sin n\theta$$

$$z_{10}(\theta) = \frac{d_1}{2} \left[\frac{\cos (\overline{n-1}\,\theta + \phi)}{n-1} \quad \frac{\cos (\overline{n+1}\,\theta - \phi)}{n+1} \right] + \frac{d_8\, e^{-d_3\theta}}{1 + d_3^2}$$

$$(n \sin n\theta - d_3 \cos \theta) - \frac{d_4}{n} \sin n\theta$$

$$\therefore\ I_n = \sqrt{\frac{1}{2}\left(x_n^{\ 2} + y_n^{\ 2}\right)}\ , \quad n \neq 1, \quad n = 3, 5, 7, \ldots$$

Input RMS Fundamental Current, I_1:

$$x_1 = \frac{2}{M\pi}\left[\ w_{11}(\alpha_1) - w_{11}(0) + w_{12}(\beta_1) - w_{12}(\alpha_1) + w_{13}(\pi) - w_{13}(\beta_1)\right]$$

$$y_1 = \frac{2}{M\pi}\left[\ z_{11}(\alpha_1) - z_{11}(0) + z_{12}(\beta_1) - z_{12}(\alpha_1) + z_{13}(\pi) - z_{13}(\beta_1)\right]$$

$$w_{11}(\theta) = \frac{d_1}{2}\left[\ \theta \cos\phi - \frac{1}{2}\sin(2\theta - \phi)\ \right] - \frac{d_6\ e^{-d_3\theta}}{1 + d_3^{\ 2}}\left(d_3 \sin\theta + \cos\theta\right)$$

$$+ d_4 \cos\theta$$

$$w_{12}(\theta) = 2d_1\ \left[\ \theta \cos\phi - \frac{1}{2}\sin(2\theta - \phi)\ \right] - \frac{2d_7\ e^{-d_3\theta}}{1 + d_3^{\ 2}}\left(d_3 \sin\theta + \cos\theta\right)$$

$$+ 2d_4 \cos\theta$$

$$w_{13}(\theta) = \frac{d_1}{2}\left[\ \theta \cos\phi = \frac{1}{2}\sin(2\theta - \phi)\ \right] - \frac{d_8\ e^{-d_3\theta}}{1 + d_3^{\ 2}}\left(d_3 \sin\theta + \cos\theta\right)$$

$$+ d_4 \cos\theta$$

$$z_{11}(\theta) = \frac{d_1}{2}\left[\ -\ \theta \sin\phi - \frac{1}{2}\cos(2\theta - \phi)\ \right] + \frac{d_6\ e^{-d_3\theta}}{1 + d_3^{\ 2}}\left(\sin\theta - d_3 \cos\theta\right)$$

$$- d_4 \sin\theta$$

$$z_{12}(\theta) = 2d_1 \; [\; - \; \theta \; \sin \phi - \frac{1}{2} \cos \; (2\theta - \phi) \;] + \frac{2d_7 \; e^{-d_3\theta}}{1 + d_3^{\;2}} \; (\sin \theta - d_3 \; \cos \theta)$$

$$- \; 2d_4 \; \sin \theta$$

$$z_{13}(\theta) = \frac{d_1}{2} \; (\; - \; \theta \; \sin \phi - \frac{1}{2} \cos \; (2\theta - \phi) \;] + \frac{d_8 \; e^{-d_3\theta}}{1 + d_3^{\;2}} \; (\sin \theta - d_3 \; \cos \theta)$$

$$-d_4 \; \sin \theta$$

$$I_1 = \sqrt{\frac{1}{2} \; (x_1 2 + y_1^{\;2})}$$

Case 3:

$$\boxed{\frac{2}{3} < E_a < 1.0 \text{ pu:}} \qquad \alpha_2 = \alpha_3 = 0, \; 0 < \alpha_1 < \frac{\pi}{2} < \beta_1 < \pi$$

$$E_a = \frac{1}{6} \; (4 + \cos \alpha_1 - \cos \beta_1), \; \boxed{\alpha_1 = \cos^{-1} \; (6E_a - 4 + \cos \beta_1)}$$

$$i_a = 2d_1 \; \sin \; (\theta - \phi) + d_9 \; e^{-d_3\theta} - d_4 \quad , \; 0 < \theta < \alpha_1$$

$$= 3d_1 \; \sin \; (\theta - \phi) + d_{10} \; e^{-d_3\theta} - d_4 \; , \; \alpha_1 < \theta < \beta_1$$

$$= 2d_1 \; \sin \; (\theta - \phi) + d_{11} \; e^{-d_3\theta} - d_4 \; , \; \beta_1 < \theta < \pi$$

$$d_9 = I_0 + d_4 + 2d_1 \sin \phi$$

$$d_{10} = [\ I\alpha_1 + d_4 - 3d_1 \sin (\alpha_1 - \phi)\ ]\ e^{d_3 \alpha_1}$$

$$d_{11} = [\ I\beta_1 + d_9 - 2d_1 \sin (\beta_1 - \phi)\ ]\ e^{d_3 \beta_1}$$

$$i_p = \frac{2i_a}{M},\ 0 < \theta < \alpha_1$$

$$= \frac{3i_a}{M},\ \alpha_1 < \theta < \beta_1$$

$$= \frac{2i_a}{M},\ \beta_1 < \theta < \pi$$

Motor Average Current, I_{av}:

$$I_{av} = \frac{1}{\pi}\ [\ w_{14}(\alpha_1) - w_{14}(0) + w_{15}(\beta_1) - w_{15}(\alpha_1) + w_{16}(\pi) - w_{16}(\theta)\ ]$$

$$w_{14}(\theta) = -\ 2d_1 \cos (\theta - \phi) - \frac{d_9}{d_3}\, e^{-d_3 \theta} - d_4 \theta$$

$$w_{15}(\theta) = -3d_1 \cos (\theta - \phi) - \frac{d_{10}}{d_3}\, e^{-d_3 \theta} - d_4 \theta$$

$$w_{16}(\theta) = -\ 2d_1 \cos (\theta - \phi) - \frac{d_{11}}{d_3}\, e^{-d_3 \theta} - d_4 \theta$$

Motor RMS Current, $I_{a_{rms}}$:

$$I_{a_{rms}} = \sqrt{\frac{1}{\pi}\left[\, z_{14}(\alpha_1) - z_{14}(0) + z_{15}(\beta_1) - z_{15}(\alpha_1) + z_{16}(\pi) + z_{16}(\beta_1)\right]}$$

$$z_{14}(\theta) = (2d_1^{\,2} + d_4^{\,2})\,\theta = d_1^{\,2}\sin(2\theta - 2\phi) - \frac{d_9^{\,2}}{2d_3}\,e^{-2d_3\theta} - \frac{4d_1d_9}{1+d_3^{\,2}}\,e^{-d_3\theta}$$

$$[\, d_3\sin(\theta-\phi) + \cos(\theta-\phi)\,] + 4d_1d_4\cos(\theta-\phi) + \frac{2d_4d_9}{d_3}\,e^{-d_3\theta}$$

$$z_{15}(\theta) = (\tfrac{9}{2}\,d_1^{\,2} + d_4^{\,2})\,\theta - \frac{9}{4}\,d_1^{\,2}\sin(2\theta - 2\phi) - \frac{d_{10}^{\,2}}{2d_3}\,e^{-2d_3\theta} - \frac{6d_1d_{10}}{1 + d_3^{\,2}}$$

$$e^{-d_3\theta}\,[\, d_3\sin(\theta-\phi) + \cos(\theta-\phi)\,] + 6d_1d_4\cos(\theta-\phi)$$

$$+ \frac{2d_4d_{10}}{d_3}\,e^{-d_3\theta}$$

$$z_{16}(\theta) = (2d_1^{\,2} + d_4^{\,2})\,\theta - d_1^{\,2}\sin(2\theta - 2\phi) - \frac{d_{11}^{\,2}}{2d_3}\,e^{2d_3\theta} - \frac{4d_1d_{11}}{1 + d_3^{\,2}}$$

$$e^{-d_3\theta}\,[\, d_3\sin(\theta-\phi) - \cos(\theta-\phi)\,] + 4d_1d_4\cos(\theta-\phi)$$

$$+ \frac{2d_4d_{11}}{d_3}\,e^{-d_3\theta}$$

Input RMS Current, I:

$$I = \sqrt{\frac{1}{\pi}\left[\ 4(z_{14}(\alpha_1)-z_{14}(0)] + 9[z_{15}(\beta_1)-z_{15}(\alpha_1)]+4[z_{16}(\pi)-z_{16}(\beta_1)]\ \right]}$$

Input Harmonic Currents, I_n ($n \neq 1$):

$$x_n = \frac{2}{M\pi}[\ w_{17}(\alpha_1) - w_{17}(0) + w_{18}(\beta_1) - w_{18}(\alpha_1) + w_{19}(\pi) - w_{19}(\beta_1)\ ]$$

$$y_n = \frac{2}{M\pi}[\ z_{17}(\alpha_1) - z_{17}(0) + z_{18}(\beta_1) - z_{18}(\alpha_1) + z_{19}(\pi) - x_{19}(\beta_1)\ ]$$

$$w_{17}(\theta) = 2d_1\left[\frac{\sin(\overline{n-1}\,\theta + \phi)}{n-1} - \frac{\sin(\overline{n+1}\,\theta - \phi)}{n+1}\right] - \frac{2d_9\ e^{-d_3\theta}}{n^2 + d_3^2}$$

$$(d_3 \sin n\theta + n \cos n\theta) + \frac{2d_4}{n}\cos n\theta$$

$$w_{18}(\theta) = \frac{9d_1}{2}\left[\frac{\sin(\overline{n-1}\,\theta + \phi)}{n-1} - \frac{\sin(\overline{n+1}\,\theta - \phi)}{n+1}\right] - \frac{3d_{10}\ d^{-d_3\theta}}{n^2 + d_3^2}$$

$$(d_3 \sin n\theta + n \cos n\theta) + \frac{3d_4}{n}\cos n\theta$$

$$w_{10}(\theta) = 2d_1\left[\frac{\sin(\overline{n-1}\,\theta + \phi)}{n-1} - \frac{\sin(\overline{n+1}\,\theta - \phi)}{n+1}\right] - \frac{2d_{11}\ e^{-d_3\theta}}{n^2 + d_3^2}$$

$$(d_3 \sin n\theta + n \cos n\theta) + \frac{2d_4}{n}\cos n\theta$$

$$z_{17}(\theta) = 2d_1 \left[\frac{\cos (\overline{n-1}\ \theta + \phi}{n-1} - \frac{\cos (\overline{n+1}\ \theta - \phi)}{n+1} \right] + \frac{2d_9\ e^{-d_3\theta}}{n^2 + d_3^{\ 2}}$$

$$(d \sin n\theta - d_3 \cos n\theta) - \frac{2d_4}{n} \sin n\theta$$

$$z_{18}(\theta) = \frac{9d_1}{2} \left[\frac{\cos (\overline{n-1}\ \theta + \phi}{n-1} - \frac{\cos (\overline{n+1}\ \theta - \phi)}{n+1} \right] + \frac{3d_{10}\ e^{-d_3\theta}}{n^2 + d_3^{\ 2}}$$

$$(n \sin n\theta - d_3 \cos n\theta) - \frac{3d_4}{n} \sin n\theta$$

$$z_{19}(\theta) = 2d_1 \left[\frac{\cos (\overline{n-1}\ \theta - \phi)}{n-1} = \frac{\cos (\overline{n+1}\ \theta - \phi)}{n+1} \right] + \frac{2d_{11}\ d^{-d_3\theta}}{n^2 + d_3^{\ 2}}$$

$$(n \sin n\theta - d_3 \cos n\theta) - \frac{2d_4}{n} \sin n\theta$$

$$I_n = \sqrt{\frac{1}{2} (x_n^{\ 2} + y_n^{\ 2})}$$

Input RMS Fundamental Current, I_1:

$$x_1 = \frac{2}{M\pi} \left[w_{20}(\alpha_1) - w_{20}(0) + w_{20}(\beta_1) - w_{20}(\alpha_1) + w_{21}(\pi) - w_{21}(\beta_1) \right]$$

$$y_1 = \frac{2}{M\pi} \left[z_{20}(\alpha_1) - z_{20}(0) + z_{20}(\beta_1) - z_{20}(\alpha_1) + z_{21}(\pi) - z_{21}(\beta_1) \right]$$

$$w_{20}(\theta) = 2d_1 \left[\theta \cos \phi - \frac{1}{2} \sin (2\theta - \phi) \right] - \frac{2d_9\ e^{-d_3\theta}}{1 + d_3^{\ 2}} (d_3 \sin \theta + \cos \theta)$$

$$+ 2d_4 \cos \theta$$

$$w_{21}(\theta) = \frac{9d_1}{2}\left[\ \theta \cos\phi - \frac{1}{2}\sin(2\theta-\phi)\ \right] - \frac{3d_{10}\ e^{-d_3\theta}}{1 + d_3^{\,2}}$$

$$(d_3 \sin\theta + \cos\theta) + 3d_4 \cos\theta$$

$$w_{22}(\theta) = 2d_1\ \left[\ \theta \sin\phi - \frac{1}{2}\cos(2\theta-\phi)\ \right] + \frac{2d_{11}\ e^{-d_3\theta}}{1 + d_3^{\,2}}$$

$$(d_3 \sin\theta + \cos\theta) + 2d_4 \cos\theta$$

$$z_{20}(\theta) = 2d_1\ \left[\ -\theta \sin\phi - \frac{1}{2}\cos(2\theta-\phi)\ \right] + \frac{2d_9\ e^{-d_3\theta}}{1 + d_3^{\,2}}$$

$$(\sin\theta - d_3 \cos\theta) - 2d_4 \sin\theta$$

$$z_{21}(\theta) = \frac{9d_1}{2}\left[\ -\theta \sin\phi - \frac{1}{2}\cos(2\theta-\phi)\ \right] + \frac{3d_{10}\ e^{-d_3\theta}}{1 + d_3^{\,2}}$$

$$(\sin\theta - d_3 \cos\theta) - 3d_4 \sin\theta$$

$$z_{22}(\theta) = 2d_1\ \left[\ -\theta \sin\phi - \frac{1}{2}\cos(2\theta-\phi)\ \right] + \frac{2d_{11}\ e^{-d_3\theta}}{1 + d_3^{\,2}}$$

$$(\sin\theta - d_3 \cos\theta) - 2d_4 \sin\theta$$

$$I_1 = \sqrt{\frac{1}{2}\left(x_1^{\,2} + y_1^{\,2}\right)}$$

Also compute λ, δ, h and η.

A.5 ANALYSIS OF A PULSE-WIDTH-MODULATED AC/DC CONVERTER SUPPLYING A DC TRACTION MOTOR

A.5.1 General

In the phase-controlled rectifiers, with or without sector control, the supply current consists of one pulse per half cycle. This results in a high content of lower harmonics which are difficult to filter out. An improvement in this situation can be effected by turning the thyristors on and off several times during each half cycle. The width of the resulting pulses could be changed to control the output voltage. Lower-order harmonics could be reduced or eliminated by selecting the type of modulation for the pulse widths and the number of pulses per half cycle. The resulting increase in higher-order harmonics can be filtered out fairly easily.

A.5.2 Sinusoidal Pulse Width Control

Figure A.5.1 gives the connection diagram for a pulse-width-modulated (PWM) ac/dc converter supplying a dc traction motor. Figure A.5.2 shows the corresponding waveforms of voltages and currents of a pulse-width-modulated ac-dc converter.

A.5.3 Definition of Variables

As a reference for the analysis to follow, a list of variables and circuit parameters is summarized below.

C = impact filter capacitance

f_c = carrier frequency

f_r = reference sine signal frequency

I = carrier ratio = f_c/f_r

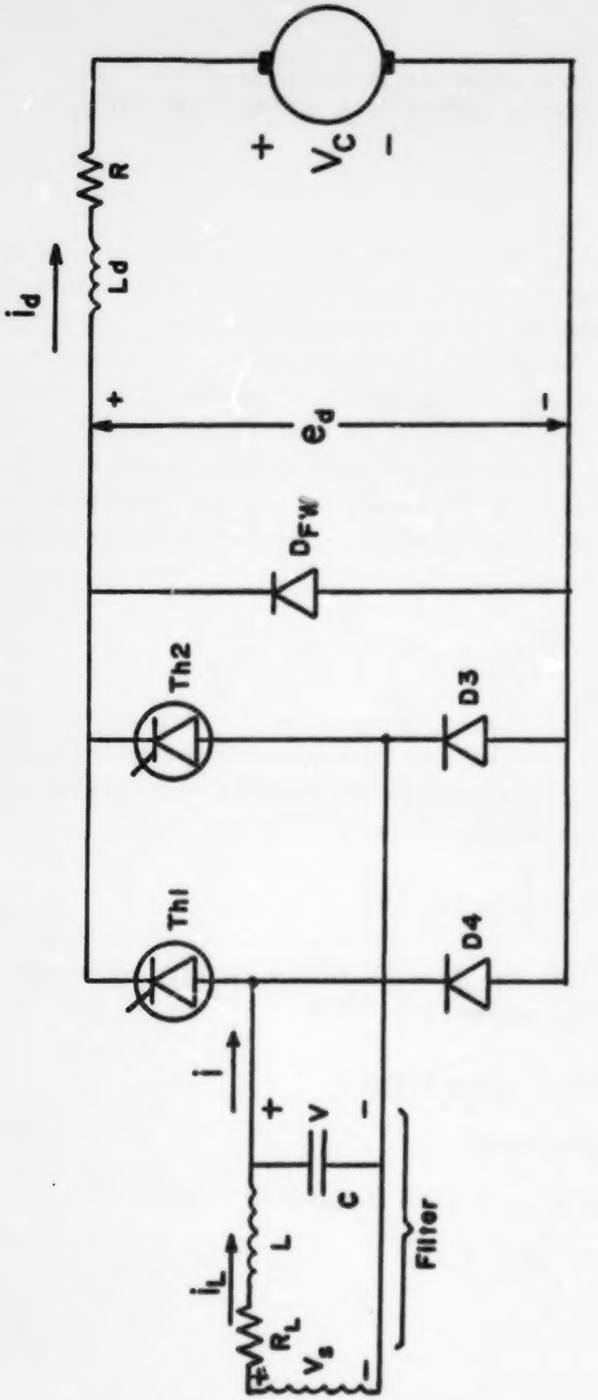

Figure A.5.1 Pulse-Width-Modulated AC-DC Converter Supply for a Separately-Excited or Series DC Motor

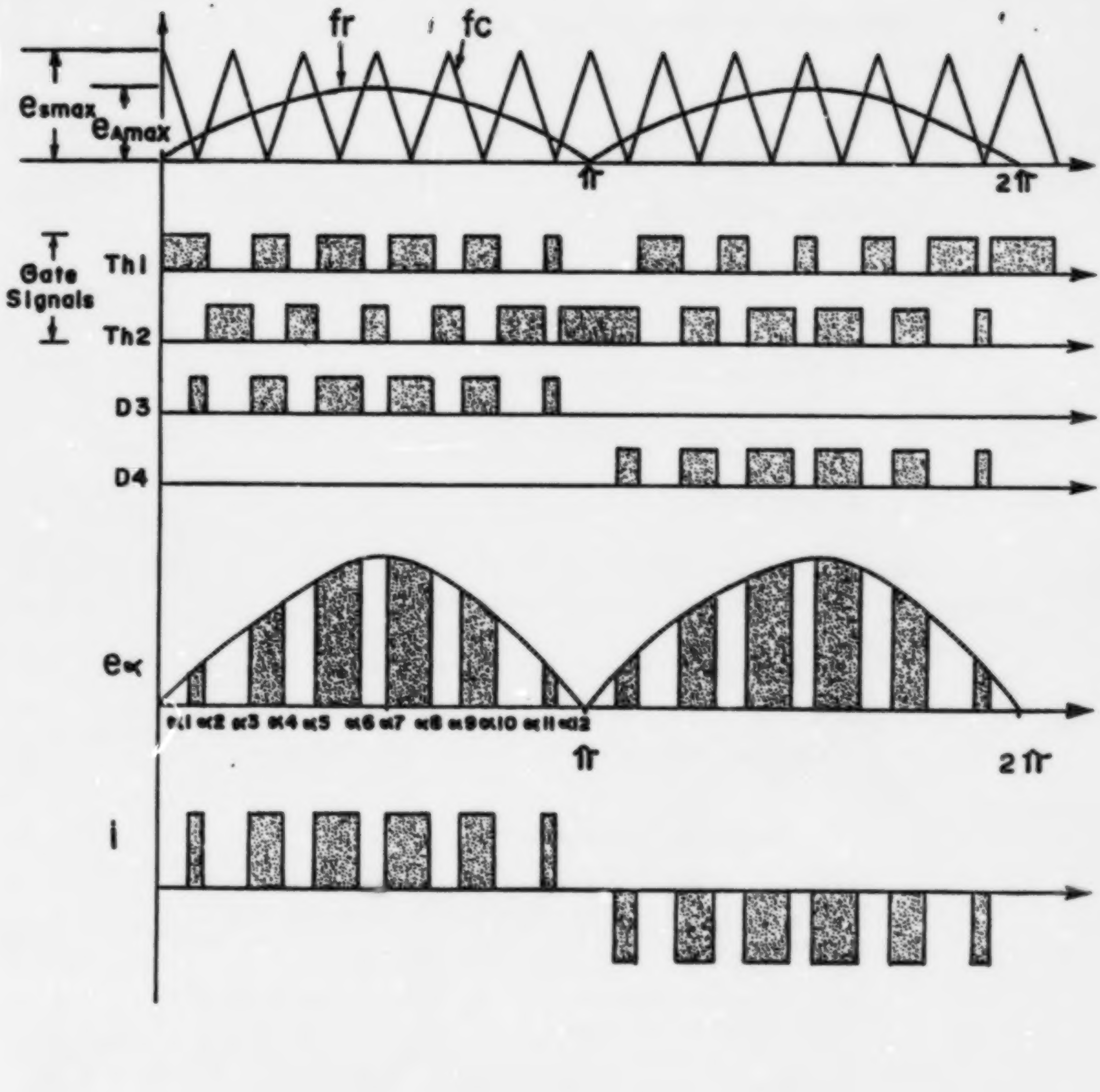

Figure A.5.2 Waveforms of Voltages and Currents of a Pulse-Width Modulated AC-DC Converter

L = input filter inductance

L_d = equivalent motor inductance

M = modulation index = $e_{smax}/e_{\Delta max} < 1$

R = armature winding equivalent resistance

R_L = input filter inductance resistance plus transformer winding resistance

t_q = commutation time

V_c = dc motor back emf

V_D = forward diode drop (typically 2V)

V_s = transformer secondary rms voltage

ω = supply angular frequency (2 f)

A.5.4 Assumptions

The computational complexity can be reduced while still maintaining reasonable accuracy with the following assumptions:

- the dc motor current (i_d) contains a small amount of ripple
- sinusoidal modulation of the PWM control scheme is used
- the capacitors are lossless
- whenever commutation takes place, the dc motor current (i_d) flows through the free-wheeling diode
- the dc motor back emf (V_c) depends on the type of motor (series or shunt)
- a high efficiency transformer is used.

A.5.5 Computation Algorithm

The computation of voltages, currents, power losses, efficiency and power factor of the PWM ac/dc converter follows the flow chart in Figure A.5.3, with the detailed expressions presented in the following sections. For a specified output power from the motor and a specified speed, the dc motor current (I_0) can be determined. Using this value of current and an assumed modulation index (M), calculations can be made to determine a calculated motor power. This value is compared with the specified power and, if different, the modulation index is changed until the specified and calculated powers agree. Auxiliary values such as harmonic factor, losses, efficiency and power factor are then calculated. Repetition of this approach leads to a graph of modulation index, voltages, currents and auxiliary values as a function of output power.

A.5.5.1 Iteration to Obtain Alphas

The magnitude of the triangular carrier wave can be described by a series of straight lines where:

1st line: $y = \frac{2I}{\pi} e_{\Delta max} (X = \frac{\pi}{2I})$, where $I = \frac{f_c}{f_r}$

2nd line: $y = + \frac{2I}{} e_{\Delta max} (X - \frac{\pi}{2I})$

3nd line: $y = - \frac{2I}{} e_{\Delta max} (X - \frac{3\pi}{2I})$

ith line: $y = (-1)^i \frac{2I}{\pi} e_{max} [x - \frac{[2i - 1 - (-1)^i]\pi}{4I}]$

The reference sine signal in the region 0 to π is described by:

$$y = e_{smax} \sin x$$

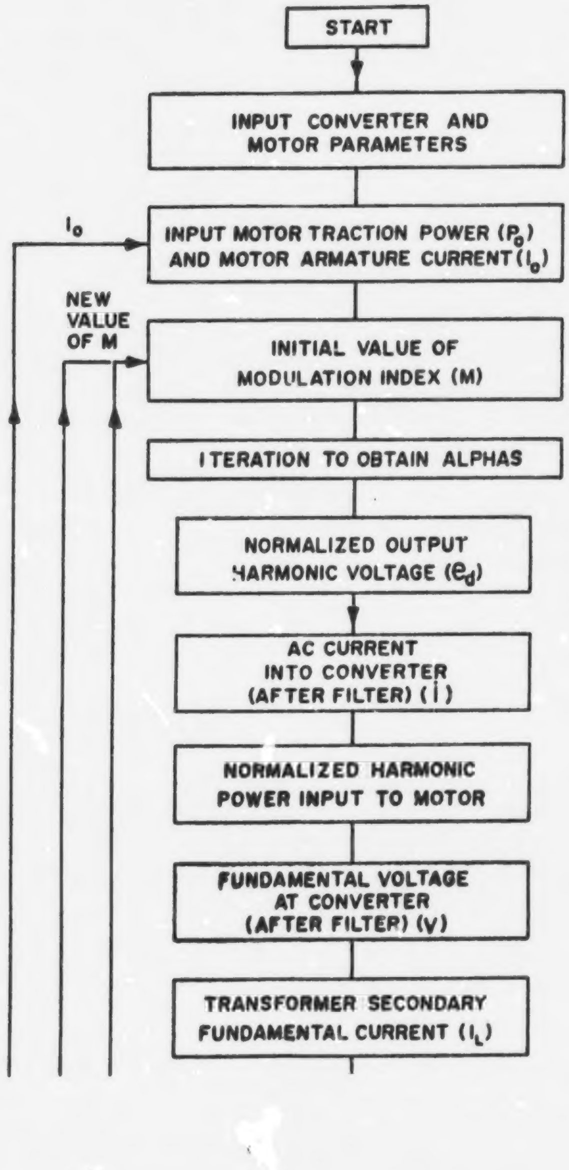
START
INPUT CONVERTER AND MOTOR PARAMETERS
I_o
INPUT MOTOR TRACTION POWER (P_o) AND MOTOR ARMATURE CURRENT (I_o)
NEW VALUE OF M
INITIAL VALUE OF MODULATION INDEX (M)
ITERATION TO OBTAIN ALPHAS
NORMALIZED OUTPUT HARMONIC VOLTAGE (e_d)
AC CURRENT INTO CONVERTER (AFTER FILTER) (I)
NORMALIZED HARMONIC POWER INPUT TO MOTOR
FUNDAMENTAL VOLTAGE AT CONVERTER (AFTER FILTER) (V)
TRANSFORMER SECONDARY FUNDAMENTAL CURRENT (I_L)

Figure A.5.3 Flow Chart for Determining Performance of Pulse-Width-Modulated AC-DC Converter Supplying a DC Traction Motor

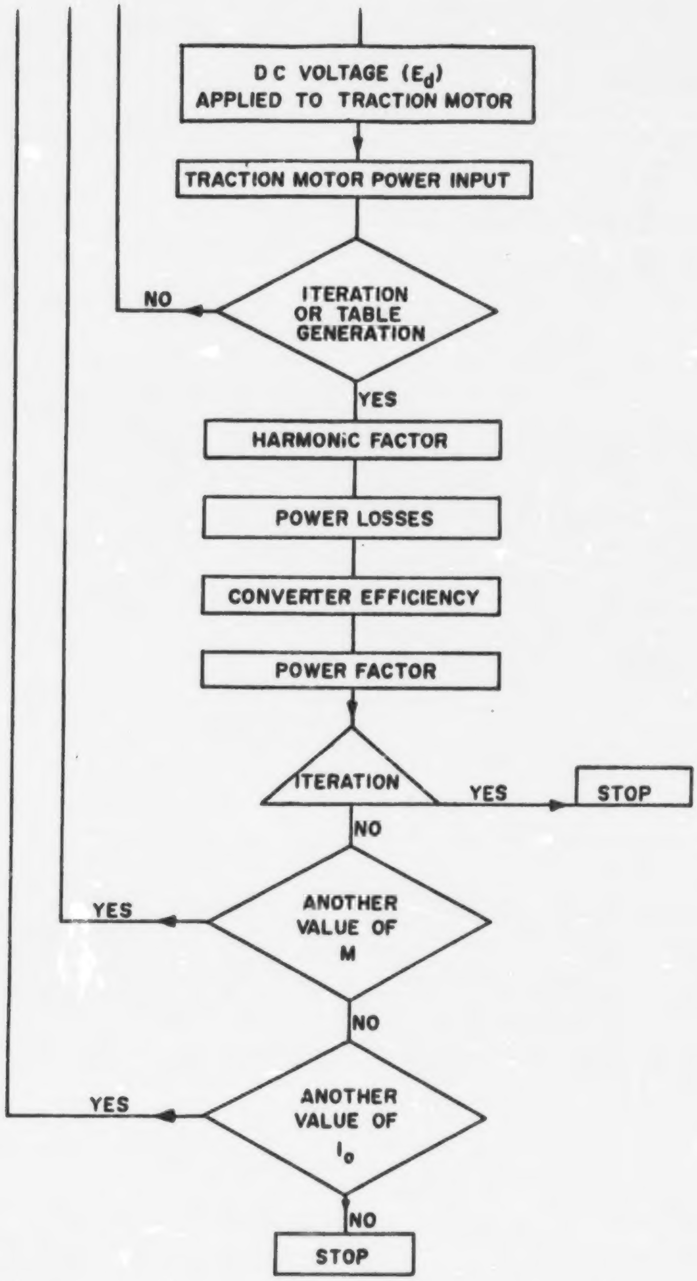

Figure A.5.3 Cont'd)

The solution of the angles of intersection of the triangular carrier wave and reference sine signal are obtained by equating the two functions:

$$(-1)^i \frac{2I}{\pi} e_{\Delta max} \left[x - \frac{[\, 2i - 1 - (-1)^i \,]\pi}{4I} \right] = e_{smax} \sin x$$

and determining α_i by setting $x = \alpha_i$.

$$\alpha_i = \frac{e_{smax}}{e_{\Delta max}} \frac{\pi}{2I} (-1)^i \sin \alpha_i + \frac{[\, 2i - 1 - (-1)^i \,]\pi}{4I}$$

$$\boxed{\begin{array}{l} \alpha_i = (-1)^i \frac{M}{I} \pi \sin \alpha_i + \frac{[\, 2i - 1 - (-1)^i \,]\pi}{4I} \\ \text{where: } M = \frac{e_{smax}}{e_{\Delta max}} < 1 \text{ , } I = \frac{f_c}{f_r} \end{array}}$$

The angles of intersection, which establish the gate firing timing, can be evaluated interactively using the computer.

A.5.5.2 Normalized Output Harmonic Voltage (e_d)

The traction motor voltage (e_d) can be expressed as:

$$e_d = E_d + \sum_{n=1}^{\infty} a_n \cos nwt + b_n \sin nwt$$

where the dc component, E_d, can be determined from:

$$E_d = \frac{1}{\pi} \int_0^{\pi} e_d \, dwt$$

$$= \frac{\sqrt{2}\, V}{\pi} \sum_{i=1}^{I} (\cos \alpha_{2i-1} - \cos\alpha_{2i})$$

and the coefficients, a_n and b_n, are determined from:

$$a_n = \frac{2}{\pi} \int_0^{\pi} e_d \cos nwt \, dwt$$

$$= \frac{2}{\pi} \sum_{i=1}^{I} \int_{\alpha_{2i-1}}^{\alpha_{2i}} \sqrt{2}\, V \sin wt \cos nwt \, dwt$$

$$= \frac{2\sqrt{2}\, V}{\pi} \sum_{i=1}^{I} \int_{\alpha_{2i-1}}^{\alpha_{2i}} \frac{1}{2} [\, \sin (n+1)\, wt - \sin (n-1)\, wt \,]\, dwt$$

$$a_n = \frac{\sqrt{2}\, V}{\pi} \sum_{i=1}^{I} \left[\frac{\cos (n-1)\, wt}{n-1} - \frac{\cos (n+1)\, wt}{n+1} \right]_{\alpha_{2i-1}}^{\alpha_{2i}}$$

Similarly,

$$b_n = \frac{\sqrt{2}\, V}{\pi} \sum_{i=1}^{I} \left[\frac{\sin (n-1)\, wt}{n-1} - \frac{\sin (n+1)\, wt}{n+1} \right]_{\alpha_{2i-1}}^{\alpha_{2i}}$$

For calculations of harmonic power, only the normalized values of the coefficients are required in the form:

$$a_n' = a_n \Big/ \frac{\sqrt{2}\,V}{\pi}$$

$$b_n' = b_n \Big/ \frac{\sqrt{2}\,V}{\pi}$$

A.5.5.5 AC Current Into Converter (After Filter) (i)

The ac current into the converter is assumed to have no dc component or even harmonics. It can be expressed as:

$$i = \sum_{n=1}^{\infty} d_n \sin nwt \qquad n = 1,3,5,\ldots$$

where: $d_n = \frac{2I_0}{n\pi} \sum_{i=1}^{I} (\cos n\alpha_{2i-1} - \cos n\alpha_{2i})$

With the dc motor current (I_0) known, the ac current can be determined.

A.5.5.6 Normalized Harmonic Power Input to Motor

The harmonic power input to the motor is given by:

$$P_H = \sum |C_n| I_{dn} \cos \phi_n$$

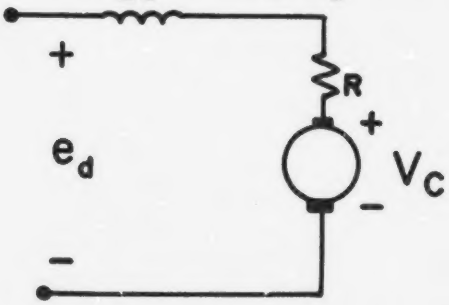

where: $\phi_n = \tan^{-1} \frac{nwL_d}{R}$

The normalized harmonic power input can obtain from:

$$P_H' = \sum_{n=1}^{\infty} \frac{|C_n'|^2 R}{R^2 + (nwL_d)^2}$$

where: $|C_n'|^2 = \frac{a_n' + b_n'}{2}$

A.5.5.5 Fundamental Voltage At Converter (After Filter) (V)

With reference to the circuit, the fundamental current of the secondary of the transformer can be obtained from the fundamental of the ac current into the converter (Section A.5.5.3) by the expression:

$$I(1) = I_L(1) \frac{-jXc}{R_T = jXc}$$

$$I_L(1) = I(1)\ (1 + j \frac{R_T}{Xc})$$

$$= I(1) + j \frac{V}{X_c}$$

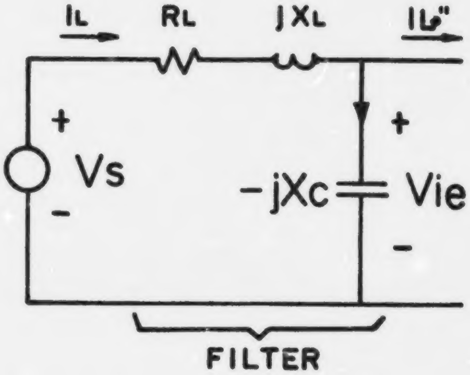

$$\boxed{I_L(1) = \sqrt{I(1)^2 + \frac{V}{X_c})^2} \quad \angle \tan^{-1} \frac{V}{I(1)\ X_c}}$$

The known transformer secondary voltage (V_s) can be developed as follows:

$$V_s = I_L \; (R_L + j \; X_L) + V \; \underline{|0^0}$$

$$= (I(1) + j \; \frac{V}{X_c}) \; (R_L + j \; X_L) + V$$

$$= I(1) \; R_L \; \frac{V \; X_L}{X_c} + V + j \; \frac{V \; R_L}{X_c} + j \; I(1) \; X_L$$

$$= V \; (1 - \frac{X_L}{X_c}) + I(1) \; R_L + j \; (I(1) \; X_L + \frac{V \; R_L}{X_c})$$

The magnitude of the secondary voltage becomes:

$$|V_s|^2 = (V \; (1 - \frac{X_L}{X_c}) + I(1) \; R_L)^2 + (I(1) \; X_L + \frac{V \; R_L}{X_c})^2$$

$$= V^2 \; (1 - \frac{X_L}{X_c})^2 + 2 \; (1 - \frac{X_L}{X_c}) \; I(1) \; R_L \; V + (I(1) \; R_L)^2 + (I(1) \; X_L)^2$$

$$+ 2 \; I(1) \; X_L \; \frac{R_L}{X_c} \; V + V^2 \; (\frac{R_L}{X_c})^L$$

$$= [(1 - \frac{X_L}{X_c})^2 + (\frac{R_L}{X_c})^2] \; V^2 + 2 \; I(1) \; R_L \; V + (I(1) \; R_L)^2 + (I(1) \; X_L)^2$$

which can be rearranged to obtain a quadratic equation in terms of the fundamental voltage (V) at the converter.

$$[(1 - \frac{X_L}{X_c})^2 + (\frac{R_L}{X_c})^2] \; V^2 + 2 \; I(1) \; R_L \; V + (I(1) \; R_L)^2 + (I(1) \; X_L)^2 - V_S{}^2 = 0$$

If the following constants are defined:

$$\text{Let } A = (1 - \frac{X_L}{X_c})^2 + (\frac{R_L}{X_c})^2$$

$$B = 2\ I(1)\ R_L$$

$$C = I(1)^2\ (R_L^{\ 2} + X_L^{\ 2}) - V_S^{\ 2}$$

then the fundamental voltage at the converter is equal to:

$$V = \frac{-\ B + \sqrt{B^2 - 4\ AC}}{2A}$$

A.5.5.6 Transformer Secondary Fundamental Current (I_L)

From the current expressicn developed in Section E.5.5, the magnitude of the transformer secondary fundamental current is calculated from:

$$I_L(1) = \sqrt{I^2(1) + (\frac{V}{X_c})^2}$$

while the transformer secondary harmonic currents ($n \geq 2$) can be obtained from:

$$I_{Ln} = I_n \frac{X_c/_n}{\frac{X_c}{n} - nX_L}$$

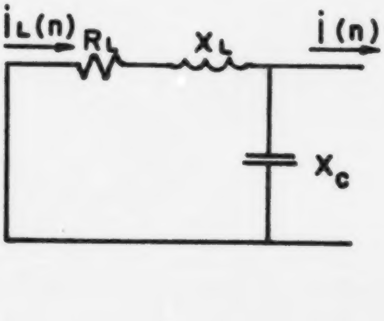

A.5.5.7 DC Voltage (E_d) Applied to Traction Motor

The value of dc voltage applied to the traction motor was given in Section A.5.5.2 as:

$$E_d = \frac{\sqrt{2}\,V}{\pi} \sum_{i=1}^{I} (\cos \alpha_{2i-1} - \cos \alpha_{2i})$$

A.5.5.8 Traction Motor Power Input

The dc power input is given by:

$$P_{DC} = E_d \, I_0$$

where: I_0 = given or known traction motor dc current

E_d = dc voltage applied to traction motor (Section A.5.5.6).

The harmonic power can be obtained from the normalized harmonic power (Section A.5.5.4) using the expression:

$$P_H \left(\frac{\sqrt{2}\,V}{\pi}\right)^2 P^1_H$$

Thus, the total input power into the tracton motor equals:

$$P = P_{DC} + P_H$$

If the correct modulation index is used, the traction motor (P_0) should be equal to:

$$P_0 = P_{DC} - I_0^2 R$$

The value of the modulation index may have to be determined iteratively with the equality of given and calculated powers determining the correct value. For all calculations, the carrier ratio (f_c/f_r) was assumed to be six.

Once the correct modulation index has been determined, the following auxiliary values can be computed.

A.5.5.9 Harmonic Factor

The harmonic factor is, by definition, expressed as:

$$HF = \sqrt{\sum_{n=2}^{\infty} I_{Ln}^2 / I_L^2(1)}$$

where the currents are obtained from the expression presented in Section A.5.5.6.

A.5.5.10 Transformer Secondary RMS Current

The transformer secondary rms current is obtained from:

$$I_{Lrms} = \sqrt{\sum_{n=1}^{\infty} I_{Ln}^2}$$

where the currents are obtained from Section A.5.5.6.

A.5.5.11 Power Losses

Three power losses are taken into account:

(i) filter losses:

$$P_{FILT} = I_{Lrms}^2 \; F_L$$

(ii) switching losses:

$$P_s = \frac{t_q}{T} I_0 \sum_{i=1}^{I} e_d (\alpha_{2i})$$

where: t_q = commutation time

$T = \frac{\pi}{2W}$

ω = supply frequency (rad/sec)

$e_d(\alpha_{2i}) = \sqrt{2}\ V \sin (\alpha_{2i})$

(iii) conduction losses.

The conduction losses due to the device drop can be expressed as:

$$P_c = I_0 \left[\frac{2V_D}{\pi} \sum_{i=1}^{I} (\alpha_{2i} - \alpha_{2i-1}) \right] \text{(SCR's)}$$

$$+ I_0 \left[\frac{V_D}{\pi} \left[\pi - \sum_{i=1}^{I} (\alpha_{2i} - \alpha_{2i-1}) \right] \right] \text{(free wheeling diode)}$$

This expression can be reduced to:

$$P_c = \frac{I_0 V_D}{\pi} \left[\pi + \sum_{i=1}^{I} (\alpha_{2i} - \alpha_{2i-1}) \right]$$

where V_D = device voltage drop.

A.5.5.12 Converter Efficiency

The overall ac/dc converter per cent efficiency is given by:

$$\% \; n = \frac{P}{P + P_{FILT} + P_s + P_c} \times 100\%$$

where the powers are determined in Sections A.5.5.8 and A.5.5.11.

A.5.5.13 Power Factor

The power factor is defined in terms of the angle between the fundamental transformer secondary voltage (V_s) and the funamental transformer secondary current (I_L). From Section A.5.5.5. for the real part of V_s, let:

$$Q_2 = V \left(1 - \frac{X_L}{X_c}\right) + I(1) \, R_L$$

and for the imaginary part, let:

$$Q_1 = I(1) \, X_L + \frac{V \, R_L}{X_c}$$

Then the angle of V_s equals:

$$\underline{\left| V_s \right.} = \tan^{-1} (Q_1/Q_2)$$

Alos from Section A.5.5.5, the angle of I_L equals:

$$\underline{\left| I_L \right.}(1) = \tan^{-1} (v \, / \, (I(1) \, X_c))$$

Thus, the angle between the transformer secondary voltage and current is:

$$\theta = \angle V_s - \angle I_L(1)$$

and the power factor (pf) becomes:

$$pf = \cos \theta$$

A.6 AN AC-DC-DC LINK USING A TYPE A CHOPPER SUPPLYING A SEPARATELY-EXCITED MOTOR

A.6.1 General

A very popular means of speed control of dc motors is the use of dc choppers. Essentially choppers convert a fixed dc voltage to a variable dc output voltage. From the point of view of harmonic penetration into the ac supply, the configuration of dc choppers considered here includes a full wave rectifier on the input side of the chopper.

A.6.2 Type A Chopper Supplied from an AC Line

Figure A.6.1 shows the connection diagram for a dc chopper supplied from an ac line through a single-phase transformer, full wave rectifier and LC filter. The chopper supplies a separately-excited dc traction motor. This scheme is similar to a configuration used by General Electric Co. (commonly known as the GE chopper) for traction motor control. Unlike the present scheme, analyzed in detail in the succeeding sections, the GE chopper employs controlled rectifiers on the input side of the chopper.

A.6.3 Definition of Symbols Used in this Analysis

ALPHA = duty ratio = ton/TCHOP

C1 = input filter capacitance

EFF = efficiency

FLTLOS = input filter losses

HF = harmonic factor

ICHOP_{DC} = dc component of chopping current

I_{LDC} = dc component of filter inductor current, ILDC = ICHOP_{DC}

IOD = output dc current into motor

ISRMS = rms current at transformer secondary side

L = load inductance (motor armature inductance)

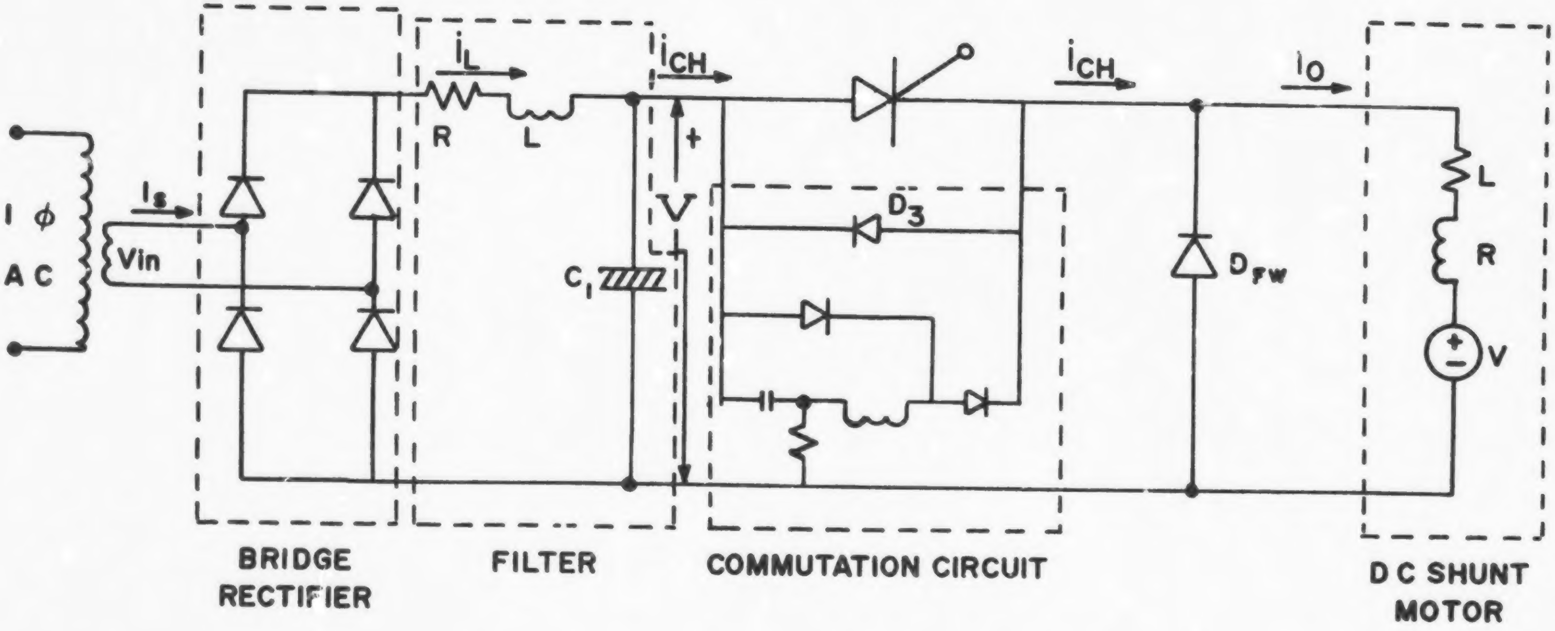

Figure A.6.1 An AC-DC-DC Link, Type A Chopper

L_1 = input filter inductance

P_C = conduction losses (main thyristor plus diodes)

PF = power factor

P_H = total power input to motor

P_S = switching loss

P_{TOT} = total losses = PS + PC + FLTLOS

R_{L1} = filter inductor resistance plus loading resistance

TCHOP = chopping period (fchop = 1/Tchop)

ton = switching device conduction time within a cycle

t_q = thyristor turn off time (20 sec here)

t_x = time variable, for determination of continuous or discontinuous current mode operation

V = chopper input voltage

V_c = motor back emf

V_D = diode or thyristor forward voltage drop

v_0 = chopper output voltage, dc components only

v_{in} = transformer secondary voltage

A.6.4 Analysis of a Type A Chopper with Filter

Figures A.6.2 and A.6.3 give the voltage and wave forms of the chopper output for two possible cases: Case 1, continuous current operation, and Case 2, discontinuous current. The cases are distinguished by the value of t_x as:

Case 1: $t_x \geq$ TCHOP → continuous mode

Case 2: $t_x <$ TCHOP → discontinuous mode

t_x is given as:

$$t_x = \tau \ln \left[e^{ton/\tau} \left[1 + \frac{V-V_c}{V_c} (1-e^{-ton/\tau}) \right] \right]$$

where: $\tau = L/R$

$V_c = Ka\ \phi\ N$

V = input voltage to chopper (assume dc)

$= \frac{2\sqrt{2}}{\pi}$ Vin rms

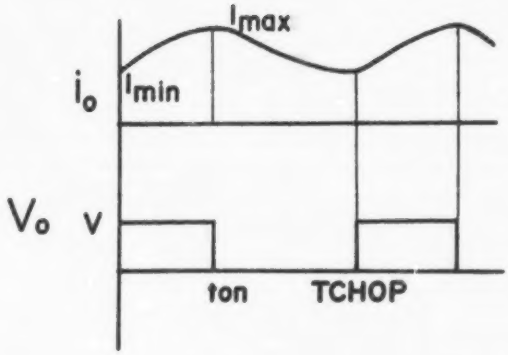

Figure A.6.2 Continuous current operation

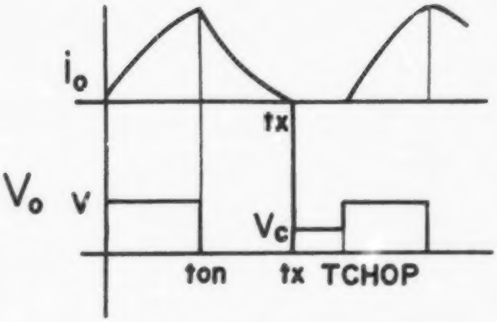

Figure A.6.3 Discontinuous current operation

Case 1: $t_x \geq$ TCHOP (continuous mode)

Usually the chopper will operate in continuous current mode if the load has enough inductance to sustain the current. The chances of going into discontinuous mode will increase when the chopper is operating at low-duty ratio (ton/TCHOP). Low-duty ratio implies decreasing ton. In most cases, with a reasonable amount of load inductance and a chopping frequency of 400 Hz, it was experienced that the mode of operation stays continuous even at low-duty ratio (say, for a duty ratio of 0.1). The following analysis is based on continuous-mode operation.

The output voltage and current waveform in this case refers to Figure A.6.2.

v_0, the output voltage, is given by:

$$v_a = v_0 + \sum_{n=1}^{\infty} (a_n \sin nwt + b_n \cos nwt)$$

where: $v_0 = V \, . \, ton/TCHOP$

$$a_n = \frac{V}{n\pi}(1 - \cos nwton)$$

$$b_n = \frac{V}{n\pi}\sin nwton$$

$$|Cn| = \sqrt{a_-^{\,2} + b_n^{\,2}}$$

$$= \frac{\sqrt{2}\, V}{n\pi}(1 - \cos nwton)^{1/2}$$

Consider i_{CH}, chopper input current:

$$I_m = \frac{v-v_c}{R}$$

$$i_{CH} = ICH_{DC} + \sum_{n=1}^{\infty} (a_n \sin nwt + b_n \cos nwt)$$

$$I_{min} = \frac{V}{R}\,\frac{(e^{ton/\tau} - 1)}{(e^{TCHOP/\tau} - 1)} - \frac{V_c}{R}$$

$$ICH_{DC} = \frac{1}{TCHOP}\left[\, I_m\, ton + \tau(I_m - I_{min})\,(e^{-ton/\tau} - 1)\,\right]$$

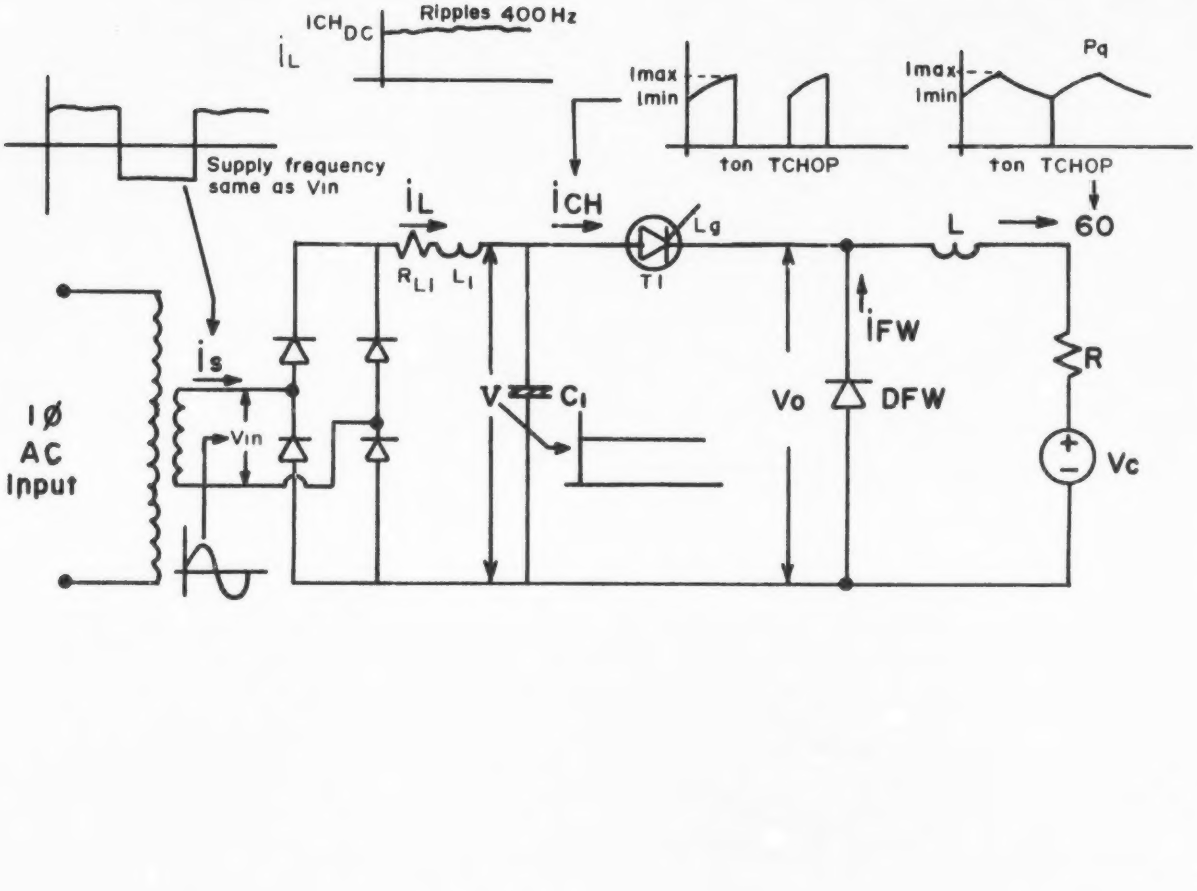

Figure A.6.4 Waveforms for Continuous Current Mode Operation

$$a_n = \frac{2}{\mathrm{TCHOP}} \left[\frac{I_m}{nw} (1 - \cos nwton) - \frac{(I_m - I_{min})\, nw\tau^2}{1 + (nw\tau)^2} \right.$$

$$\left. + \frac{(I_m - I_{min})\ \tau e^{-ton/\tau}}{\sqrt{1 + (nw\tau)^2}} \sin (nwton + \tan^{-1} nw\tau) \right]$$

$$b_n = \frac{2}{\mathrm{TCHOP}} \left[\frac{I_m}{nw} \sin nwt - (I_m - I_{min}) \frac{e^{-t/\tau}\ nw\tau^2}{1 + (nw\tau)^2} \right.$$

$$\left. \left(\sin nwt - \frac{\cos nwt}{nw\tau}\right) \right] \Bigg|_0^{ton}$$

Consider i_L (Figure A.6.6):

$$i_L - I_{LDC} + \text{harmonics } (i_{Ln})$$

$$I_{LDC} = ICH_{DC}$$

The harmonics of i_L can be obtained from the harmonics of i_{CH}:

$$i_{Ln} = \left[\frac{1}{(n \frac{f_{CH}}{f_r})^2 - 1} \right] i_{CHn}$$

$$i_{CHn} = \sqrt{\frac{a_n^2 + b_n^2}{2}}$$

where: $f_r = \dfrac{1}{2\pi \sqrt{L_1 C_1}}$

$$f_{CH} = \frac{1}{\mathrm{TCHOP}}$$

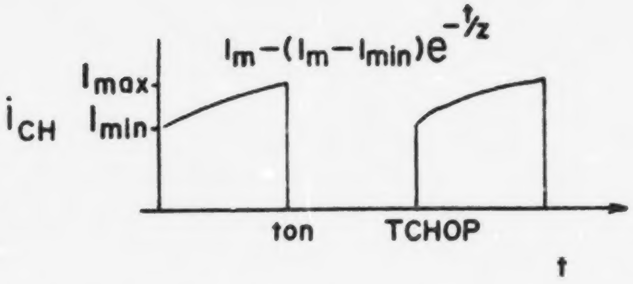

Figure A.6.5

Wave Form of i_{CH}

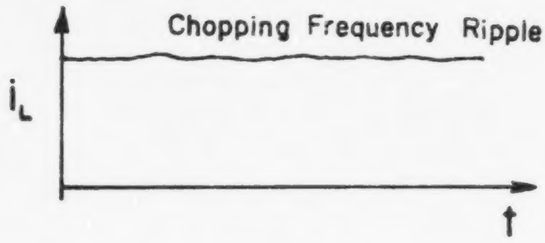

Figure A.6.6

Wave form of i_L

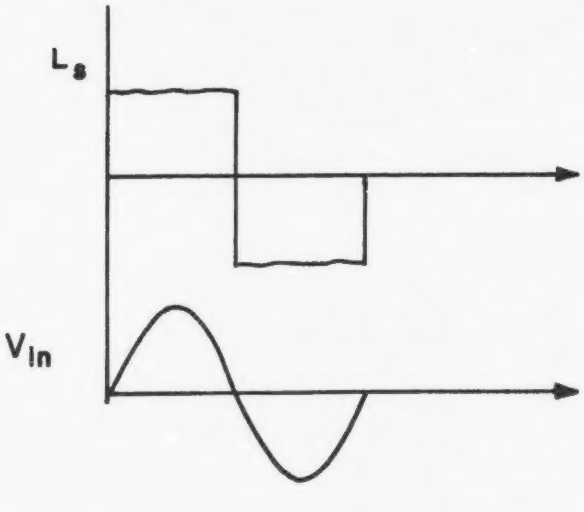

Figure A.6.7

Wave Forms of i_L
and V_{in}

a_n and b_n are given in Section A.6.3.

Consider i_s, the transformer secondary current:

- the frequency of i_s is the supply frequency, same as v_{in}.
- i_s has no dc component.

The harmonics of i_s are computed from i_L. Knowing the discrete values of i_L in time domain for one period, these discrete values are inputted to a Fast Fourier transform program. The corresponding harmonics of i_s can then be obtained. Since i_s is approximately a square wave when i_L is ripple-free, the harmonics of i_s can never be better than $1/n\tau$.

Power Input to Motor (P_H)

Input power consists of dc and harmonics input:

$$P_H = \underbrace{\frac{v_0\ (v_0 - V_c)}{R}}_{\substack{\text{dc}\\ \text{power}}} + \underbrace{\sum_{n=1}^{\infty} \frac{|\ V_n\ |^2\ R}{R^2 + (nwL)^2}}_{\substack{\text{harmonic}\\ \text{power}}}$$

$$|\ V_n\ |^2 = \frac{|\ C_n\ |^2}{2}$$

where: $|\ C_n\ |$ is given on page 93.

After currents and voltages have been computed, the associated power losses can be obtained as follows:

Switching Losses (P_S)

$$P_S = V\ .\ ICH_{DC}\ \frac{t_q}{TCHOP}$$

Conduction Losses (PC)

$$P_c = \underbrace{V_D\, I_{00}}_{\substack{\text{main thyristor}\\ \text{plus free-}\\ \text{wheeling diode}}} + \underbrace{2\, V_D\, ICH_{DC}}_{\substack{\text{front-end}\\ \text{rectifier,}\\ \text{4 diodes}}}$$

Filter Losses (FLTLOS)

$$FLTLOS = \underbrace{i_{L\,rms}^{2}\, R_{L1}}_{\substack{\text{loss in}\\ \text{inductor}}} + \underbrace{i_c^{2}\, R_{c1}}_{\substack{\text{loss in}\\ \text{filtering}\\ \text{capacitor } C_1}}$$

R_{L1} is a lumped parameter. It includes the line resistance plus the winding resistance of the filter inductor, where:

$$i_{LRMS} = \sqrt{I_{LDC}^{2} + \boxed{\sum_{n=1}^{\infty} i_{LN}^{2}}}$$

only 80 terms in program

$$\sum_{n=1}^{80} i_{Ln}^{2}$$

Transformer losses, motor higher harmonic hysteresis and eddy current losses were neglected in our analysis.

Harmonic Factor (HF)

$$HF = \frac{\left(\sum_{n=2}^{\infty} I_{sn}^{2}\right)^{1/2}}{I_{s1}}$$

where: I_{sn} = rms value of the n^{th} harmonic input current, computed from FFT subroutine

I_{s1} = fundamental component of i_s

Power Factor (PF)

Assume transformer secondary voltage is a pure sinusoidal.

$$PF = \frac{I_{s1}}{I_{srms}} = \frac{I_{s1}}{\sqrt{\underbrace{\sum_{n=1}^{\infty}}_{\text{only 80 terms in program}} I_{sn}^{2}}}$$

Note: i_s has no dc component.

Efficiency (EFF)

$$\%\ EFF = [\ \frac{P_H}{P_H + P_{TOT}}\ ] \times 100$$

$$P_{TOT} = P_S + P_C + FLTLOS$$

Case 2: $t_x < T_{CHOP}$ (discontinuous current)

Voltage and current waveform in this case refer to Figure A.6.3. General waveforms are given in Figure A.6.4.

Compute V_0 as follows:

$$w = 2\pi/T_{CHOP}$$

$$v_0 = V_0 + \sum_{n=1}^{\infty} a_n \sin nwt + \sum_{n=1}^{\infty} b_n \cos nwt$$

$$= V_0 + \sum_{n=1}^{\infty} C_n \sin (nwt + \theta_n)$$

$$a_n = \frac{V}{n\pi} (1 - \cos nwton) - \frac{V_c}{n\pi} (1 - \cos nwt_x)$$

$$b_n = \frac{V}{n\pi} \sin nwton - \frac{V_c}{n\pi} \sin nwt_x$$

$$c_n = \sqrt{a_n^{\ 2} + b_n^{\ 2}}$$

$$= \frac{\sqrt{2}}{n\pi} [V^2 + V_c^{\ 2} - V^2 \cos(nwton) + VV_c \cos(nwton) - VV_c$$

$$- VV_c \cos (nw (t_x - ton)) - V_c^{\ 2} \cos nwt_x + VV_c \cos nwt_x]^{1/2}$$

$$\theta_n = \tan^{-1} (\frac{a_n}{b_n})$$

$$V_0 = V \frac{ton}{T_{CHOP}} + (\frac{T_{CHOP} - t_x}{T_{CHOP}}) V_c$$

All the equations for i_{CH}, L_i, . . , power loss, HF, PF, etc., are the same as the continuous current case, except I_{min} in Case 2 is zero and analysis of V_0 will be different.

APPENDIX B

TRAIN CONFIGURATIONS

Identity Number	Locomotive Axles	Car Type and Number			Van	Segment
		1	2	3		
010	6	Box 69			1	ARTEDM
011	16	Bulk 114			1	ARTEDM
012	4	TOFC 82			1	EDMART
013	10	Box 74			1	KINTOR
014	10	Box 73			1	TORKIN
015	8	TOFC 77			1	TORKIN
016	14	Box 81			1	MOJWAL
017	32	Bulk 115			1	MOJWAL
018	8	TOFC 79			1	WALMOJ
019	6	Box 69			1	SPYSAS
020	16	Bulk 114			1	SPYSAS
021	4	TOFC 98			1	SASSPY
022	8	Box 84			1	MTLTOR
023	22	Bulk 107			1	TORMTL
024	8	TOFC 83			1	TORMTL
025	4	Box 62			1	BICSWN
026	12	Bulk 116			1	BICSWN
027	4	TOFC 88			1	SWNBIC
028	16	Bulk 156			1	BICSWN
029	16	Bulk 127			1	BICSWN
030	8	Bulk 126			1	BICSWN
031	8	Bulk 156(e)			1	SWNBIC
032	8	Box 71	Bulk 72(e)		1	SWNBIC
033	8	Coal 116(e)			1	SWNBIC
034	8	Box 58	Bulk 59(e)		1	SWNBIC
035	8	Box 12	TOFC 47	Bulk 58(e)	1	SWNBIC
036	8	Coal 115(e)			1	SWNBIC
037	4	Box 59	Bulk 59(e)		1	SWNBIC
038	4	Box 12	TOFC 47	Bulk 59(e)	1	SWNBIC
039	4	Box 62			1	EDMBIC
040	12	Bulk 116			1	EDMBIC
041	4	TOFC 88			1	BICEDM
042	10	Box 75			1	IGNKEN
043	12	Bulk 108			1	KENIGN
044	4	TOFC 77			1	KENIGN
045	10	Box 79			1	CALSTE
046	22	Bulk 107			1	CALSTE
047	20	TOFC 86			1	STECAL
048	14	Box 86			1	GLDMTL
049	28	Bulk 115			1	MTLGLD

		Car Type and Number				
Identity Number	Locomotive Axles	1	2	3	Van	Segment
050	8	TOFC 70			1	MTLGLD
051	12	Box 83			1	NBNVAN
052	26	Bulk 112			1	NBNVAN
053	20	TOFC 81			1	VANNBN
054	10	Box 79			1	STEGOL
055	22	Bulk 107			1	STEGOL
056	20	TOFC 86			1	GOLSTE
057	6	Box 69			1	SUXWHT
058	14	Bulk 113			1	WHTSUX
059	4	TOFC 69			1	WHTSUX
060	8	Box 76			1	RPSVAN
061	18	Bulk 106			1	RPSVAN
062	6	TOFC 76			1	VANRPS
101	6	Box 56			1	ARTEDM
102	6	Box 45			1	ARTEDM
103	16	Bulk 113			1	ARTEDM
014	16	Bulk 93			1	ARTEDM
105	4	TOFC 86			1	EDMART
106	4	TOFC 52			1	EDMART
107	10	Box 80			1	KINTOR
108	10	Box 67			1	KINTOR
109	10	Box 78			1	TORKIN
110	10	Box 65			1	TORKIN
111	8	TOFC 81			1	TORKIN
112	8	TOFC 61			1	TORKIN
113	14	Box 91			1	MOJWAL
114	32	Bulk 129			1	MOJWAL
115	4	TOFC 86			1	SASSPY
116	4	TOFC 53			1	SASSPY
117	8	Box 68			1	MTLTOR
188	8	Box 59			1	MTLTOR
199	22	Bulk 116			1	TORMTL
120	22	Bulk 104			1	TORMTL
121	8	TOFC 86			1	TORMTL
122	8	TOFC 70			1	TORMTL
123	4	Box 61			1	BICSWN
124	4	Box 52			1	BICSWN
125	12	Bulk 113			1	BICSWN
126	12	Bulk 102			1	BICSWN
127	4	TOFC 79			1	SWNBIC
128	4	TOFC 59			1	SWNBIC
129	4	Box 61			1	EDMBIC
130	4	Box 49			1	EDMBIC

		Car Type and Number				
Identity Number	Locomotive Axles	1	2	3	Van	Segment
131	12	Bulk 113			1	EDMBIC
132	12	Bulk 96			1	EDMBIC
133	4	TOFC 79			1	BICEDM
134	4	TOFC 56			1	BICEDM
135	12	Bulk 106			1	KENIGN
136	12	Bulk 84			1	KENIGN
137	4	TOFC 71			1	KENIGN
138	4	TOFC 45			1	KENIGN
139	10	Box 86			1	CALSTE
140	10	Box 75			1	CALSTE
141	20	TOFC 100			1	STECAL
142	22	Bulk 116			1	CALSTE
143	14	Box 96			1	GLDMTL
144	8	TOFC 75			1	MTLGLD
145	8	TOFC 65			1	MTLGLD
146	20	TOFC 95			1	VANNBN
147	20	TOFC 100			1	GOLSTE
148	4	TOFC 66			1	WHTSUX
149	4	TOFC 55			1	WHTSUX
150	8	Box 70			1	RPSVAN
151	8	Box 61			1	RPSVAN
152	18	Bulk 113			1	RPSVAN
153	18	Bulk 100			1	RPSVAN
154	16	Bulk 151			1	BICSWN
155	8	Bulk 122			1	BICSWN
156*	10	Bulk 132			1	EDMART
157	10	Bulk 96			1	EDMART
158*	10	Bulk 132			1	SASSPY
159	10	Bulk 98			1	SASSPY
160	18	Bulk 138			1	MTLTOR
161	18	Bulk 114			1	MTLTOR
162	12	Bulk 119			1	SWNBIC
163	12	Bulk 105			1	SWNBIC
164	24	Bulk 121			1	IGNKEN
165	24	Bulk 56			1	STECAL
166	24	Bulk 53			1	VANNBN
167	24	Bulk 56			1	GOLSTE
168	20	Bulk 123			1	VANRPS
169	12	Bulk 129			1	EDMART
170	12	Bulk 100			1	EDMART
171	12	Bulk 129			1	SASSPY
172	12	Bulk 101			1	SASSPY

* Train stalled, no results for this configuration

APPENDIX C

TRAIN TIMES

Segment		Train	Train Run Time		Track Time (minutes)	Train Delay (minutes)	Train Tons	Axles	Train Length (feet)
			650 hp (minutes)	1300 hp (minutes)					
ARTEDM									
West:	**Box**	010	272.40	217.60	200.30	1.548	5320.0	6	3584.
	Box	101	248.50	211.00	200.30	1.267	4358.0	6	2934.
	Box	102	230.80	207.10	200.30	1.030	3544.0	6	2384.
	Bulk	011	265.90	216.60	200.30	2.352	14202.0	16	5444.
	Bulk	103	264.70	216.30	200.30	2.332	14082.0	16	5399.
	Bulk	104	243.60	210.80	200.30	1.944	11682.0	16	4499.
East:	**Bulk**	169	301.90	237.90	200.30	4.913	15879.0	12	6059.
	Bulk	157	286.10	227.30	200.30	3.660	11857.0	10	4514.
	Bulk	170	269.20	221.30	200.30	3.854	12399.0	12	4754.
	TOFC	105	340.80	260.90	200.30	3.595	4969.0	4	4434.
	TOFC	012	332.60	253.10	200.30	3.433	4745.0	4	4234.
	TOFC	106	271.40	218.90	200.30	2.217	3065.0	4	2734.
KINTOR									
West:	**Box**	107	196.10	172.70	163.12	0.847	6257.0	10	4194.
	Box	013	192.00	171.30	163.12	0.787	5813.0	10	3894.
	Box	108	187.40	169.90	163.12	0.716	5295.0	10	3544.
East:	**Box**	111	198.00	174.10	163.12	2.998	6109.0	10	4094.
	Box	014	194.10	172.90	163.12	2.815	5739.0	10	3844.
	Box	112	188.50	171.20	163.12	2.522	5147.0	10	3444.
	TOFC	109	220.90	177.50	163.12	3.108	4812.0	8	4244.
	TOFC	015	216.00	176.20	163.12	2.962	4588.0	8	4044.
	TOFC	110	197.30	171.40	163.12	2.376	3692.0	8	3244.
MOJWAL									
West:	**Box**	113	281.00	264.30	257.43	4.715	7194.0	14	4804.
	Box	016	274.70	263.60	257.43	4.230	6454.0	14	4304.
	Bulk	114	279.30	266.00	257.43	6.225	16494.0	32	6359.
	Bulk	017	273.90	265.20	257.43	5.613	14814.0	32	5729.
East:	**TOFC**	018	291.50	261.60	257.43	0.221	4700.0	8	4144.
SPYSAS									
West:	**Box**	019	359.00	289.40	263.31	3.748	5320.0	6	3584.
	Bulk	020	351.70	289.00	263.31	5.662	14202.0	16	5444.
East:	**Bulk**	171	427.10	309.80	263.31	7.442	15879.0	12	6059.
	Bulk	159	406.10	300.60	263.31	6.670	12097.0	10	4604.
	Bulk	172	375.00	290.60	263.31	5.907	12519.0	12	4799.
	TOFC	021	613.30	395.50	263.31	6.194	5641.0	4	5034.
	TOFC	115	487.60	348.90	263.31	5.463	4969.0	4	4434.
	TOFC	116	380.90	290.30	263.31	3.452	3121.0	4	2784.
MTLTOR									
West:	**Box**	022	511.20	441.10	396.05	26.302	6492.0	8	4393.
	Box	117	476.10	432.10	396.05	22.339	5308.0	8	3594.
	Box	118	458.80	427.50	396.05	19.954	4642.0	8	3144.
	Bulk	160	540.70	454.30	396.05	35.279	17143.0	18	6524.
	Bulk	161	500.50	443.30	396.05	30.827	14263.0	18	5444.

Segment		Train	Train Run Time		Track Time (minutes)	Train Delay (minutes)	Train Tons	Axles	Train Length (feet)
			650 hp (minutes)	1300 hp (minutes)					
East:	Bulk	119	446.70	436.00	396.05	27.224	14626.0	22	5594.
	Bulk	023	459.60	433.70	396.05	25.805	13546.0	22	5189.
	Bulk	120	457.20	432.90	396.05	25.326	13186.0	22	5054.
	TOFC	121	495.30	434.70	396.05	23.330	5092.0	8	4494.
	TOFC	024	489.70	433.20	396.05	22.795	4924.0	8	4344.
	TOFC	122	466.20	427.50	396.05	20.069	4196.0	8	3694.
BICSWN									
West:	Box	025	133.70	98.30	78.87	0.519	4741.0	4	3234.
	Box	123	132.40	97.60	78.87	0.511	4667.0	4	3184.
	Box	124	121.20	91.20	78.87	4.439	4001.0	4	2734.
	Bulk	030	181.50	119.00	78.87	0.941	15396.0	8	5864.
	Bulk	155	177.50	116.90	78.87	0.912	14916.0	8	5684.
	Bulk	028	134.30	97.50	78.87	1.177	19242.0	16	7334.
	Bulk	026	133.80	97.50	78.87	0.879	14319.0	12	5474.
	Bulk	154	131.80	96.20	78.87	1.141	18642.0	16	7109.
	Bulk	125	131.90	96.40	78.87	0.857	13959.0	12	5339.
	Bulk	126	124.40	92.30	78.87	0.778	12639.0	12	4844.
	Bulk	029	119.80	89.80	78.87	0.968	15762.0	16	6029.
East:	Bulk	162	121.00	91.90	78.87	1.219	14679.0	12	5609.
	Bulk	163	113.60	89.10	78.87	1.082	12999.0	12	4979.
	TOFC	037	146.00	102.30	78.87	1.247	6289.0	4	5739.
	TOFC	038	140.20	99.80	78.87	1.247	5443.0	4	5739.
	TOFC	027	133.80	101.20	78.87	0.985	5081.0	4	4534.
	TOFC	127	125.90	94.60	78.87	0.888	4577.0	4	4084.
	TOFC	032	111.50	88.40	78.87	1.518	7690.0	8	6984.
	TOFC	128	109.30	87.20	78.87	0.670	3457.0	4	3084.
	TOFC	034	102.20	85.20	78.87	1.250	6338.0	8	5749.
	TOFC	035	100.00	84.40	78.87	1.251	5536.0	8	5754.
	TOFC	031	99.40	84.30	78.87	1.563	4956.0	8	7214.
	TOFC	033	90.80	82.00	78.87	1.161	3842.0	8	5340.
	TOFC	036	90.30	81.60	78.87	1.167	3841.0	8	5369.
EDMBIC									
West:	Box	039	287.60	201.20	173.71	2.663	4741.0	4	3234.
	Box	129	284.30	200.10	173.71	2.622	4667.0	4	3184.
	Box	130	247.10	188.70	173.71	2.128	3779.0	4	2584.
	Bulk	040	284.20	200.30	173.71	4.507	14319.0	12	5474.
	Bulk	131	279.00	198.80	173.71	4.396	13959.0	12	5339.
	Bulk	132	250.40	190.50	173.71	3 766	11919.0	12	4574.
East:	TOFC	041	226.90	191.10	173.71	3.046	5081.0	4	4534.
	TOFC	133	220.50	187.90	173.71	3.044	4577.0	4	4084.
	TOFC	134	199.70	181.10	173.71	1.971	3289.0	4	2934.
IGNKEN									
West:	Box	042	186.30	178.20	171.29	3.944	5887.0	10	3944.
	Bulk	164	187.40	179.20	171.29	4.662	15288.0	24	5879.
East:	Bulk	043	252.70	189.70	171.29	4.801	13359.0	12	5114.
	Bulk	135	250.00	189.00	171.29	4.764	13119.0	12	5024.
	Bulk	136	221.30	182.70	171.29	4.283	10479.0	12	4034.
	TOFC	044	297.60	208.80	171.29	4.253	4465.0	4	3984.
	TOFC	137	283.50	202.50	171.29	4.047	4129.0	4	3684.
	TOFC	138	223.80	181.00	171.29	2.843	2673.0	4	2384.

Segment		Train	Train Run Time						
			650 hp (minutes)	1300 hp (minutes)	Track Time (minutes)	Train Delay (minutes)	Train Tons	Axles	Train Length (feet)
CALSTE									
West:	Box	139	232.50	178.30	167.23	3.443	6701.0	10	4494.
	Box	045	221.60	176.20	167.23	3.180	6183.0	10	4144.
	Box	140	215.60	175.20	167.23	3.030	5887.0	10	3944.
	Bulk	142	229.50	178.30	167.23	4.270	14626.0	22	5594.
	Bulk	046	219.20	176.60	167.23	3.965	13546.0	22	5189.
East:	Bulk	165	171.20	170.60	167.23	2.622	7488.0	24	2954.
	TOFC	141	172.30	171.60	167.23	4.715	62445.0	20	5374.
	TOFC	047	171.70	171.10	167.23	4.109	5461.0	20	4674.
GLDMTL									
West:	Box	143	403.40	364.30	339.81	11.794	7564.0	14	5054.
	Box	048	391.80	361.00	339.81	10.643	6824.0	14	4554.
East:	Bulk	049	419.70	369.90	339.81	15.000	14691.0	28	5669.
	TOFC	144	461.90	374.30	339.81	10.483	4476.0	8	3944.
	TOFC	050	448.70	369.80	339.81	9.829	4196.0	8	3694.
	TOFC	145	435.70	365.90	339.81	9.165	3916.0	8	3444.
NBNVAN									
West:	Box	051	244.00	239.90	222.78	11.590	6541.0	12	4404.
	Bulk	052	246.90	243.20	222.78	14.406	14269.0	26	5474.
East:	Bulk	166	232.20	230.70	218.00	6.956	7128.0	24	2819.
	TOFC	146	238.20	236.30	218.00	12.644	5965.0	20	5124.
	TOFC	053	235.60	234.10	218.00	10.916	5181.0	20	4424.
STEGOL									
West:	Box	054	137.00	136.90	135.06	0.785	6183.0	10	4144.
	Bulk	055	137.30	137.30	135.06	0.983	13546.0	22	5189.
East	Bulk	167	134.70	124.80	123.42	0.559	7488.0	24	2954.
	TOFC	147	135.40	125.20	123.42	1.018	6245.0	20	5374.
	TOFC	056	128.80	124.90	123.42	0.885	5461.0	20	4674.
SUXWHT									
West:	Box	057	264.90	239.70	230.81	2.716	5320.0	6	3584.
East:	Bulk	058	279.40	241.30	230.81	3.371	14260.0	14	5339.
	TOFC	059	307.00	245.90	230.81	2.263	4017.0	4	3534.
	TOFC	148	300.60	244.20	230.81	2.168	3849.0	4	3434.
	TOFC	149	278.40	238.90	230.81	1.821	3233.0	4	2884.
RPSVAN									
West:	Box	060	902.80	887.70	856.99	19.162	5900.0	8	3994.
	Box	150	897.90	885.30	856.99	17.723	5456.0	8	3694.
	Box	151	891.60	882.00	856.99	15.564	4790.0	8	3244.
	Bulk	152	911.00	895.80	856.99	25.868	14143.0	18	5399.
	Bulk	061	906.90	893.60	856.99	24.374	13303.0	18	5084.
	Bulk	153	903.50	891.80	856.99	23.093	12583.0	18	4814.
East:	Bulk	168	975.30	901.50	856.99	29.966	15405.0	20	5909.
	TOFC	062	993.40	894.10	856.99	19.992	4470.0	6	3934.

APPENDIX D

SPEED FACTORS

Segment		Train No.	Exponent	Constant	Target hp/Ton	Target hp/Axle
ARTEDM						
West	Box	101	4.51911	236.708	2.06736	1584.62
		102	6.79359	230.842	2.53284	1263.59
	Bulk	103	3.68124	235.668	1.74369	1635.27
		104	5.12927	233.017	2.06791	1593.30
East	Bulk	169	3.18054	229.032	1.41806	2027.71
		170	3.84104	229.744	1.57400	1744.45
	TOFC	105	2.78107	256.976	1.90311	2506.15
		106	3.41553	250.824	2.07654	1678.74
KINTOR						
West	Box	107	5.73785	194.629	2.67411	1734.20
		108	7.40466	190.806	3.09069	1688.15
East	Box	111	5.65753	197.425	2.65593	1682.08
		112	7.52942	192.657	3.11902	1655.55
	TOFC	109	3.29048	221.477	2.57081	1605.00
		110	5.10634	208.566	3.25802	1548.58
MOJWAL						
West	Box	113	11.49383	286.219	2.74457	1426.80
		016	17.05650	279.936	3.16213	1472.53
	Bulk	114	14.43909	283.357	2.83005	1475.25
		017	21.80074	277.920	3.31671	1550.28
East	TOFC	018	6.51168	294.884	2.40798	1433.53
SPYSAS						
West	Box	019	3.47221	315.392	1.78182	1695.03
	Bulk	020	3.82659	312.351	1.77215	1688.28
East	Bulk	171	2.34165	292.207	1.19554	1753.83
		172	2.95082	302.751	1.41387	1610.50
	TOFC	115	2.20702	340.638	1.68706	2257.07
		116	2.70172	341.290	1.94579	1619.52
MTLTOR						
West	Box	117	8.30553	461.691	2.26580	1666.81
		118	11.33008	454.550	2.72899	1731.55
	Bulk	160	4.51967	473.551	1.52509	1625.82
		161	6.59818	468.930	1.85875	1642.82
East	Bulk	119	11.65002	457.746	2.48943	1795.83
		120	14.47069	453.593	2.90383	1873.84
	TOFC	121	5.98652	481.188	2.27734	1592.89
		122	9.01818	467.730	2.87018	1634.61

Segment		Train No.	Exponent	Constant	Target hp/Ton	Target hp/Axle
BICSWN						
West	Box	123	2.40247	98.813	1.69244	2096.06
		124	2.57196	98.206	1.73289	1837.40
	Bulk	030	1.72738	89.093	1.20937	2527.68
		029	2.53607	97.382	1.65517	1733.05
East	Bulk	162	2.69704	90.988	1.41087	1853.13
		163	3.05269	92.144	1.54245	1783.58
	TOFC	037	2.07263	88.848	1.23921	2111.95
		033	7.10796	93.833	3.09946	1538.49
EDMBIC						
West	Box	129	2.06135	203.657	1.34581	1674.00
		130	2.69653	207.635	1.56556	1563.09
	Bulk	131	2.14048	202.462	1.31569	1633.95
		132	2.66326	205.754	1.48261	1560.94
East	TOFC	133	4.68577	190.017	1.41485	1720.72
		134	7.57590	190.984	1.88288	1621.33
IGNKEN						
West	Box	042	17.53111	185.519	2.71684	1711.52
	Bulk	164	16.44214	186.639	2.63531	1738.03
East	Bulk	135	2.64194	195.499	1.31878	1557.18
		136	4.02426	196.283	1.56611	1511.19
	TOFC	137	2.27579	209.680	1.50234	1766.61
		138	3.89116	204.869	1.88215	1487.97
CALSTE						
West	Box	139	2.63567	224.708	2.09765	1459.43
		140	3.45007	218.178	2.35256	1432.21
	Bulk	142	2.83468	222.781	2.09913	1448.91
		046	3.31445	218.830	2.25604	1438.53
East	Bulk	165	202.92808	171.788	9.93707	3125.41*
	TOFC	141	174.97708	172.986	2.86592	919.95
		047	202.80178	172.407	3.51337	981.24
GLDMTL						
West	Box	143	7.43865	405.806	2.90497	1670.76
		048	9.21772	398.568	3.27337	1686.87
East	Bulk	049	5.95197	425.633	2.95411	1648.27
	TOFC	144	3.53523	464.996	2.72198	1627.79
		145	4.26049	452.655	3.02909	1577.68

Segment		Train No.	Exponent	Constant	Target hp/Ton	Target hp/Axle
NBNVAN						
West	Box	051	44.43212	244.318	6.33581	3532.87*
	Bulk	052	49.85238	247.156	7.78207	4350.73*
East	Bulk	166	111.07831	233.731	70.27325	20906.97*
	TOFC	146	89.81260	240.136	37.47584	11213.14*
		053	112.10237	237.445	60.48079	15698.79*
RPSVAN						
West	Box	150	52.19445	895.558	3.41934	2389.52*
		151	67.64439	891.659	4.32937	2642.71*
	Bulk	152	44.18716	905.051	2.99572	2419.47*
		153	56.62896	900.921	3.76369	2689.45*
East	Bulk	168	9.35346	948.482	1.87264	1506.78
	TOFC	062	6.95806	961.998	1.90376	1481.14
STEGOL						
West	Box	054	958.01246	137.005	3460.7364	1239781.7*
	Bulk	055				
East	Bulk	167	9.11940	145.855	4.40949	1380.37
	TOFC	147	8.88822	146.935	4.38016	1372.32
		056	22.63740	133.795	5.28805	1447.94
SUXWHT						
West	Box	057	7.26746	251.283	1.70342	1562.91
	Bulk	058	4.96258	251.149	1.41505	1501.69
East	TOFC	148	3.46758	263.101	1.52446	1523.93
		149	4.70505	262.264	1.75793	1468.74

---

* The predicted high values reflect situations where train times are very insensitive to increasing power. Thus, although predicted requirements are high, warranted power levels are in fact very low.

POOR

QUALITY

ORIGINAL